Mathematisches Forschungsinstitut Oberwolfach

Report No. 10/2024

DOI: 10.4171/OWR/2024/10

Hyperbolic Balance Laws: Interplay between Scales and Randomness

Organized by
Rémi Abgrall, Zürich
Mauro Garavello, Milano
Mária Lukáčová-Medvid'ová, Mainz
Konstantina Trivisa, College Park

25 February – 1 March 2024

Abstract. Hyperbolic balance laws are fundamental in the mathematical modeling of transport-dominated processes in natural, socio-economic and engineering sciences. The aim of the workshop was to discuss open questions in the area of nonlinear hyperbolic conservation and balance laws. We have focused on a delicate interplay between scale hierarchies and random/stochastic effects and discuss them from analytical, numerical and modeling point of view. This leads to questions of admissibility criteria connecting to ill-posedness of weak entropy solutions, hyperbolic problems with nonlocal terms, mean field theory, multiscale and structure preserving numerical methods, random solutions and uncertainty quantification methods, as well as data-based methods.

Mathematics Subject Classification (2020): 35L65, 35L40, 35L60, 35R60, 65M08, 60H15, 76F10, 82B40.

Introduction by the Organizers

The workshop *Hyperbolic Balance Laws: Interplay between Scales and Randomness* was organized by Rémi Abgrall (Zürich), Mauro Garavello (Milano), Mária Lukáčová-Medvid'ová (Mainz), and Konstantina Trivisa (College Park). The workshop was well attended with over 40 participants with broad geographic representation from all continents.

We have discussed fundamental problems, including novel probabilistic solution concepts, admissibility criteria for weak entropy solutions, non-local hyperbolic

problems, randomness, and multiscale effects. These themes are inter-connected through analytical and numerical methods developed by the hyperbolic balance laws community over the last years. These mathematical techniques are now emerging in a new light with the aid of control theory, mean field games, uncertainty quantification and data science.

The Oberwolfach workshop gave a broad mix of talks covering modelling, analysis and numerics of hyperbolic balance laws. We had 30 talks given by senior and junior researchers; on Wednesday afternoon we organized a trip to Saint Roman. The atmosphere in Oberwolfach was stimulating, we enjoyed talks, afternoon coffee and cake joined with a free discussion time. The extensive scientific exchange has produced many new ideas that will be elaborated in the future. We also had good luck having nice weather, blue sky, and shining sun...

The organizers and participants thank the "Mathematisches Forschungsinstitut Oberwolfach" for having provided a comfortable and inspiring environment for the workshop.

Acknowledgement: The MFO and the workshop organizers would like to thank the National Science Foundation for supporting the participation of junior researchers in the workshop by the grant "US Junior Oberwolfach Fellows".

Workshop: Hyperbolic Balance Laws: Interplay between Scales and Randomness

Table of Contents

Abstracts

Preserving stationary states on unstructured grids

Wasilij Barsukow
(joint work with Raphaël Loubère, Pierre-Henri Maire)

1. Abstract

The consistency condition of Harten-Lax-van Leer [6] imposes equality of numerical fluxes both sides of an interface between cells. We give up this condition (which leaves us with free parameters in the definition of the approximate Riemann solver) and impose that the sum of all fluxes around a node vanishes (which allows to fix some of those parameters after imposing some additional identifications). For this setup to work out one needs to consider half-cells with possibly different fluxes on each of them (and on each of its sides). We show that a particular choice of such a solver for 2-d linear acoustics admits a discrete analogue of curl grad = 0, and give arguments why for any such node-based solver this identity can only be expected on grids consisting of polygons with at most 4 edges.

2. Introduction

The paramount hyperbolic equation in 1 spatial dimension is linear advection

$$\partial_t q + c\partial_x q = 0 \qquad q\colon \mathbb{R}_0^+ \times \mathbb{R} \to \mathbb{R} \tag{1}$$

Concepts such as stability and high order of accuracy for numerical methods, as well as limiting and TVD traditionally are first developed for (1). Linear systems in 1-d reduce to such equations componentwise by diagonalization.

This is no longer the case in multiple spatial dimensions, because Jacobians in different directions may not commute and systems no longer reduce to a set of decoupled advection equations. The most prominent system in this context is that of linear acoustics

$$\partial_t \mathbf{v} + \nabla p = 0 \qquad \mathbf{v}\colon \mathbb{R}_0^+ \times \mathbb{R}^d \to \mathbb{R}^d \tag{2}$$

$$\partial_t p + \nabla \cdot \mathbf{v} = 0 \qquad p\colon \mathbb{R}_0^+ \times \mathbb{R}^d \to \mathbb{R} \tag{3}$$

The behaviour of its solutions is very different from pure transport: For example, solutions to bounded initial data can become L^∞ unbounded ([1, 3]). System (2)–(3) possesses an involutional constraint of stationary vorticity

$$\partial_t(\nabla \times \mathbf{v}) = 0 \tag{4}$$

and non-trivial stationary states governed by

$$\nabla p = 0 \qquad \nabla \cdot \mathbf{v} = 0 \tag{5}$$

The key question pursued here is: *What are the stationary states of a numerical method for* (2)–(3)*?*

3. Cartesian grids

Some answers for the case of Cartesian grids have already been given in [2]. They shall be summarized next. Consider (for simplicity the modified equation of) an upwind, dimensionally-split numerical method for (2)–(3) in two spatial dimensions

$$\partial_t u + \partial_x p = \Delta x \partial_x^2 u \tag{6}$$

$$\partial_t v + \partial_y p = \Delta x \partial_y^2 v \tag{7}$$

$$\partial_t p + \partial_x u + \partial_y v = \Delta x (\partial_x^2 p + \partial_y^2 p) \tag{8}$$

where $\mathbf{v} := (u, v)$ and $\Delta x = \Delta y$. If the initial data are chose to correspond to a stationary state, one is, at least at initial time, left with

$$\partial_t u = \Delta x \partial_x^2 u \tag{9}$$

$$\partial_t v = \Delta x \partial_y^2 v \tag{10}$$

$$\partial_t p = 0 \tag{11}$$

i.e. a heat equation in x for u and in y for v. One thus concludes that

$$\partial_x u \overset{t\to\infty}{\longrightarrow} 0 \qquad\qquad \partial_y v \overset{t\to\infty}{\longrightarrow} 0 \tag{12}$$

Summing up, one does still have $\partial_x u + \partial_y v = 0$, but (12) are a poor subset of all divergencefree velocity fields, because $\partial_x u$ and $\partial_y v$ vanish individually already. Such a method is called *not stationarity preserving*. The precise arguments involve analyzing the behaviour of discrete Fourier modes of the upwind method and are presented in [2]. They lead to the same conclusion (12). Moreover, (12) can be easily observed in a numerical experiment.

On Cartesian grids a very convincing solution has been proposed in several works (e.g. [9, 7, 10, 8, 2]). One aims at finding a numerical method whose modified equation would be

$$\partial_t u + \partial_x p = \Delta x \partial_x (\partial_x u + \boxed{\partial_y v}) \tag{13}$$

$$\partial_t v + \partial_y p = \Delta x \partial_y (\boxed{\partial_x u} + \partial_y v) \tag{14}$$

$$\partial_t p + \partial_x u + \partial_y v = \Delta x (\partial_x^2 p + \partial_y^2 p) \tag{15}$$

with the boxed terms having been added. The challenge is to achieve this discretely, and it turns out that special multi-dimensional finite differences are necessary here. Note that the idea is not to make sure that terms cancel at leading order, but to find discrete derivatives $D_x, D_y, D_{xx}, D_{xy}, D_{yy}$ which mimic the behaviour of their continuous versions (*structure preservation*):

$$D_x(D_x u + D_y v) = D_{xx} u + D_{xy} v \qquad D_y(D_x u + D_y v) = D_{xy} u + D_{yy} v \tag{16}$$

Standard finite differences do not fulfill these relations. The methods developed in the above-mentioned references are all using such special finite differences; they are *stationarity preserving*. As has been mentioned in [8, 2] they also preserve a discretization of the vorticity $\nabla \times \mathbf{v}$ exactly: they are *vorticity preserving*.

4. A non-classical Finite Volume method

Inspired by challenges faced by collocated Lagrangian methods, a new kind of approximate Riemann solver was introduced in [5, 4]. To this end recall that the consistency condition of [6] arises upon integration of the conservation law $\partial_t q + \partial_x f(q) = 0$ over space time volumes $[0,t] \times [-\lambda t, 0]$ and $[0,t] \times [0, \lambda t]$. One assumes that at $t = 0$ Riemann data are given with the discontinuity at $x = 0$, together with an approximate solution of this Riemann problem in the space-time wedge bounded by the left-running and right-running waves (speeds $\pm\lambda$). This allows to compute the flux averages over $[0,t]$ at the locations $x = 0^{\pm}$. Continuity of these fluxes is the consistency condition.

Here, it is proposed not to make use of it. This, on the one hand, implies less conditions imposed during the construction of the approximate Riemann solver, i.e. free parameters. On the other hand, this implies a loss of conservation. This, however, is replaced by *nodal conservation*, which amounts to 1 equation per node. Some additional assumptions allow to reduce the number of free parameters to one per node, and this latter can then be imposed by applying nodal conservation.

Some notation is necessary to make these concepts more precise. We denote by

- $\mathcal{C}, \mathcal{N}, \mathcal{E}$ the sets of cells, nodes and edges on the grid,
- $\mathcal{C}(n), \mathcal{C}(e)$ the sets of cells adjacent to a node n and to an edge e,
- $\mathcal{N}(c)$ the set of nodes around a cell c

We subdivide every edge $e \in \mathcal{E}$ in two, refer to them as *subedges* and denote their set as $\mathcal{SE}$. The set of subedges surrounding a cell c is denoted by $\mathcal{SE}(c)$, the set of subedges around a node n is denoted by $\mathcal{SE}(n)$ and the set of (2) subedges around a node n which are adjacent to cell c is denoted by $\mathcal{SE}(n,c)$.

We denote by $\hat{f}_{s,c}$ a numerical flux from the cell c through the subedge s. The Finite Volume update formula then reads

$$\partial_t q_c + \frac{1}{|c|} \sum_{s \in \mathcal{SE}(c)} |s| \hat{f}_{s,c} = 0 \tag{17}$$

where q_c denotes the cell average of q in cell $c \in \mathcal{C}$ and $|c|$ and $|s|$ are the area of c and the length of s. Global conservation implies

$$0 = \partial_t \left(\sum_{c \in \mathcal{C}} |c| q_c \right) = - \sum_{c \in \mathcal{C}} \sum_{s \in \mathcal{SE}(c)} |s| \hat{f}_{s,c} \tag{18}$$

Reorganize the sum:

$$= - \sum_{n \in \mathcal{N}} \sum_{c \in \mathcal{C}(n)} \sum_{s \in \mathcal{SE}(n,c)} |s| \hat{f}_{s,c} \tag{19}$$

Instead of the classical "localization" of conservation on an edge $\sum_{c \in \mathcal{C}(e)} \hat{f}_{e,c} = 0$ we impose to localize the conservation on a node:

$$\sum_{c\in\mathcal{C}(n)}\sum_{s\in\mathcal{SE}(n,c)}|s|\hat{f}_{s,c}=0 \tag{20}$$

The free parameter that we choose to keep during the derivation of the Riemann solver is a *nodal pressure*, for which condition (20) yields the following expression (see [4] for details):

$$p_n^*:=\frac{\displaystyle\sum_{s\in\mathcal{SE}(n)}|s|\left(\frac{p_\mathrm{L}+p_\mathrm{R}}{2}-\mathbf{n}_s\cdot\frac{\mathbf{v}_\mathrm{R}-\mathbf{v}_\mathrm{L}}{2}\right)}{\displaystyle\sum_{s\in\mathcal{SE}(n)}|s|} \tag{21}$$

Here, $\mathbf{n}_s$ is a unit normal associated to a subedge s once and for all, and cells L/R are such that $\mathbf{n}_s$ is pointing from L to R. Denote by $\mathbf{n}_{s,c}$ the unit normal to s pointing out of c. Then, if $\mathbf{n}_s=\mathbf{n}_{s,c}$, then c is L, if $\mathbf{n}_s=-\mathbf{n}_{s,c}$, then c is R. Thus, one can rewrite

$$\sum_{s\in\mathcal{SE}(n)}|s|\mathbf{n}_s\cdot(\mathbf{v}_\mathrm{R}-\mathbf{v}_\mathrm{L})=-\sum_{c\in\mathcal{C}(n)}\mathbf{v}_c\cdot\underbrace{\left(\sum_{s\in\mathcal{SE}(n,c)}|s|\mathbf{n}_{s,c}\right)}_{=:\ell_{nc}\mathbf{n}_{nc}} \tag{22}$$

The vector $\mathbf{n}_{nc}$ is called the unit *node normal*.

5. Some discrete operators on unstructured grids

Definition 1. *Denote by*

$$\mathrm{GRAD}_c\phi:=\frac{1}{|c|}\sum_{n\in\mathcal{N}(c)}\ell_{nc}\mathbf{n}_{nc}\phi_n \qquad \mathrm{GRAD}\colon\mathcal{N}\to\mathcal{C}^2 \tag{23}$$

$$\mathrm{DIV}_n\mathbf{v}:=-\frac{1}{|c_n|}\sum_{c\in\mathcal{C}(n)}\ell_{nc}\mathbf{n}_{nc}\cdot\mathbf{v}_c \qquad \mathrm{DIV}\colon\mathcal{C}^2\to\mathcal{N} \tag{24}$$

where c_n is the dual cell around node n, i.e. the polygon consisting of cell centroids and edge midpoints around n.

The dual cell is chosen only to guarantee

$$\sum_{c\in\mathcal{C}}|c|=\sum_{n\in\mathcal{N}}|c_n|+\text{b.t.} \tag{25}$$

Theorem 1. GRADϕ *is a consistent discretization of* $\nabla\phi$ *in the sense that it is exact for affine* ϕ*.*

Theorem 2. DIV$\mathbf{v}$ *is a weakly consistent discretization of* $\nabla\cdot\mathbf{v}$ *in the sense that it is the* ℓ^2 *dual of* GRAD*.*

Proof. Ignoring boundaries:

(26)
$$\sum_{n\in\mathcal{N}} |c_n|\phi_n \mathrm{DIV}_n\mathbf{v} = -\sum_{n\in\mathcal{N}} \phi_n \sum_{c\in\mathcal{C}(n)} \ell_{nc}\mathbf{n}_{nc}\cdot\mathbf{v}_c = -\sum_{c\in\mathcal{C}} \mathbf{v}_c \cdot \sum_{n\in\mathcal{N}(c)} \ell_{nc}\mathbf{n}_{nc}\phi_n$$

(27)
$$= -\sum_{c\in\mathcal{C}} \mathbf{v}_c \cdot \mathrm{GRAD}_c\phi$$

□

One thus can rewrite the nodal pressure as

(28)
$$p_n^* = \frac{\displaystyle\sum_{s\in\mathcal{SE}(n)} |s|\frac{p_\mathrm{L}+p_\mathrm{R}}{2} - \frac{1}{2}|c_n|\mathrm{DIV}_n\mathbf{v}}{\displaystyle\sum_{s\in\mathcal{SE}(n)} |s|}$$

6. Stationarity preservation of node-based methods

The full method, without giving the details of the derivation which are available in [4], reads

(29)
$$\frac{\mathrm{d}}{\mathrm{d}t}\mathbf{v}_c = -\frac{1}{|c|}\sum_{n\in\mathcal{N}(c)} \ell_{nc}\mathbf{n}_{nc}p_n^* = -\mathrm{GRAD}_c p^*$$

(30)
$$\frac{\mathrm{d}}{\mathrm{d}t}p_c = -\frac{1}{|c|}\sum_{n\in\mathcal{N}(c)}\sum_{s\in\mathcal{SE}(n,c)} |s|(p_c - p_n^*)$$

One easily concludes the following

Theorem 3. *If* $p = \mathrm{const}$ *and* $\mathrm{DIV}_n\mathbf{v} = 0 \quad \forall n \in \mathcal{N}$ *initially, then these data remain stationary.*

In view of what has been said in the Introduction, one needs to avoid that stationary states of a numerical method for acoustics turn out to be a poor subset of all divergencefree vector fields. As the discrete divergence here is defined on the nodes, it is natural to make the following

Definition 2. *A linear numerical method of the form* (29)–(30) *is called* stationarity preserving *if it has as many linearly independent stationary states as there are nodes on the grid (up to modifications related to boundaries).*

The linear system $\mathrm{DIV}\,\mathbf{v} = 0$ consists of $\#\mathcal{N}$ equations for $2\#\mathcal{C}$ variables. It thus has at least $2\#\mathcal{C} - \#\mathcal{N}$ solutions. The same number appears in a different context, too. Consider operators that annihilate GRAD identically. Seen as a matrix, GRAD has $2\#\mathcal{C}$ rows and $\#\mathcal{N}$ columns. Its left kernel thus has dimension at least $2\#\mathcal{C} - \#\mathcal{N}$.

The number $2\#\mathcal{C} - \#\mathcal{N}$ can be estimated assuming that the grid consists of cells with α edges. Then $\#\mathcal{E} = \frac{\alpha}{2}\#\mathcal{C}$, and from Euler's formula one obtains

$$2\#\mathcal{C} - \#\mathcal{N} = \frac{6-\alpha}{\alpha-2}\#\mathcal{N} \tag{31}$$

This proves

Theorem 4. *The method* (29)–(30) *with the nodal pressure* (28) *is stationarity preserving on triangular-quadrangular grids* ($\#\mathcal{E}(c) \leq 4$).

For hexagonal grids there are no non-trivial solutions of $\mathrm{DIV}\,\mathbf{v} = 0$.

Without proof (which can be found in [4]) we also state the following

Theorem 5. *If* $\#\mathcal{E}(c) \leq 4$, *then the method* (29)–(30) *is vorticity preserving, i.e. it keeps the following weakly consistent discretization of the curl of* $\mathbf{v}$ *exactly stationary:*

$$\mathrm{CURL}_n\mathbf{v} = -\frac{1}{|c_n|}\sum_{c\in\mathcal{C}(n)} \ell_{nc}\mathbf{n}_{nc} \times \mathbf{v}_c \tag{32}$$

and CURL GRAD $= 0$.

7. Conclusions

We have exemplified a numerical method that involves a nodal pressure. It has been derived from the idea of nodal conservation and is characterized by discrete differential operators that map from the primary (cells) to the dual (nodes) mesh. The resulting method is collocated on the primary mesh. The particular choice presented here is shown to be stationarity preserving on grids of cells with at most 4 edges; it reduces to well-known stationarity preserving methods of truly multi-dimensional nature on Cartesian grids. Based on rather fundamental arguments it was also shown, however, that a method which uses a gradient operator that maps from nodes to cells cannot be vorticity preserving on grids containing pentagons and other polygons with more than 4 edges, independently of further details of the numerical method.

References

[1] D. Amadori and L. Gosse, *Error Estimates for Well-Balanced Schemes on Simple Balance Laws: One-Dimensional Position-Dependent Models*, BCAM Springer Briefs in Mathematics, Springer, 2015.

[2] W. Barsukow, *Stationarity preserving schemes for multi-dimensional linear systems*, Mathematics of Computation, **88** (2019), 1621–1645.

[3] W. Barsukow and C. Klingenberg, *Exact solution and a truly multidimensional Godunov scheme for the acoustic equations*, ESAIM: M2AN, **56** (2022).

[4] W. Barsukow, R. Loubère, and P.-H. Maire, *A high-order cell-centered Lagrangian scheme for two-dimensional compressible fluid flows on unstructured meshes*, submitted to Math. Comp., (2023).

[5] G. Gallice, A. Chan, R. Loubère, and P.-H. Maire, *Entropy stable and positivity preserving godunov-type schemes for multidimensional hyperbolic systems on unstructured grid*, J. Comput. Phys., **468** (2022), 111493.

[6] A. Harten, P. D. Lax, and B. van Leer. *On upstream differencing and Godunov-type schemes for hyperbolic conservation laws*, SIAM review, **25** (1983), 35–61.
[7] R. Jeltsch and M. Torrilhon, *On curl-preserving finite volume discretizations for shallow water equations*, BIT Numerical Mathematics, **46** (2006), 35–53.
[8] T. B. Lung and P. L. Roe, *Toward a reduction of mesh imprinting*, International Journal for Numerical Methods in Fluids, **76** (2014), 450–470.
[9] K. W. Morton and P. L. Roe, *Vorticity-preserving Lax-Wendroff-type schemes for the system wave equation*, SIAM J. Sci. Comput., **23** (2001), 170–192.
[10] S. Mishra and E. Tadmor, *Constraint preserving schemes using potential-based fluxes II. genuinely multi-dimensional central schemes for systems of conservation laws*, ETH preprint, **32** (2009).

High-Order Semi-implicit Schemes for Evolutionary Partial Differential Equations with Higher Order Derivatives

Sebastiano Boscarino

Many time-dependent PDEs which arise in physics or engineering involve the computation of high order spatial derivatives. In this paper, we are interested in proposing a semi-implicit (SI) approach with an IMEX RK setting for solving several types of PDEs with high order spatial derivatives.

We consider a sequence of such PDEs with increasingly higher order derivatives. To simplify the presentation, the PDEs examples below are only one-dimensional equations.

- The second order diffusion problem

$$u_t - (a(u)u_x)_x = 0, \tag{1}$$

where $a(u) \geq 0$ is smooth and bounded and it is a PDE with second order derivatives.

Many PDE of the form (1) which arise in physics or engineering, usually involve the computation of nonlinear diffusion terms, such as: the miscible displacement in porous media [6] which is widely used in the exploration of underground water, oil, and gas, the carburizing model [8] which is derived in the chemical heat treatment in mechanical industry, the high-field model in semiconductor device simulations [9, 10], and so on.

In this paper we also consider one-dimensional version of the convection-diffusion equation

$$u_t + f(u)_x - (a(u)u_x)_x = 0. \tag{2}$$

- The dispersive equation [11, 16] with third derivatives

$$u_t + f(u)_x + (r'(u)g(r(u)_x)_x)_x = 0, \tag{3}$$

where $f(u)$, $r(u)$ and $g(u)$ are arbitrary (smooth) functions. The Korteweg-de Vries (KdV) equation [12] which is widely studied in fluid dynamics and plasma physics, is a special case of Eq. (3) for the choice of the functions $f(u) = u^2$, $g(u) = u$ and $r(u) = u$. The KdV-type equations play an important role in the long-term evolution of initial data [14], are often used

to model the propagation of waves in a variety of nonlinear and dispersive media [13].

Another choice of the functions $f(u) = u^3$, $r(u) = u^2$ and $g(u) = u/2$, gives the so called general KdV equation [16]

$$u_t + (u^3)_x + (u(u_{xx}^2))_x = 0. \tag{4}$$

Eq. (4) is known to have compacton solutions of the form:

$$u(x,t) = \begin{cases} \sqrt{2\lambda}\cos\left(\frac{x-\lambda t}{2}\right), & |x-\lambda t| \le \pi, \\ 0, & \text{otherwise.} \end{cases} \tag{5}$$

Furthermore, Eq. (4) is a particular case of the nonlinear dispersive equation [17]

$$u_t + (u^m)_x + (u(u_{xx}^n))_x = 0, \quad m > 1, \quad m = n + 1, \tag{6}$$

with $m = 3$ and $n = 2$. In the numerical tests section we will consider Eq. (6) with $m = 3$, $n = 2$ and $m = 2$, $n = 1$.

Note that in general, the prototype of nonlinear dispersive equations is the $K(m;n)$ equation (6), introduced by Rosenau and Hyman in [18]. For certain values of m and n, the $K(m;n)$ equation has solitary waves which are compactly supported. These structures, the so-called compactons, have several things in common with soliton solutions of the Korteweg–de Vries (KdV) equation where a nonlinear dispersion term replaces the linear dispersion term in the KdV equation.

- The fourth order diffusion equation

$$u_t + (a(u_x)u_{xx})_{xx} = 0, \tag{7}$$

is a special biharmonic-type equation, where the nonlinearity could be more general but we just present (7) as an example. In this paper we will also concentrate on the one dimensional case biharmonic type equation

$$u_t + f(u)_x + (a(u_x)u_{xx})_{xx} = 0. \tag{8}$$

The fourth order diffusion problem has wide applications in the modeling of thin beams and plates, strain gradient elasticity, and phase separation in binary mixtures [15].

It is well known that the time discretization is a very important issue for time dependent PDEs. For the k-th ($k \ge 2$) order PDEs, explicit methods always suffer from stringent and severe time step restriction, i.e., $\Delta t = \mathcal{O}(\Delta x^k)$, for the stability where Δt is the time step and Δx is the mesh size. This time step is too small, resulting in excessive computational cost and rendering the explicit schemes impractical. On the other hand, implicit methods can overcome the drastic time step size restriction imposed by the stability condition for explicit schemes. However, nonlinear algebraic system must be solved (e.g. by Newton iteration) at each time step.

To cope with both the shortcomings of the explicit and implicit methods, one possible approach is to use implicit-explicit (IMEX) methods. These methods

have been proposed and studied by many authors, for example [2, 4, 25, 3]. IMEX schemes have been successfully applied to various problems, such as convection-diffusion-reaction systems [2, 31, 3], hyperbolic systems with relaxation [25, 5], and collisional kinetic equations [7].

In the case of evolutionary partial differential equations with higher-order derivatives, IMEX methods can be used to treat the different derivative terms differently. Specifically, the higher-order derivative terms are treated implicitly, while the rest of the terms are treated explicitly. Using IMEX methods can help to alleviate the stringent time step restriction and reduce the difficulty of solving algebraic equations when the higher-order derivative terms are linear. However, for equations with nonlinear high derivative terms, IMEX methods may be much more expensive than explicit methods because nonlinear algebraic system must be solved (e.g. by Newton iteration) at each time step. In order to overcome this constraint in [24] the authors introduced the explicit-implicit-null (EIN) time-marching method. This method consists to add and subtract a sufficiently large linear highest derivative term on one side of the considered equation. After that, the linear highest derivative term is treated implicitly, while the remaining term is treated explicitly using an IMEX R-K setting.

In [1] we discuss an alternative approach to [24] for solving time dependent PDEs with high order spatial derivatives by using high order IMEX-RK methods in a much more general context than usually found in the literature, obtaining very effective schemes. The basic idea is to propose a new strategy, called *semi-implicit* (SI), based on IMEX Runge-Kutta methods (SI-IMEX-RK), for the construction of a class of schemes for the solution of equations (1), (2), (6) (7) and (8). Furthermore, in the literature, IMEX-RK schemes have been already used in a SI-IMEX-RK strategy for solving: relaxation problems containing degenerate and/or fully nonlinear diffusion terms [20], a class of degenerate convection-diffusion problems [21, 22], fourth order nonlinear degenerate diffusion equation and surface diffusion of graph, [23].

The above strategy is really convenient and useful in the case in which we have a linearly implicit evaluation for the unknown variable in the term involving high order spatial derivatives, as in equations (1), (2), (6), (7) and (8). The linearly implicit evaluation is the key to the methods working for our problems. However, in other cases for time-dependent PDEs with fully nonlinear high order spatial derivatives, as for example equation (3), the approach proposed in [24] is more suitable.

In order to apply the SI-IMEX-RK idea, we take the nonlinear diffusion equation (1) as an example to introduce the approach in detail. Assume that the semi-discrete formulation of (1) can be written as

$$\frac{dU(t)}{dt} = \frac{1}{\Delta x^2}\mathcal{B}(U(t))U(t), \tag{9}$$

where $U(t) = (U_1(t), U_2(t), ..., U_M(t))^T$, with $U_i(t)$ is the approximate solution at spatial position x_i for $i = 1, ..., M$, i.e., $U_i(t) \approx (u(x_i, t)$, for $i = 1, ..., M$, and uniform grid spacing $\Delta x_i = x_{i+1} - x_i$. $\mathcal{B} \in R^{M\times M}$ is a tridiagonal matrix

arising from the discretization of $(a(u)u_x)_x$. Here we emphasize that the matrix $\mathcal{B}$ inherits its discontinuous dependence on U from that of $a(u)$ on u. The SI-IMEX-RK approach is based in choosing the time discretization by an implicit and explicit RK scheme, respectively, of an IMEX pair of schemes accordingly. Roughly speaking, in the product $\mathcal{B}(U)U$ the implicit treatment is applied only to that second factor U, while the nonlinear term $\mathcal{B}(U)$ is treated explicitly. This approach does not require solutions for nonlinear systems since the new methods require only solving a discretized diffusion equation with a linear diffusion term in which the matrix $\mathcal{B}(U)$ is given.

An advantage of this approach with respect to [24] is that we can use different types of IMEX-RK schemes already exiting in the literature. In [24] the drawback in the technique of adding and subtracting the same term on one side of the considered equation is that the constant that stabilizes the scheme depends on the specific type of IMEX RK method selected. In [1] we showed several examples of equations of the form (1), (2), (6) (7) and (8) that can be efficiently solved with the SI-IMEX-RK approach, choosing different IMEX RK tableaux.

Finally, we coupled high order finite difference schemes with high-order SI-IMEX-RK time discretization for solving diffusion (1) (2), dispersive (6) and fourth order diffusion equations (7) (8), respectively. We choose the finite difference schemes to discretize the space because of its simplicity in design and coding. However, other type of space discretization can be considered as local discontinuous Galerkin schemes [26] with application to various high order PDEs, [16, 27, 28, 19, 29, 11, 30].

References

[1] S. Boscarino, *High-Order Semi-implicit Schemes for Evolutionary Partial Differential Equations with Higher Order Derivatives*, J. Sci. Comput., **96** (2023).

[2] U. M. Ascher, S. J. Ruuth, and R. J. Spiteri, *Implicit-explicit Runge-Kutta methods for time-dependent partial differential equations*, Appl. Numer. Math. **25** (1997), 151–167.

[3] M. P. Calvo, J. D. Frutos, and J. Novo, *Linearly implicit Runge-Kutta methods for advection-reaction-diffusion equations*, Appl. Numer. Math. **37** (2001), 535–549.

[4] C. A. Kennedy and M. H. Carpenter. *Additive Runge–Kutta schemes for convection–diffusion–reaction equations*, Appl. Numer. Math. **44** (2003), 139–181.

[5] S. Boscarino and G. Russo. *On a class of uniformly accurate IMEX Runge–Kutta schemes and applications to hyperbolic systems with relaxation* SIAM J. Sci. Comput. **31** (2009), 1926–1945.

[6] R. E. Ewing and M. F. Wheeler, *Galerkin methods for miscible displacement problems in porous media.* SIAM J. Numer. Anal., **17** (1980), 351–365.

[7] G. Dimarco and L. Pareschi, *Asymptotic preserving implicit-explicit Runge–Kutta methods for nonlinear kinetic equations*, SIAM J. Numer. Anal. **51.2** (2013), 1064–1087.

[8] P. Cavaliere, G. Zavarise, and M. Perillo, *Modeling of the carburizing and nitriding processes*, Comp Mater Sci, **46** (2009), 26–35.

[9] C. Cercignani, I. M. Gamba, J. W. Jerome, and C.-W. Shu,*Device benchmark comparisons via kinetic, hydrodynamic, and high-field models*, Comput Methods Appl Mech Engrg, **181** (2000), 381–392.

[10] C. Cercignani, I. M. Gamba, and C. D. Levermore, *High field approximations to Boltzmann-Poisson system boundary conditions in a semiconductor*, Appl Math Lett, **10** (1997), 111–117.

[11] J. Yan and C.-W. Shu, *A local discontinuous Galerkin method for KdV type equations*, SIAM J. Numer. Anal. **40** (2002), 769–791.
[12] D. J. Korteweg and G. De Vries, *On the change of form of long waves advancing in a rectangular canal, and on a new type of long stationary waves*, Philos. Mag. **91** (2011), 1007–1028.
[13] T. B. Benjamin, J. L. Bona, and J. J. Mahony, *Model equations for long waves in nonlinear dispersive systems*, Philos. Trans. R. Soc. Lond. Ser. A, Math. Phys. Sci. **272** (1972), 47–78.
[14] J. L. Bona, K. S. Promislow, and C. E. Wayne, *Higher-order asymptotics of decaying solutions of some nonlinear, dispersive, dissipative wave equations*, Non-linearity **8** (1995), 1179–1206.
[15] S. M. Han, H. Benaroya, and T. Wei, *Dynamics of transversely vibrating beams using four engineering theories*, Journal of Sound and Vibration, **v225** (1999), 935–988.
[16] D. Levy, C.-W. Shu, and J. Yan, *Local discontinuous Galerkin methods for nonlinear dispersive equations*, J. Comput. Phys. **196** (2004), 751–772.
[17] A. Chertock and D. Levy, *Particle methods for dispersive equations*, J. Comput. Phys., **171** (2001), 708–730.
[18] P. Rosenau, and J. M. Hyman, *Compactons: solitons with finite wavelength*, Phys. Rev. Lett., **70** (1993), 564–567.
[19] H. Wang, Q. Zhang, S. Wang, and C-W. Shu,*Local discontinuous Galerkin methods with explicit-implicit-null time discretizations for solving nonlinear diffusion problems*, Science China Mathematics, **63** (2020), 187–208.
[20] S. Boscarino, F. G. LeFloch, and G. Russo *High-order asymptotic-preserving methods for fully nonlinear relaxation problems*, SIAM J. Sci. Comput., **36** (2014), A377-A395
[21] S. Boscarino, R. Bürger, P. Mulet, G. Russo, and L. M. Villada, *Linearly implicit IMEX Runge–Kutta methods for a class of degenerate convection-diffusion problems*, SIAM J. Sci. Comput., **37** (2015), B305–B331.
[22] S. Boscarino, R. Bürger, P. Mulet,G. Russo, and L. M. Villada, *On linearly implicit IMEX Runge-Kutta methods for degenerate convection-diffusion problems modeling polydisperse sedimentation*. Bulletin of the Brazilian Mathematical Society, New Series, **47** (2016), 171-185.
[23] S. Boscarino, F. Filbet, and G. Russo, *High Order Semi-implicit Schemes for time dependnet Partial Differential Equations*, J. Sci. Comput., **68** (2016), 975–100.
[24] M. Tan, J. Cheng, and C.-W. Shu,*Stability of high order finite difference and local discontinuous Galerkin schemes with explicit-implicit-null time-marching for high order dissipative and dispersive equations*, J. Comput. Phys. **464** (2022).
[25] L. Pareschi and G. Russo, *Implicit–explicit Runge–Kutta schemes and applications to hyperbolics ystems with relaxations*, J. Sci. Comput., **25** (2005), 129–155.
[26] B. Cockburn and C.-W. Shu, *The local discontinuous Galerkin method for time-dependent convection-diffusion systems*, SIAM J. Numer. Anal., **35** (1998), 2440–2463.
[27] H. Shi and Y. Li, *Local discontinuous Galerkin methods with implicit-explicit multistep time-marching for solving the nonlinear Cahn-Hilliard equation*, J. Comput. Phys., **394** (2019), 719–731.
[28] Q. Tao, Y. Xu, and C.-W. Shu, *An ultraweak-local discontinuous Galerkin method for PDEs with high order spatial derivatives*, Math. Comput. **89** (2020), 2753–2783.
[29] Y. Xu and C.-W Shu, *Local discontinuous Galerkin methods for the Kuramoto-Sivashinsky equations and the Ito-type coupled KdV equations*, Comput. Methods Appl. Mech. Eng. **195** (2006), 3430–3437.
[30] J. Yan and C.-W. Shu, *Local discontinuous Galerkin methods for partial differential equations with higher order derivatives*, J. Sci. Comput. **17** (2002), 1–4.
[31] W. Hundsdorfer and J. Verwer, *Numerical solution of time-dependent advection-diffusion-reaction equations*, **33** (2003), Berlin: Springer.

New High-Order Numerical Methods for Hyperbolic Systems of Nonlinear PDEs with Uncertainties

Alina Chertock

(joint work with Michael Herty, Arsen S. Iskhakov, Safa Janajra, Alexander Kurganov, and Mária Lukáčová-Medvid'ová)

Many important scientific problems contain sources of uncertainties in parameters, initial and boundary conditions (ICs and BCs), etc. In partial differential equations (PDEs), uncertainties may be described with the help of random variables. In this paper, the focus is placed on hyperbolic systems of conservation and balance laws with uncertainties. Such systems read as

$$\boldsymbol{U}_t + \nabla_{\boldsymbol{x}} \cdot \boldsymbol{F} = \boldsymbol{S}, \tag{1}$$

where $\boldsymbol{U}(\boldsymbol{x}, t, \boldsymbol{\xi}) \in \mathbb{R}^N$ is an unknown vector-function, $\boldsymbol{F}(\boldsymbol{U}) : \mathbb{R}^N \to \mathbb{R}^N$ are the flux functions, and $\boldsymbol{S}(\boldsymbol{U}, \boldsymbol{x}, \boldsymbol{\xi})$ is a source term. Furthermore, t is time, and $\boldsymbol{x} \in \mathbb{R}^d$ are spatial variables. Without loss of generality, we assume that $\boldsymbol{\xi} \in \Xi \subset \mathbb{R}^s$ are real-valued random variables. We denote by $(\Xi, \mathcal{F}, \nu)$ the underlying probability space, where Ξ is a set of events, $\mathcal{F}(\Xi)$ is the σ-algebra of Borel measurable sets, and $\nu(\boldsymbol{\xi}) : \Xi \to \mathbb{R}_+$ is the probability density function (PDF), $\nu \in L^1(\Xi)$.

The system (1) arises in many applications, including fluid dynamics, geophysics, electromagnetism, meteorology, and astrophysics, to name a few. Quantifying uncertainties that appear as input quantities, as well as in the ICs and BCs due to empirical approximations or measuring errors, is essential as it helps to perform sensitivity analysis and provides guidance to improve models.

Several numerical methods have already been developed for (1). Monte Carlo-type methods are reliable but not computationally efficient due to the large number of realizations required to approximate statistical moments accurately. Another widely used approach for solving (1) is the generalized polynomial chaos (gPC), where the solution is sought in terms of a series of orthogonal polynomials with respect to the probability density in $\boldsymbol{\xi}$; see, e.g., [13]. There are two types of gPC methods: intrusive and non-intrusive ones. In non-intrusive algorithms, such as stochastic collocation (gPC-SC) methods, one seeks to satisfy the governing equations at a discrete set of nodes in the random space, employing the same numerical solver as for the deterministic problem and then using interpolation and quadrature rules to evaluate statistical moments numerically. In intrusive approaches, such as stochastic Galerkin (gPC-SG) methods, the gPC expansions are substituted into the governing equations and projected by a Galerkin approximation to obtain deterministic equations for the expansion coefficients. Solving the coefficient equations yields the statistical moments of the original uncertain problem solution.

Several challenges are associated with applying the gPC-SC and gPC-SG methods to nonlinear hyperbolic systems (1). It is well-known that spectral-type gPC-based methods exhibit fast convergence when the solution depends smoothly on the random parameters. However, one of the main problems in using these methods is related to the lack of smoothness of their solutions, which may break down

in finite time due to the development of shock and contact waves. Although these discontinuities appear in spatial variables, their propagation speed can be affected by uncertainty, causing discontinuities in random variables and triggering aliasing errors and Gibbs-type phenomena. Another open question in gPC-based stochastic methods is the representation of strictly positive quantities such as gas density or water depth and/or the enforcement of discrete bound-preserving constraints. It can also be shown that the gPC-based methods, which are highly accurate for moment estimation, might fail to approximate PDF, even for one-dimensional (1-D) noise [4]. An additional numerical difficulty associated with implementing the gPC-SG methods is posed by the fact that the deterministic Jacobian of the projected system differs from the random Jacobian of the original system. Therefore, when applied to general nonlinear hyperbolic systems, the gPC-SG method results in a system for expansion coefficients, which is not necessarily globally hyperbolic [3]. Consequently, additional effort is needed to develop stable numerical methods for (potentially ill-posed) systems for the gPC coefficients.

In this talk, we present a new approach in which we conduct the approximation in the random space using weighted essentially non-oscillatory (WENO) interpolants rather than orthogonal polynomial expansions, which are highly oscillatory in the case of nonsmooth solutions. The new approach is realized in the semi-discrete finite-volume framework. The system (1) is integrated over the $(\boldsymbol{x}, \boldsymbol{\xi})$-cells and the solution is obtained in terms of cell averages, which are evolved in time using numerical fluxes in the $\boldsymbol{x}$-directions. These fluxes are evaluated with the help of a second-order piecewise linear reconstruction in $\boldsymbol{x}$ and a Gauss-Legendre quadrature in $\boldsymbol{\xi}$ implemented using high-order WENO interpolants. This allows one to achieve high accuracy in $\boldsymbol{\xi}$ even in the generic case of discontinuous solutions. We refer the reader to related work in [1, 2, 6, 10, 11], where a similar idea has been used in the framework of stochastic finite-volume methods. In this work, we implement a second-order finite-volume method in physical space. It is combined with a high-order WENO interpolation in the random space. Notice that by using a high-order WENO interpolation, we not only keep a high-order approximation in the random space but also properly (without the Gibbs phenomenon) resolve discontinuities that may propagate into the random directions.

The new family of methods may use different numerical fluxes, piecewise-linear reconstructions, and high-order interpolations. A particular choice made in this work is the following. We use the Riemann-problem-solver-free central-upwind (CU) fluxes introduced in [7, 8]; the generalized minmod reconstruction in $\boldsymbol{x}$; the fifth-order Gauss-Legendre quadrature; and the recently proposed fifth-order affine-invariant WENO-Z (Ai-WENO-Z) interpolation in $\boldsymbol{\xi}$ (see [5, 9, 12]), which is a stabilized version of the original WENO-Z interpolation. It should be observed that the lack of BCs in the random space imposes an additional difficulty, as it requires the development of a special high-order interpolation technique near the boundary. We overcome this difficulty by designing a new one-sided Ai-WENO-Z interpolation. In addition, we restrict our consideration to the simplest 1-D case ($d = s = 1$) and two higher-dimensional extensions ($d = 1$, $s = 2$ and $d = 2$,

$s = 1$). We test the resulting scheme on several numerical examples for the Euler equations of gas dynamics and the Saint-Venant system of shallow water equations, both considered with different probability densities in random variables. For the shallow water application, we enforce the well-balanced (WB) property, that is, to make the scheme capable of exactly preserving "lake-at-rest"/still-water steady-state solutions.

References

[1] R. Abgrall and S. Mishra, *Uncertainty quantification for hyperbolic systems of conservation laws*, Handbook of numerical methods for hyperbolic problems, Handb. Numer. Anal., vol. 18, Elsevier/North-Holland, Amsterdam, (2017), 507–544.

[2] R. Abgrall and S. Tokareva, *The stochastic finite volume method*, Uncertainty quantification for hyperbolic and kinetic equations, SEMA SIMAI Springer Ser., vol. 14, Springer, Cham, (2017), 1–57.

[3] B. Després, G. Poëtte, and D. Lucor, *Robust uncertainty propagation in systems of conservation laws with the entropy closure method*, Uncertainty quantification in computational fluid dynamics, Lect. Notes Comput. Sci. Eng., vol. 92, Springer, Heidelberg, (2013), 105–149.

[4] A. Ditkowski, G. Fibich, and A. Sagiv, *Density estimation in uncertainty propagation problems using a surrogate model*, SIAM/ASA J. Uncertain. Quantif. **8** (2020), no. 1, 261–300.

[5] W. S. Don, R. Li, B.-S. Wang, and Y. H. Wang, *A novel and robust scale-invariant WENO scheme for hyperbolic conservation laws*, J. Comput. Phys. **448** (2022), Paper No. 110724, 23 pp.

[6] G. Geraci, P. M. Congedo, R. Abgrall, and G. Iaccarino, *A novel weakly-intrusive non-linear multiresolution framework for uncertainty quantification in hyperbolic partial differential equations*, J. Sci. Comput. **66** (2016), 358–405.

[7] A. Kurganov, S. Noelle, and G. Petrova, *Semidiscrete central-upwind schemes for hyperbolic conservation laws and Hamilton-Jacobi equations*, SIAM J. Sci. Comput. **23** (2001), 707–740.

[8] A. Kurganov and G. Petrova, *A second-order well-balanced positivity preserving central-upwind scheme for the Saint-Venant system*, Commun. Math. Sci. **5** (2007), 133–160.

[9] P. Li, T. T. Li, W. S. Don, and B.-S. Wang, *Scale-invariant multi-resolution alternative WENO scheme for the Euler equations*, J. Sci. Comput. (2023), Paper No. 15, 32 pp.

[10] M. Petrella, S. Tokareva, and E. F. Toro, *Uncertainty quantification methodology for hyperbolic systems with application to blood flow in arteries*, J. Comput. Phys. **386** (2019), 405–427.

[11] S. Tokareva, A. Zlotnik, and V. Gyrya, *Stochastic finite volume method for uncertainty quantification of transient flow in gas pipeline networks*, Appl. Math. Model. **125** (2024), no. part B, 66–84.

[12] B.-S. Wang and W. S. Don, *Affine-invariant WENO weights and operator*, Appl. Numer. Math. **181** (2022), 630–646.

[13] D. Xiu, *Numerical methods for stochastic computations*, Princeton University Press, Princeton, NJ, 2010, A spectral method approach.

Space Dependent Conservation Laws and Hamilton-Jacobi Equations

Rinaldo M. Colombo
(joint work with Vincent Perrollaz, Abraham Sylla)

We are concerned with conservation laws and Hamilton - Jacobi equations

$$\partial_t u + \partial_x H(x,u) = 0 \qquad \partial_t U + H(x, \partial_x U) = 0 \tag{1}$$

in the scalar one dimensional case. The problems we address are:

(1) well posedness;
(2) correspondence between the solutions to the 2 equations;
(3) characterization of attainable sets and inverse design.

The explicit presence of the x variable in the flux/Hamiltonian H has a deep influence on a variety of properties of the solutions to the equations in (1), see [12] for a somewhat surprising example.

1. Well Posedness

A huge literature is devoted to the existence, uniqueness and continuous dependence on initial data of the solutions to the Cauchy problems

$$\textbf{(CL)} \quad \begin{cases} \partial_t u + \partial_x H(x,u) = 0 \\ u(0,x) = u_o(x) \end{cases} \qquad \textbf{(HJ)} \quad \begin{cases} \partial_t U + H(x, \partial_x U) = 0 \\ U(0,x) = U_o(x) \end{cases}$$

where $t \in \mathbb{R}_+$ and $x \in \mathbb{R}$. As sample references, in the case of **(CL)** we recall [6, 14, 16, 19] while **(HJ)** is considered, for instance, in [4, 5, 13, 17]. However, only in few cases are these results obtained under the *same* assumptions for the 2 equations, see [8] for the x independent case.

A unique framework where both Cauchy problems **(CL)** and **(HJ)** are well posed is established in [9]. The assumptions defining this framework are:

(C3) **Smoothness** : $H \in \mathbf{C}^3(\mathbb{R}^2; \mathbb{R})$.

(CNH) **Compact NonHomogeneity** : $\exists\, X > 0 \colon \forall\, (x,u) \in \mathbb{R}^2$ if $|x| > X$ then $\partial_x H(x,u) = 0$

(UC) **Uniform Coercivity** : $\forall\, h \in \mathbb{R}\ \exists\, \mathcal{U}_h \in \mathbb{R} \colon \forall\, (x,u) \in \mathbb{R}^2$ if $|H(x,u)| \leq h$ then $|u| \leq \mathcal{U}_h$

(WGNL) **Weak Genuine NonLinearity** : for a.e. $x \in \mathbb{R}$ the set $\left\{w \in \mathbb{R} \colon \partial^2_{ww} H(x,w) = 0\right\}$ has empty interior

Note that no convexity assumption is required. Indeed, **(WGNL)** allows also the presence of a convergent sequence of inflection points of the map $u \mapsto H(x,u)$. Moreover, in the case of conservation laws, the above assumptions allow to consider fluxes that do not meet all the classical Kružkov requirements in [19], see [9, Example 1.1]. Technically, among the above assumptions, it seems that **(UC)** is the hardest one to be weakened, if possible.

Under the assumptions **(C3)**-**(CNH)**-**(UC)**-**(WGNL)** entirely specular well posedness theorems for **(CL)** and **(HJ)** can be stated, see [9, Theorem 2.18] and [9, Theorem 2.19]. Indeed, these results yield Lipschitz continuous semigroups

$$S^{CL}\colon \mathbb{R}_+ \times \mathbf{L}^\infty(\mathbb{R};\mathbb{R}) \to \mathbf{L}^\infty(\mathbb{R};\mathbb{R}) \quad \text{and} \quad S^{HJ}\colon \mathbb{R}_+ \times \mathbf{Lip}(\mathbb{R};\mathbb{R}) \to \mathbf{Lip}(\mathbb{R};\mathbb{R})$$

whose orbits are weak entropy solutions to **(CL)** and viscosity solutions to **(HJ)**.

Technically, the difficulty of providing *a priori* $\mathbf{L}^\infty$ bounds on solutions to **(CL)** is overcome providing a sufficient endowment of stationary solutions, see [11].

2. Correspondence between the Solutions to (CL) and (HJ)

If U is a *smooth* solution to Hamilton-Jacobi equation with Hamiltonian H, it is evident that $\partial_x U$ solves the conservation law with flux H. However, when dealing with weak entropy solutions to **(CL)** and with viscosity solutions to **(HJ)**, exhibiting a rigorous correspondence is not immediate. The case where H does not depend on x was closed in [8], following the previous results obtained in [18], see also [7]. Under the assumptions **(C3)**-**(CNH)**-**(UC)**-**(WGNL)**, [9, Theorem 2.20] proves that the following diagrams commute in the general — x dependent — case (1):

$$\begin{array}{ccc} U_o & \longrightarrow & S_t^{HJ}U_o \\ {\scriptstyle \partial_x}\downarrow & & \downarrow{\scriptstyle \partial_x} \\ u_o & \longrightarrow & S_t^{CL}u_o \end{array} \qquad\qquad \begin{array}{ccc} U_o & \longrightarrow & S_t^{HJ}U_o \\ {\scriptstyle \int^x}\uparrow & & \uparrow \\ u_o & \longrightarrow & S_t^{CL}u_o \end{array} \quad \text{[9, Formula (2.28)]}$$

Remarkably, it turns out that the stability properties of the two semigroups are not in full correspondence, see [9] for details.

3. Characterization of Attainable Sets and Inverse Design

Given $T > 0$ and profiles $w \in \mathbf{L}^\infty(\mathbb{R};\mathbb{R})$, $W \in \mathbf{Lip}(\mathbb{R};\mathbb{R})$, consider the sets

$$\begin{aligned} I_T^{CL}(w) &= \left\{u_o \in \mathbf{L}^\infty(\mathbb{R};\mathbb{R})\colon S_T^{CL}u_o = w\right\}, \\ I_T^{HJ}(W) &= \left\{U_o \in \mathbf{Lip}(\mathbb{R};\mathbb{R})\colon S_T^{HJ}U_o = W\right\}. \end{aligned}$$

Characterizing those w, resp. W, such that $I_T^{CL}(w) \neq \emptyset$, resp. $I_T^{HJ}(W) \neq \emptyset$, is the characterization of the *attainable set* for **(CL)**, resp. **(HJ)**. By *inverse design* we refer to the problem of characterizing the set $I_T^{CL}(w)$, resp. $I_T^{HJ}(W)$. Results in this direction were obtained by several authors, see for instance [1, 2, 3, 8, 15, 20].

Substituting both **(UC)** and **(WGNL)** with the (stronger) condition

(**CVX**) **Strong Convexity:** $\forall x \in \mathbb{R},\ p \mapsto \partial_p H(x,p)$ is an increasing $\mathbf{C}^1-$diffeomorphism of $\mathbb{R}$ onto itself

a full characterization of the attainable set for **(HJ)** is presented in [10, Theorem 3.2]. This is obtained through an explicit construction based on the connections of **(HJ)** to the optimal control of ODEs. It is then possible to explicitly characterize $I_T^{HJ}(W)$, see [10, Theorem 3.3]. Note however that, differently from the x independent case considered in [8], the set $I_T^{CL}(w)$ apparently does not admit a simple direct characterization.

As a consequence of these results one proves that $I_T^{CL}(w)$ is a closed cone (with respect to the $\mathbf{L^1_{loc}}$ topology). This seemingly fundamental property currently lacks an *a priori* justification, also at an heuristic level.

References

[1] F. Ancona and M. T. Chiri, *Attainable profiles for conservation laws with flux function spatially discontinuous at a single point*, ESAIM Control Optim. Calc. Var., **26** (2020), Paper No. 124, 33.

[2] F. Ancona and A. Marson, *On the attainable set for scalar nonlinear conservation laws with boundary control*, SIAM J. Control Optim., **36** (1) (1998), 290–312.

[3] B. Andreianov, C. Donadello, S. S. Ghoshal, and U. Razafison, *On the attainable set for a class of triangular systems of conservation laws*, J. Evol. Equ., **15** (2015), 503–532.

[4] M. Bardi and I. Capuzzo-Dolcetta, *Optimal control and viscosity solutions of Hamilton-Jacobi-Bellman equations*, Springer Science & Business Media, 2008.

[5] G. Barles, *An introduction to the theory of viscosity solutions for first-order Hamilton-Jacobi equations and applications*,In *Hamilton-Jacobi equations: approximations, numerical analysis and applications*, Springer, (2013), 49–109.

[6] A. Bressan, *Hyperbolic systems of conservation laws*, volume 20 of *Oxford Lecture Series in Mathematics and its Applications*, Oxford University Press, Oxford, 2000.

[7] G. M. Coclite and N. H. Risebro, *Viscosity solutions of Hamilton-Jacobi equations with discontinuous coefficients*, J. Hyperbolic Differ. Equ., **4** (2007), 771–795.

[8] R. M. Colombo and V. Perrollaz, *Initial data identification in conservation laws and Hamilton-Jacobi equations*, J. Math. Pures Appl. **138** (2020), 1–27.

[9] R. M. Colombo, V. Perrollaz, and A. Sylla, *Conservation laws and Hamilton–Jacobi equations with space inhomogeneity*, J. Evol. Equ., **23** (2023), 1–72.

[10] R. M. Colombo, V. Perrollaz, and A. Sylla, *Initial data identification in space dependent conservation laws and Hamilton-Jacobi equations*, 2023, arXiv, math.AP 2304.05092.

[11] R. M. Colombo, V. Perrollaz, and A. Sylla, $\mathbf{L}^\infty$ *stationary solutions to non homogeneous conservation laws*, To appear, Proceedings of the XVIII International Conference on Hyperbolic Problems: Theory, Numerics, Applications.

[12] R. M. Colombo, V. Perrollaz, and A. Sylla, *Peculiarities of space dependent conservation laws: Inverse design and asymptotics*, To appear, Proceedings of the XVIII International Conference on Hyperbolic Problems: Theory, Numerics, Applications.

[13] M. G. Crandall and P.-L. Lions, *Viscosity solutions of Hamilton-Jacobi equations*, Trans. Amer. Math. Soc., **277** (1983), 1–42.

[14] C. M. Dafermos, *yperbolic conservation laws in continuum physics*, volume 325 of *Grundlehren der mathematischen Wissenschaften [Fundamental Principles of Mathematical Sciences]*, Springer-Verlag, Berlin, fourth edition, 2016.

[15] C. Esteve-Yagüe and E. Zuazua, *Reachable set for Hamilton-Jacobi equations with non-smooth Hamiltonian and scalar conservation laws*, Nonlinear Anal., **227** (2023), Paper No. 113167, 18.

[16] H. Holden and N. H. Risebro, *Front tracking for hyperbolic conservation laws*, volume 152 of Applied Mathematical Sciences, Springer, Heidelberg, second edition, 2015.

[17] H. Ishii, *Uniqueness of unbounded viscosity solution of Hamilton-Jacobi equations*, Indiana Univ. Math. J., **33** (1984), 721–748.

[18] K. H. Karlsen and N. H. Risebro, *A note on front tracking and equivalence between viscosity solutions of Hamilton-Jacobi equations and entropy solutions of scalar conservation laws*, Nonlinear Anal., **50**(4, Ser. A: Theory Methods) (2002), 455–469.

[19] S. N. Kruzhkov, *First order quasilinear equations with several independent variables*, Mathematics of the USSR-Sbornik, **81** (1970), 228–255.

[20] T. Liard and E. Zuazua, *Initial data identification for the one-dimensional Burgers equation*, IEEE Trans. Automat. Control, **67** (2022), 3098–3104.

On well-balanced finite volume and discontinuous Galerkin schemes for the Einstein-Euler system of general relativity

Michael Dumbser

(joint work with Olindo Zanotti, Ilya Peshkov, Elena Gaburro, Gabriella Puppo)

In this talk we present a new family of well-balanced discontinuous Galerkin (DG) finite element schemes with subcell finite volume (FV) limiter for the numerical solution of the Einstein–Euler equations of general relativity based on a first order hyperbolic reformulation of the Z4 formalism. The first order Einstein-Euler Z4 system, which is composed of 64 equations, is analysed and proven to be strongly hyperbolic for a general metric. The well-balancing is achieved for arbitrary but *a priori* known equilibria by subtracting a discrete version of the equilibrium solution from the discretized time-dependent PDE system. Special care has also been taken in the design of the numerical viscosity so that the well-balancing property is achieved. As for the treatment of low density matter, e.g. when simulating massive compact objects like neutron stars surrounded by vacuum, we have introduced a new filter in the conversion from the conserved to the primitive variables, preventing superluminal velocities when the density drops below a certain threshold, and being potentially also very useful for the numerical investigation of highly rarefied relativistic astrophysical flows.

We furthermore present a novel family of central WENO finite difference schemes for a new first order reformulation of the classical BSSNOK system.

Thanks to these improvements, all standard tests of numerical relativity are successfully reproduced, reaching four main achievements: (i) we are able to obtain stable long term simulations of stationary black holes, including Kerr black holes with extreme spin, which after an initial perturbation return perfectly back to the equilibrium solution up to machine precision; (ii) a (standard) TOV star under perturbation is evolved in pure vacuum ($\rho = p = 0$) up to $t = 1000$ with no need to introduce any artificial atmosphere around the star; and, (iii) we solve the head on collision of two punctures black holes, that was previously considered untractable within the FO-Z4 formalism, (iv) we perform a stable long-time evolution of a rotating binary black hole merger based on the new CWENO schemes for first order reformulation of the BSSNOK system.

References

[1] M. Dumbser, O. Zanotti, E. Gaburro, and I. Peshkov, *A well-balanced discontinuous Galerkin method for the first-order Z4 formulation of the Einstein–Euler system*, Journal of Computational Physics **504** (2024), 112875.

[2] M. Dumbser, O. Zanotti, and G. Puppo, *A monolithic first–order BSSNOK formulation of the Einstein–Euler equations and its solution with conservative finite difference CWENO schemes*, Physical Review D, in preparation.

Monte Carlo method and the isentropic Euler system

Eduard Feireisl

(joint work with Mária Lukáčová-Medvid'ová, Hana Mizerová)

We consider one of the iconic examples of hyperbolic systems in fluid dynamics – the Euler system – in its simplified isentropic version:

$$\partial_t \rho + \nabla \cdot (\rho \vec{u}) = 0, \tag{1}$$

$$\partial_t (\rho \vec{u}) + \nabla \cdot (\rho \vec{u} \otimes \vec{u}) + a \nabla \rho^\gamma = 0,\ a > 0,\ \gamma > 1$$

supplemented with the physically relevant impermeability conditions

$$\vec{u} \cdot \vec{n}|_{\partial\Omega} = 0.$$

The problem is closed by prescribing the initial state

$$\rho(0, \cdot) = \rho_0,\ \rho \vec{u}(0, \cdot) = \rho_0 \vec{u}_0.$$

The Euler system features the well known mathematical difficulties summarized in the following list of "bad" and "good" news:

- **Good:** The problem is (locally) well–posed in a class of Sobolev data of high regularity.
- **Bad:** "Many" solutions develop singularities after a finite time – shock waves (standard), implosions (new results [4] and others).

- **Good:** Weak solutions exist globally in time for any sufficiently smooth initial data (or Riemann data).
- **Bad:** There infinitely many weak solutions for given initial data (without imposing any admissibility conditions), see the pioneering paper [2] and many more recent related results.

- **Good:** Admissible solutions (satisfying some form of energy inequality) satisfy the weak–strong uniqueness principle. In particular, the Euler system is locally well posed in the class of weak solutions if the data are smooth enough.
- **Bad:** The set of "wild" initial data giving rise to infinitely many *admissible* weak solutions (on arbitrarily short time interval) is dense in L^p, see [1].

Our main objective is to study convergence of numerical methods with uncertain data, specifically the Monte–Carlo method. We consider the class of generalized dissipative solutions satisfying

$$\partial_t \rho + \nabla \cdot \vec{m} = 0,\ \vec{m} \equiv \rho \vec{u},$$

$$\partial_t \vec{m} + \nabla \cdot \left(\frac{\vec{m} \otimes \vec{m}}{\rho} \right) + a \nabla \rho^\gamma = -\nabla \cdot \mathfrak{R},$$

$$\frac{\mathrm{d}}{\mathrm{d}t} E(t) \leq 0,\ E(t) \leq E_0,\ E_0 = \int_\Omega \left[\frac{1}{2} \frac{|\vec{m}_0|^2}{\rho_0} + \frac{a}{\gamma - 1} \rho^\gamma \right]\ dx,$$

$$E \equiv \int_\Omega \left[\frac{1}{2} \frac{|\vec{m}|^2}{\rho} + \frac{a}{\gamma - 1} \rho^\gamma \right]\ dx + c(\gamma) \int_{\overline{\Omega}} \mathrm{d}\ \mathrm{trace}[\mathfrak{R}],$$

with the energy defect represented by **Reynolds stress**

$$\mathfrak{R} \in L^\infty(0,T;\mathcal{M}^+(\overline{\Omega};R^{d\times d}_{\rm sym})).$$

The dissipative solutions can be "identified" with limits of consistent (numerical) approximations of the original Euler system, see [3].

As the Euler system is essentially ill–posed, our approach is based on multivalued solution mappings and abstract version of the Strong law of large numbers in this framework. Specifically, we consider the mapping

$$(\rho_0,\vec{m}_0) \in (\text{data space}) \mapsto \mathcal{U}(\rho_0,\vec{m}_0) \subset \mathcal{T} \text{ (trajectory space)},$$

$$\mathcal{U}(\rho_0,\vec{m}_0) = \Big\{(\rho,\vec{m}) \in \mathcal{T} \ \Big|\ (\rho,\vec{m}) \text{ a dissipative solution of the Euler system,}\ (\rho,\vec{m})(0,\cdot) = (\rho_0,\vec{m}_0)\Big\}$$

Here, the trajectory space

$$\mathcal{T} = \Big\{(\rho,\vec{m}) \ \Big|\ (\rho,\vec{m}) \in C_{\rm weak}([0,T];L^\gamma(\Omega)\times L^{\frac{2\gamma}{\gamma+1}}(\Omega;R^d))\Big\}$$

is endowed either with the strong topology

$$\mathcal{T}_{\rm strong} \hookrightarrow L^q((0,T)\times\Omega;R^{d+1}),\ 1<q\leq \frac{2\gamma}{\gamma+1} = \min\left\{\gamma;\frac{2\gamma}{\gamma+1}\right\}$$

or with the weak topology

$$\mathcal{T}_{\rm weak} \hookrightarrow C([0,T];W^{-\ell,2}(\Omega;R^{d+1})),\ \ell > d.$$

We claim the following results concerning convergence of the Monte–Carlo method applied to random consistent approximations of the Euler system:

Monte–Carlo method, weak form: Suppose $(\rho_{0,n},\vec{m}_{0,n})_{n=1}^\infty$ is a family of pairwise i.i.d. copies of initial data $(\rho_0,\vec{m}_0)$ satisfying

$$\frac{1}{L} \leq \rho_0(x) \leq L,\ |\vec{m}_0(x)| \leq L \text{ for a.a. } x\in\Omega.$$

with a deterministic constant L.

Let $(\vec{U}_h)_{h>0}$, $\vec{U}_h = (\rho_n,\vec{m}_h)$ be a consistent approximation.

Then

$$\mathbb{E}\left[{\rm dist}_{W^{-\ell,2}((0,T)\times\Omega;R^{d+1})}\left[\frac{1}{N}\sum_{n=1}^N \vec{U}_h(\rho_{0,n},\vec{m}_{0,n});\mathbb{E}\Big[\mathcal{U}(\rho_0,\vec{m}_0)\Big]\right]\right] \to 0$$

as $h\to 0$, $N\to\infty$ for any $\ell > d+1$.

Monte–Carlo method, strong form: Suppose $(\rho_{0,n},\vec{m}_{0,n})_{n=1}^\infty$ are a pairwise i.i.d. representations of random data $(\rho_0,\vec{m}_0)$ satisfying

$$\frac{1}{L} \leq \rho_0(x) \leq L,\ |\vec{m}_0(x)| \leq L \text{ for a.a. } x\in\Omega$$

with a deterministic constant L.

Let $(\vec{U}_h)_{h>0}$ be a consistent approximation of the Euler system.

Then any sequence $h_m \to 0$ contains a subsequence $(h_{m_k})_{k=1}^{\infty}$ such that

$$\mathbb{E}\left[\left\| \frac{1}{NK}\sum_{n=1}^{N}\sum_{k=1}^{K} \vec{U}_{h_{m_k}}(\rho_{0,n}, \vec{m}_{0,n}) - \mathbb{E}\Big[(\rho, \vec{m})\Big] \right\|_{L^q((0,T)\times\Omega;R^{d+1})}\right] \to 0$$

as $K,\ N \to \infty$ for any $1 \le q < \frac{2\gamma}{\gamma+1}$, where $(\rho, \vec{m}) \in \mathcal{U}(\rho_0, \vec{m}_0)$ is a measurable selection.

References

[1] E. Chiodaroli and E. Feireisl, *Glimm's method and density of wild data for the Euler system of gas dynamics*, Nonlinearity **37** (2024), Paper No. 035005, 12

[2] C. De Lellis and L. Székelyhidi, Jr., *On admissibility criteria for weak solutions of the Euler equations*, Arch. Ration. Mech. Anal. **195** (2010), 225–260.

[3] E. Feireisl, M. Lukáčová-Medviďová, H. Mizerová, and B. She, *Numerical analysis of compressible fluid flows*, Springer-Verlag, Cham, 2022

[4] F. Merle, P. Raphaël, I. Rodnianski, and J. Szeftel, *On the implosion of a compressible fluid II: singularity formation*, Ann. of Math. (2) **196** (2022), 779–889

A posteriori error estimates for finite volume approximations of one dimensional systems of hyperbolic conservation laws

Jan Giesselmann

(joint work with Sam G. Krupa, Aleksey Sikstel)

We are interested in the numerical approximation of systems of hyperbolic conservation laws endowed with one convex entropy/entropy flux pair. In particular, we derive a posteriori error bounds for first order finite volume approximations which are useful for (provable) error control and mesh adaptation.

We follow the paradigm of reconstruction-based a posteriori error estimates presented in [9]: A suitable reconstruction of the numerical solution is interpreted as the exact solution to a perturbed version of the system of hyperbolic conservation laws, where the perturbation – called "residual" – is computable. Then, a stability theory for hyperbolic conservation laws is used in order to bound the difference between the exact solution and the reconstruction of the numerical solution in terms of the residual. In this context, one crucial feature of a "suitable" reconstruction is that the reconstruction is an element of a suitable set of functions such that the stability theory can be applied.

In our recent manuscript [6], we present results based on stability results obtained by Bressan, Chiri and Shen in [1] that relate the $L^\infty(0,T;L^1(\mathbb{R}))$-norm of the error to the $W^{-1,1}([0,T]\times\mathbb{R})$-norm of the residual – provided the total variation and the total oscillation of the numerical solution are sufficiently small. Our main contribution is to have found a way to actually compute the $W^{-1,1}([0,T]\times\mathbb{R})$-norm of the residual locally, i.e. on space-time cells. In contrast, in [1], it was *a priori* shown for a variety of schemes that the global–in–space residual decays with a certain rate with respect to the mesh width. Being able to compute norms of residuals locally pavess the way for mesh adaptation based on

residual equi-distribution. To be more precise, the localization of the residual is achieved by introducing numerical fluxes in the definition of local residuals such that their contributions vanish when local residuals are added in order to obtain global residuals. We compute dual norms of residuals, by exploiting the fact that the residuals live in a rather low dimensional space so that it is sufficient to test with test functions from another low dimensional space. We make this rigorous by introducing a specifically designed projection operator.

A specific challenge of the stability estimates from [1] is that these require us to decompose the computational domain into trapezoids distinguishing between trapezoids that contain (sufficiently strong and separated) discontinuities and those that do not. We achieve this by multiresolution analysis techniques that enable us to identify discontinuities of any prescribed strength in a reliable way. Additionally, Hartens prediction strategy provides a heuristic to detect shock formation in presumably smooth parts of the domain, [8].

In another recent manuscript, [5], we derive a posteriori error estimates based on novel quantitative stability estimates that extend the theory of shifts, and in particular, the framework for proving stability developed by Krupa and Vasseur [7]. This is the first time the theory of shifts has been used for quantitative estimates. This is made possible by linking shifts to relative entropy dissipation so that we obtain computable upper bounds for the sizes of shifts. Although we only consider scalar problems in [5] we provide a framework that we believe can be extended to also cover systems. Indeed, we work entirely within the context of the theory of shifts and a-contraction, techniques that can be extended to systems as can be seen in the recent publication [2]. This is possible since the theory of shifts relies on only one entropy.

In a certain sense, our approach is close to the one pursued in [3] and [4] where Lipschitz continuous reconstructions of the numerical solution were computed and the relative entropy framework was used to bound the $L^\infty(0,T;L^2(\mathbb{R}))$-norm of the error by the $L^1(0,T;L^2(\mathbb{R}))$-norm of the residual. The results in [5] significantly improve upon those in [3] and [4] as they provide an estimator that is convergent post shock formation. This is closely linked with the fact that the theory of shifts can consider solutions from a broader class than the original weak-strong theory based on relative entropy. In particular, the theory of shifts is not restricted to studying the stability of a smooth solution $\bar{u}$ among the class of weak solutions u, but can allow for arbitrarily many shocks to exist in the otherwise smooth solution $\bar{u}$. Moreover, the theory of shifts and a-contraction have no small-data limitations, and are able to treat large shocks. Thus, we hope that the results from [5] can be extended in such a way that a posteriori stability of large-data solutions to hyperbolic systems becomes available.

However, a posteriori error estimates based on the theory of shifts come with a certain cost. As mentioned above, the theory of shifts allows us to generalize the relative entropy theory to allow for shocks in an otherwise smooth solution $\bar{u}$. However, to achieve this, it must allow for the discontinuities in $\bar{u}$ to move somewhat unpredictably, not necessarily following the Rankine-Hugoniot jump

condition. Due to this uncertainty of discontinuity positions, we need to numerically simulate extensions for each continuous piece of $\bar{u}$. These extensions are global in space and time. Therefore, instead of solving one initial value problem numerically we need to solve as many initial value problems as there are discontinuities in the initial data. In addition, we have to track approximate positions and position error bounds for each discontinuity in order to have control on which numerical solution might be revealed where and when. This is a significant additional computational load but it is somewhat mitigated by the fact that all the individual solutions will remain smooth so that we may use high order numerical schemes without stabilization. For each numerical solution, we use reconstructions as described in [3] and [4] that lead to residuals that scale optimally with mesh width for smooth solutions (and for certain classes of numerical fluxes). By combining relative entropy estimates in the smooth regions with control on the error of discontinuity positions we can, overall, control the $L^\infty(0,T;L^2(\mathbb{R}))$-norm of the error in terms of the $L^1(0,T;L^2(\mathbb{R}))$-norms of the residuals.

References

[1] A. Bressan, M. T. Chiri, and W. Shen, *A Posteriori Error Estimates for Numerical Solutions to Hyperbolic Conservation Laws*, Archive for Rational Mechanics and Analysis, **241** (2021), 357–402.

[2] G. Chen, S. G. Krupa, and A. F. Vasseur, *Uniqueness and weak-BV stability for 2 × 2 conservation laws*. Arch. Ration. Mech. Anal., **246** (2022), 299–332.

[3] A. Dedner and J. Giesselmann, *A posteriori analysis of fully discrete method of lines discontinuous Galerkin schemes for systems of conservation laws*, SIAM J. Numer. Anal., **54** (2016), 3523–3549.

[4] J. Giesselmann, Ch. Makridakis, and T. Pryer, *A posteriori analysis of discontinuous Galerkin schemes for systems of hyperbolic conservation laws*, SIAM J. Numer. Anal., **53** (2015), 1280–1303.

[5] J. Giesselmann and S. G. Krupa, *Theory of shifts, shocks, and the intimate connections to L^2-type a posteriori error analysis of numerical schemes for hyperbolic problems*, Arxiv 2306.06538.

[6] J. Giesselmann and A. Sikstel, *A-posteriori error estimates for systems of hyperbolic conservation laws*, Arxiv 2305.01340.

[7] S. G. Krupa and A. F. Vasseur, *On uniqueness of solutions to conservation laws verifying a single entropy condition*. J. Hyperbolic Differ. Equ., **16** (2019), 157–191.

[8] A. Harten, *Multiresolution algorithms for the numerical solution of hyperbolic conservation laws*. Comm. Pure Appl. Math., **48** (1995), 1305–1342.

[9] Ch. Makridakis, *Space and time reconstructions in a posteriori analysis of evolution problems*, ESAIM Proc., **21** (2007), 31–44.

Towards the Development of Fully Discrete Active Flux Methods

Christiane Helzel

(joint work with Erik Chudzik, Yannick Kiechle, Donna Calhoun, and Mária Lukáčová-Medvid'ová)

The Active Flux method is a finite volume method for hyperbolic conservation laws which uses cell average values as well as point values as degrees of freedom. The method was introduced by Eymann and Roe [5] and is in its simplest form, i.e. for one-dimensional linear advection, equivalent to scheme V described in van Leer's influential paper from 1977.

The point values in Active Flux methods are typically located along the grid cell boundaries and used both for the reconstruction as well as for the computation of numerical fluxes. The numerical fluxes are typically computed using Simpson's rule. During the last years, Active Flux methods have been developed using either a method of lines approach [1, 2] or a fully discrete approach [5, 8, 9]. A common feature of both approaches is that the governing equations are used twice, once in characteristic form to evolve the point values and once in conservative form to update the cell average values.

Our current work, which was presented at the workshop, is concerned with the further development of fully discrete Active Flux methods. Klingenberg presented recent work of his group related to semi-discrete Active Flux methods which use a method of lines approach. Fully discrete methods use a compact stencil in space as well as time. This leads to methods which use as little information as possible outside the true domain of dependence. Roe [8] pointed out that such methods produce accurate results even on coarse grids.

In fully discrete Active Flux methods, the point values are evolved in time using truly multi-dimensional evolution operators. For linear advection and acoustics exact evolution operators are known and have been used in one- and two-dimensional Active Flux methods. For nonlinear scalar hyperbolic problems characteristic theory can be used to evolve the point values. As an example we recently developed an Active Flux method for the Vlasov-Poisson system [6]. For higher-dimensional kinetic equations accuracy on coarse grids is an important property and thus Active Flux methods are interesting candidates. For more complex hyperbolic systems exact evolution operators are in general not available. We therefore used the method of bicharacteristics [7] to obtain truly multi-dimensional approximative evolution operators. Our recent results, which were presented in the talk, are described in [3]. Furthermore, we recently developed Cartesian grid Active Flux methods for adaptively refined grids [4] that make use of the compact stencil.

References

[1] R. Abgrall, *A combination of residual distribution and the active flux formulations or a new class of schemes that can combine several writings of the same hyperbolic problem: application to the 1d Euler equations*, Commun. Appl. Math. Comput., **5** (2023), 370–402.

[2] R. Abgrall and W. Barsukow, *Extensions of active flux to arbitrary order of accuracy*, ESAIM: M2AN, **57** (2023), 991–1027.

[3] E. Chudzik, C. Helzel, and M. Lukáčová-Medvid'ová, *Active flux methods for hyperbolic systems using the method of bicharacteristics*, J. Sci. Comput., **99** (2024), 16.
[4] D. Calhoun, E. Chudzik, and C. Helzel, *The Cartesian grid active flux method with adaptive mesh refinement*, J. Sci. Comput., **94** (2023), 54.
[5] T. A. Eymann and P. L. Roe, *Multidimensional active flux schemes*, In: 21st AIAA computational fluid dynamics conference (2013), p. 2940.
[6] Y. F. Kiechle, E. Chudzik, and C. Helzel, *An active flux method for the Vlasov-Poisson system*, In: Franck, E., Fuhrmann, J., Michel-Dansac, V., Navoret, L. (eds) Finite Volumes for Complex Applications X-Volume 2, Hyperbolic and Related Problems. FVCA 2023.
[7] M. Lukáčová-Medvid'ová, K. W. Morton, and G. Warnecke, *Evolution Galerkin methods for hyperbolic systems in two space dimensions*, Math. Comput., **69** (2000), 1355–1384.
[8] P. L. Roe, *Designing CFD methods for bandwidth–a physical approach*, Computers & Fluids, **214** (2021), 104774.
[9] I. Samani and P. L. Roe, *Acoustics on a coarse grid*, AIAA SCITECH 2023 Forum (2023).

Global existence of dissipative solutions to the Camassa–Holm equation with transport noise

Helge Holden
(joint work with Luca Galimberti, Kenneth H. Karlsen, Peter H. C. Pang)

We consider the nonlinear stochastic partial differential equation that equals the Camassa–Holm equation perturbed by a convective, position-dependent, noise term. Specifically, we study the Cauchy problem for

$$\begin{aligned} 0 &= \mathrm{d}u + \left[u\,\partial_x u + \partial_x P\right]\mathrm{d}t + \sigma\partial_x u \circ \mathrm{d}W, \\ -\partial_{xx}^2 P + P &= u^2 + \frac{1}{2}\left|\partial_x u\right|^2, \quad \text{for } (t,x) \in (0,T)\times\mathbb{S}^1, \end{aligned} \tag{1}$$

where $\mathbb{S}^1 = \mathbb{R}/(2\pi\mathbb{Z})$ is the 1D torus (circle), T is a positive final time, $\sigma = \sigma(x) \in W^{2,\infty}(\mathbb{S}^1)$ is a position-dependent noise function, and W is a 1D Wiener process defined on a standard filtred probability space $\mathcal{S} = \big(\Omega, \mathcal{F}, \{\mathcal{F}_t\}_{t\in[0,T]}, \mathbb{P}\big)$. Formally, by the Itô–Stratonovich conversion formula, the Stratonovich differential $\sigma\,\partial_x u \circ \mathrm{d}W$ in (1), normally denoted as a gradient, transport or convection noise term, can be expanded into $-\frac{1}{2}\sigma(x)\partial_x\left(\sigma(x)\partial_x u\right)\mathrm{d}t + \sigma(x)\partial_x u\,\mathrm{d}W$. Moreover, the elliptic equation for P can be solved to yield

$$P = P[u] := K * \left(u^2 + \frac{1}{2}\left|\partial_x u\right|^2\right), \quad K(x) = \frac{\cosh\left(x - 2\pi\,\mathrm{int}\left(\frac{x}{2\pi}\right) - \pi\right)}{2\sinh(\pi)}, \tag{2}$$

where K is the Green's function of $1 - \partial_{xx}^2$ on $\mathbb{S}^1$, $\mathrm{int}(x)$ is the integer part of x, and $*$ means convolution in x. Consequently, (1) takes the form of the nonlinear nonlocal stochastic partial differential equation

$$\begin{aligned} 0 &= \mathrm{d}u + \left[u\,\partial_x u + \partial_x P\right]\mathrm{d}t - \frac{1}{2}\sigma\partial_x\left(\sigma\partial_x u\right)\mathrm{d}t + \sigma\partial_x u\,\mathrm{d}W, \\ P &= K * \left(u^2 + \frac{1}{2}\left|\partial_x u\right|^2\right). \end{aligned} \tag{3}$$

The deterministic Camassa–Holm equation, studied in [1], is obtained by setting $\sigma = 0$.

We start by establishing existence of solutions for a regularized version (1) by adding a viscous term $\varepsilon\partial_{xx}^2 u_\varepsilon$. Thus we study

$$
\begin{aligned}
0 &= \mathrm{d}u_\varepsilon + \left[u_\varepsilon\,\partial_x u_\varepsilon + \partial_x P_\varepsilon - \varepsilon\partial_{xx}^2 u_\varepsilon\right]\,\mathrm{d}t - \frac{1}{2}\sigma_\varepsilon\partial_x\left(\sigma_\varepsilon\partial_x u_\varepsilon\right)\,\mathrm{d}t + \sigma_\varepsilon\partial_x u_\varepsilon\,\mathrm{d}W,\\
P_\varepsilon &= P[u_\varepsilon] := K * \left(u_\varepsilon^2 + \frac{1}{2}\left|\partial_x u_\varepsilon\right|^2\right).
\end{aligned}
\tag{4}
$$

This is carefully analyzed in [3].

Subsequently, we analyze the limit as $\varepsilon \to 0$, and we obtain the following result. The detailed analysis can be found in [2].

Theorem 6. *Let $\sigma \in W^{2,\infty}(\mathbb{S}^1)$, and fix some $p_0 > 4$. For any initial probability distribution Λ supported on $H^1(\mathbb{S}^1)$, satisfying*

$$
\int_{H^1(\mathbb{S}^1)} \|v\|_{H^1(\mathbb{S}^1)}^{p_0}\,\Lambda(\mathrm{d}v) < \infty,
$$

there exists a dissipative weak martingale solution $\left(\tilde{\mathcal{S}}, \tilde{u}, \tilde{W}\right)$ to the stochastic CH equation (3) with random initial data $\tilde{u}_0$ distributed according to Λ ($\tilde{u}_0 \sim \Lambda$), where $\tilde{\mathcal{S}} = \left(\tilde{\Omega}, \tilde{\mathcal{F}}, \{\tilde{\mathcal{F}}_t\}_{t\in[0,T]}, \tilde{\mathbb{P}}\right)$ is a stochastic basis. Besides, the following energy inequality holds $\tilde{\mathbb{P}}$–a.s., for a.e. $s \in [0,T)$ and every t with $s < t \le T$,

$$
\begin{aligned}
&\int_{\mathbb{S}^1} \left(\tilde{u}^2 + \left|\partial_x\tilde{u}\right|^2\right)\mathrm{d}x\Big|_s^t\\
&\qquad \le \int_s^t \int_{\mathbb{S}^1} \left(\frac{1}{4}\partial_{xx}^2\sigma^2\tilde{u}^2 + \left(\left|\partial_x\sigma\right|^2 - \frac{1}{4}\partial_{xx}^2\sigma^2\right)\left|\partial_x\tilde{u}\right|^2\right)\mathrm{d}x\,\mathrm{d}t'\\
&\qquad\quad + \int_s^t \int_{\mathbb{S}^1} \partial_x\sigma\left(\tilde{u}^2 - \left|\partial_x\tilde{u}\right|^2\right)\mathrm{d}x\,\mathrm{d}\tilde{W}.
\end{aligned}
\tag{5}
$$

Specifically, it holds for $s = 0$ and any $t \in (0,T]$, with $\int_{\mathbb{S}^1}\left(\tilde{u}^2 + \left|\partial_x\tilde{u}\right|^2\right)\mathrm{d}x\big|_{s=0}$ replaced by $\int_{\mathbb{S}^1}\left(\tilde{u}_0^2 + \left|\partial_x\tilde{u}_0\right|^2\right)\mathrm{d}x$.

The talk is based on the two papers [3, 2]. Further references can be found in the cited papers.

References

[1] R. Camassa and D. D. Holm, *An integrable shallow water equation with peaked soliton*, Phys. Rev. Lett. **71** (11) (1993), 1661–664.

[2] L. Galimberti, H. Holden, K. H. Karlsen, and P. H.C. Pang, *Global existence of dissipative solutions to the Camassa–Holm equation with transport noise*, J. Differ. Equations, **387** (2024), 1–103.

[3] H. Holden, K. H. Karlsen, and P. H.C. Pang, *Global well-posedness of the viscous Camassa–Holm equation with gradient noise*, Discrete Contin. Dyn. Syst., **43** (2) (2022), 568–61.

A new genuinely multi-dimensional structure preserving numerical method for compressible flow equations

Christian Klingenberg

Multi-dimensional conservation laws possess many more phenomena than their one-dimensional counterparts. Examples are vortices in turbulent flow and also low Mach number flow, where the flow is almost incompressible (a solenoidal velocity is multi-dimensional).

We propose a new hybrid finite element - finite volume method (based on [2]), that achieves upwinding by locally evolving continuous data, instead of solving Riemann problems. In particular cell averages of the solution and its moments are updated together with point values of the solution in a semi-discrete fashion. The original Active Flux method (see [3]) had been presented as a fully discrete third order method, that required an exact evolution operator for the point value updates. For nonlinear problems such an operator is difficult to obtain, in particular for multiple space dimensions. The new approach makes it possible to apply the Active Flux method to any system of multi-dimensional conservation laws, and this method now is of arbitrary high order.

As a first step, in [1] the new generalized Active Flux method is presented in two space dimension for the compressible Euler equations, it is of third order. It includes a limiting strategy.

It can be proven that this new scheme, when applied to the linear hyperbolic equations, is asymptotic preserving for Mach number going to zero, maintains vortices and also preserves stationary states. These properties are shown to hold in numerical experiments when applied to the non-linear compressible Euler equations. In upcoming work we will present an arbitrary high order version of [1].

This is joint work among others with Wasilij Barsukow and Lisa Lechner (Würzburg).

References

[1] R. Abgrall, W. Barsukow, and C. Klingenberg, *The Active Flux method for the Euler equations on Cartesian grids*, preprint, see https://arxiv.org/abs/2310.00683 (2023)

[2] R.Abgrall and W. Barsukow, *A hybrid finite element-finite volume method for conservation laws*, Proc. of the NumHyp21 conference, AMC 447 (see https://arxiv.org/abs/2208.14477) (2023)

[3] T. A. Eymann and P. L. Roe, *Multidimensional active flux schemes*, In 21st AIAA computational fluid dynamics conference, 2013

Stochastic NSE with L^p data

Igor Kukavica

(joint work with Fanhui Xu, Fei Wang, and Mohammed Ziane)

For the stochastic Navier-Stokes equations with a multiplicative white noise on $\Omega = \mathbb{T}^3$ or $\Omega = \mathbb{R}^3$, we prove that there exists a unique strong solution locally in time when the initial datum belongs to $L^p(\Omega; L^p)$ for $p > 3$. We also prove the

existence of global strong solutions for small data. The local existence result also holds in $\mathbb{R}^n$. All results are joint with Fanhui Xu (Harvard). Also, some are done in collaboration with Fei Wang (Shanghai) and M. Ziane (USC).

Central-upwind schemes for hyperbolic system with uncertainties

Alexander Kurganov
(joint work with Alina Chertock, Michael Herty, Mária Lukáčová-Medvid'ová)

We study nonlinear hyperbolic systems with uncertainties. In the one-dimensional case, such systems of balance laws read as

$$\boldsymbol{U}_t + \boldsymbol{F}(\boldsymbol{U})_x = \boldsymbol{S}(\boldsymbol{U}, x, \xi),$$

where x is the spatial variable, t is time, ξ is a random variable, $\boldsymbol{U} = \boldsymbol{U}(x, t, \xi)$ is the unknown random vector function, $\boldsymbol{F}$ is the flux, and $\boldsymbol{S}$ is the source term. The uncertainties may appear in the system parameters as well as in the initial and/or boundary data due to empirical approximations or measuring errors.

Nonlinear hyperbolic systems with uncertainties appear in a wide variety of applications. Quantifying the uncertainties is important since it helps to conduct sensitivity analysis and provide guidance for improving the models.

In recent years, a wide variety of uncertainty quantification methods for nonlinear hyperbolic systems has been proposed and investigated. One of the popular class methods employ Monte Carlo-type simulations, which are robust, but not very efficient due to a possibly large number of realizations required. In addition to the Monte Carlo methods, a widely used approach for random PDEs is the generalized polynomial chaos (gPC), where stochastic processes are represented in terms of orthogonal polynomials series of random variables. In principle, there are two distinct gPC approaches: intrusive and non-intrusive ones. In non-intrusive algorithms, like stochastic collocation methods, one seeks to satisfy the governing equations at a discrete set of points in the random space and then use global interpolation and quadrature rules to numerically evaluate statistical moments. Therefore, in the stochastic collocation approach, as well as in the Monte-Carlo methods, one can use numerical methods designed for the corresponding deterministic systems.

In the case of an intrusive approach, like stochastic Galerkin (SG) methods, gPC expansions are substituted into the governing equations and projected by a Galerkin approximation to obtain deterministic equations for the expansion coefficients. Solving the coefficient equations gives the stochastic moments of the random solution. The equations for the expansion coefficients are, in general, nonlinear and coupled. Nevertheless, the gPC methods are typically more accurate than their non-intrusive counterparts when the same number of modes in the gPC expansion is used and therefore a higher accuracy of the numerical solution can be achieved with a lower degree of the gPC expansion.

Development and implementation of the SG methods for nonlinear hyperbolic PDEs are, however, especially challenging due to a possible loss of hyperbolicity.

This is not the case for linear hyperbolic systems and kinetic equations. In the scalar case several approaches exist to prevent this loss. In the case of isentropic Euler equations and full Euler equations a transformation to either Roe or entropy variables has proven successful to circumvent the loss of hyperbolicity. In the case of the Saint-Venant system of shallow water equations, the hyperbolicity may be enforced by ensuring that the computed water depth is nonnegative.

However, neither of these approaches can be directly extended to the studied hyperbolic system of balance laws since they may not lead to a WB and positivity preserving method.

We consider the Saint-Venant system of shallow water equations, which is widely used for modeling flows in rivers, lakes and coastal areas, as well as in models emerging in oceanography and atmospheric sciences.

In the one-dimensional case, the studied system reads as

$$\begin{cases} h_t + q_x = 0, \\ q_t + \left(hu^2 + \dfrac{g}{2}h^2\right)_x = -ghZ_x, \end{cases} \tag{1}$$

where the water depth h, mean velocity u, and water discharge $q := hu$ are functions of x, t, and ξ. In the current setting, the bottom topography $Z(x,\xi)$ is a random field independent of time and g is the acceleration due to gravity. The system (1) is considered subject to random initial data

$$h(x,0,\xi) = h_0(x,\xi), \quad q(x,0,\xi) = q_0(\xi).$$

It is well-known that the random shallow water system (1) is hyperbolic as long as $h(x,t,\xi) \geq 0$. It is also easy to show that (1) admits a family of smooth steady-state solutions

$$q(x,\xi) = C_1(\xi), \quad \frac{u^2(x,\xi)}{2} + g\big[h(x,\xi) + Z(x,\xi)\big] = C_2(\xi), \tag{2}$$

Among all of the solutions in (2), the simplest "lake at rest" equilibria satisfying

$$q(x,\xi) \equiv 0, \quad w(x,\xi) := h(x,\xi) + Z(x,\xi) = C_2(\xi) \tag{3}$$

are often physically relevant since in many practical situations the water waves can be viewed as small perturbations of a "lake at rest" state. Capturing such waves numerically is a challenging task even in the deterministic case, because the magnitude of these perturbations may be smaller than the size of the truncation error, especially when a practically affordable course mesh is used. In order to overcome this difficulty one needs to develop a so-called well-balanced (WB) schemes, which are capable of exactly preserving the corresponding deterministic version of the steady-states solutions (2) (or at least of the "lake at rest" states (3)) at the discrete level. An additional difficulty arises due to the fact that the water depth must remain non-negative during the evolution. In the deterministic case, a number of positivity preserving schemes were proposed. Development of WB and especially positivity preserving numerical methods for the random system is even more challenging.

We implement the gPC-SG method for the Saint-Venant system (1) with uncertainty. We numerically solve the system for the gPC coefficients by a semi-discrete second-order central-upwind scheme. The choice of the central-upwind scheme is motivated by the fact that this scheme is Riemann-problem-solver-free and thus can be applied as a "back-box solver" to any hyperbolic system as long as the largest and smallest eigenvalues of its Jacobian can be estimated. The system for the gPC coefficients is a $2(K+1)\times 2(K+1)$ system as we use $K+1$ terms in each of the gPC expansions

$$\boldsymbol{U}(x,t,\xi)\approx \boldsymbol{U}^K(x,t,\xi)=\sum_{i=0}^{K}\widehat{\boldsymbol{U}}_i(x,t)\Phi_i(\xi).$$

Here, $\{\Phi_i(\xi)\}_{i=0}^K$ are orthonormal polynomials of degree up to $K\geq 1$. The choice of the polynomials depends on the distribution function of ξ. For instance, a Gaussian distribution defines the Hermite polynomials; a uniform distribution defines the Legendre polynomials, etc.

As mentioned above, the main attractive feature of the gPC-SG method is its spectral accuracy in the stochastic space, which allows one to use relatively small number of gPC coefficients. This makes the central-upwind scheme plausible as the eigenvalues of the Jacobian can be efficiently computed numerically. In addition, we ensure that the developed central-upwind scheme is WB in the sense it is capable of exactly preserve the "lake at rest" steady states (3) by extending the techniques developed in the deterministic case.

Implementing the WB central-upwind scheme may be, however, not enough for computing a reliable solution as negative values of the water depth may appear and the method then fails. The latter is related to the emergence of spurious oscillations which may be generated during the time evolution of the gPC coefficients. In order to control these oscillations, one may apply filters. This, however, can yield the loss of statistical information on the solution if the filtering is used to damp large magnitude oscillations, for instance, in the case of the Gibbs phenomenon. We propose another approach for controlling the nonnegativity of the water depth using the "draining timestep" technique originally developed in the deterministic case. In addition, we use the positivity correction procedure from to ensure the non-negativity of the water depth mean, which is the zeroth coefficient in the gPC expansion of h.

We have tested the developed gPC-SG method on a number of challenging numerical examples, in which we demonstrate both WB and positivity preserving properties. Though in some of the considered benchmarks, we obtain accurate mean and standard deviation of the stochastic solution, we have realized that when strong dicontinuities and almost dry areas are present, small oscillations appearing near the discontinuities propagate into the stochastic field and cause quite significant oscillations in both spatial and random spaces. In our numerical examples, we demonstrate that enforcing the nonnegativity of the computed water depth (and thus the hyperbolicity!) does not guarantee the lack of oscillations attributed to the Gibbs phenomenon. This demonstrates the limitations in the

applicability of the stochastic Galerkin method to the problems with discontinuous solutions.

An arbitrarily high-order well-balanced active flux like method for shallow water models

Yongle Liu

(joint work with Rémi Abgrall, Wasilij Barsukow)

I will introduce an arbitrarily high-order accurate fully well-balanced numerical method for the one-dimensional shallow water models, including the Saint-Venant systems of equations and blood flow model in an artery. The developed method is based on a continuous representation of the solution and a natural combination of the conservative and primitive formulations of the studied PDEs [1]. The degrees of freedom are defined as point values at cell interfaces and moments of the conservative variables inside the cell [2, 3]. The well-balanced property, in the sense that capable of exactly preserving both the zero and non-zero velocity equilibria, is achieved by a well-balanced approximation of the source term in the conservative formulation and a well-balanced residual computation in the primitive formulation. Several numerical tests are shown to prove its well-balanced and high-order accuracy properties.

References

[1] R. Abgrall, *A combination of residual distribution and the active flux formulations or a new class of schemes that can combine several writings of the same hyperbolic problem: application to the 1D euler equations*, Commun. Appl. Math. Comput., **5** (2023), 370–402.

[2] R. Abgrall and W. Barsukow, *Extensions of Active Flux to arbitrary order of accuracy*, ESAIM: Mathematical Modelling and Numerical Analysis, **57** (2023), 991–1027.

[3] R. Abgrall and W. Barsukow, *A hybrid finite element–finite volume method for conservation laws*, Appl. Math. Comput., **447** (2023), 127846.

A node-conservative cell-centered Finite Volume method for solving multidimensional Euler equations over unstructured grids

Pierre-Henri Maire

(joint work with Vincent Delmas, Raphaël Loubère)

The numerical simulation of hypersonic flows remains a domain of primary importance not only to design hypersonic flight vehicles but also to assess their aerodynamic and aerothermal characteristics [1]. The hypersonic regime is characterized by very strong shock waves and rarefaction ones, among other things, and is thus particularly demanding in terms of robustness and accuracy with respect to the employed numerical methods. Here, we shall focus more precisely on the numerical discretization of the inviscid part of the flow which is governed by the compressible Euler equations. Since its introduction at the beginning of the eighties, the shock capturing Finite Volume (FV) method has become the cornerstone of any modern

aerodynamics code. A quite complete panorama of this classical approach might be found for instance into [10]. The cell-centered FV method consists in writing the integral formulation of the conservation laws of mass, momentum and total energy over each cell of the computational grid. The primary unknowns are the cell-averaged values of mass, momentum and total energy. For a given cell, the time increment of the cell-averaged value results from the summation of the normal fluxes located at each cell face. In this classical framework, the normal flux approximation is obtained in a unique manner at each face through the use of an approximate Riemann solver such as the Roe one [9], which is probably one of the most popular among the available ones [10]. Even if this type of method is characterized by a positive return of experience it is also admitted that it is plagued by several flaws such as the so-called odd-even decoupling and carbuncle numerical instabilities, refer to [7, 8]. There is thus still a strong need to design robust and accurate Finite Volume methods able to cope with production engineering simulations of hypersonic flows on any type of grids.

As quoted by Candler and his co-authors [2]: *There remain a number of outstanding numerical issues in the simulation of hypersonic flows. A particular difficulty is associated with the simulation of high Mach number blunt capsule geometries that have a very large region of subsonic flow near the stagnation point. This class of flow magnifies numerical error generated at the strong shock wave; this error then accumulates in the stagnation region and corrupts the solution. The main remedies for this problems are:*

- *The grid must be aligned with the bow shock.*
- *Eigenvalue limiters must be used judiciously; other forms of dissipation can also be used to counter-act the error generated by the strong gradients across the bow shock.*

None of these "fixes" actually solve the underlying problem, rather they reduce its magnitude and mask its effects with additional dissipation. Clearly, fundamental work needs to be done to reduce the sensitivity of the solution to the grid and specific details of the numerical method. The present work is an attempt to answer to this difficult question. This presentation describes a novel subface flux-based FV method for discretizing multi-dimensional compressible Euler equations on general unstructured grids [5]. This novel numerical method relies on the partition of the cell interfaces into subfaces. The subface flux numerical approximation stems from the notion of simple Riemann solver introduced in the seminal work [4]. The approximate Riemann solver utilized in this work is constructed by decomposing the intermediate fluxes into a convection part plus a pressure part. This peculiar splitting of the numerical flux allows to define the wave speeds of this Riemann solver in a very natural manner contrarily to what is done for the HLLC solver [10]. Moreover, it is worth noting that this decomposition of the intermediate flux implies that the present Riemann solver has an underlying Lagrangian structure through a discrete Lagrange-to-Euler mapping introduced in [4]. This fundamental feature ensures the transfer of good properties such as positivity preservation and entropy stability [3]. The subface flux computation relies not only on the mean

values of the cells located on both sides of the subface by means of the foregoing approximate Riemann solver but also on the velocity of the node from which the subface emanates. The normal component of this nodal velocity with respect to the unit normal of the subface might be viewed as a parameter in the aforementioned approximate Riemann solver. Thus, the interface flux is not uniquely defined and the Finite Volume method is not conservative anymore in the classical sense. The conservation of total momentum and energy is obtained enforcing a local balance at each node which writes under the form of a vectorial equation, the solution of which provides the expression of the nodal velocity. The resulting numerical method is able to guarantee the positivity of mass density and specific energy while ensuring entropy stability provided an explicit time step condition is satisfied. We have thus obtained a novel multi-dimensional conservative and entropy-stable FV scheme wherein the numerical fluxes are computed through a nodal solver, which is exactly the one designed for compressible Lagrangian hydrodynamics [6]. The robustness and the accuracy of this novel FV scheme are assessed through various numerical tests run on various unstructured grids. This novel Finite Volume methods appears to be insensitive to the numerical pathologies (odd-even decoupling, carbuncle) occurring when utilizing the classical shock capturing methods such as the Roe or HLLC schemes. We plan to utilize this novel FV method as a building block for the FV discretization of the Navier-Stokes equations on unstructured grids. It remains also to investigate the theoretical properties of this FV discretization to better understand its insensitivity to the carbuncle phenomenon, topic which remains a subject of active research.

References

[1] J. D. Anderson, *Hypersonic and High-Temperature Gas Dynamics*, AIAA education series (2000).

[2] G. V. Candler, D. Mavriplis, and L. Treviño, *Current Status and Future Prospects for the Numerical Simulation of Hypersonic Flows*, 47th AIAA Aerospace Sciences Meeting **AIAA 2009-513** (2009).

[3] A. Chan, G. Gallice, R. Loubère, and P.-H. Maire, *Positivity preserving and entropy consistent approximate Riemann solvers dedicated to the high-order MOOD-based Finite Volume discretization of Lagrangian and Eulerian gas dynamics*, Computers & Fluids, (2021).

[4] G. Gallice, *Positive and Entropy Stable Godunov-Type Schemes for Gas Dynamics and MHD Equations in Lagrangian or Eulerian Coordinates*, Numer. Math., **94** (2003), 673–713.

[5] G. Gallice, A. Chan, R. Loubère, and P.-H. Maire, *Entropy stable and positivity preserving Godunov-type schemes for multidimensional hyperbolic systems on unstructured grid*, J. Comput. Phys., (2022).

[6] R. Loubère, P.-H. Maire, and B. Rebourcet, *Staggered and colocated Finite Volume scheme for Lagrangian hydrodynamics*, Handbook of Numerical Methods for Hyperbolic Problems: Basic and Fundamental Issues, edited by R. Abgrall and C.-W. Shu **Chapter 13** (2016), 319–352.

[7] J. J. Quirk, *A contribution to the great Riemann solver debate*, International Journal on Numerical Methods for Fluids, **18** (1994), 555–574.

[8] A. V. Rodionov, *Artificial viscosity Godunov-type schemes to cure the carbuncle phenomenon*, J. Comput. Phys., **345** (2017), 308–329.
[9] P. L. Roe, *Approximate Riemann solvers, parameter vectors and difference scheme*, J. Comput. Phys., **43** (1981), 357–372.
[10] E. F. Toro, *Riemann solvers and Numerical Methods for Fluid Dynamics*, Springer (1999).

Efficient iterative arbitrary high order methods: an adaptive bridge between low and high order

Lorenzo Micalizzi
(joint work with Davide Torlo, Walter Boscheri, Maria Han Veiga)

The focus of the talk is an efficient modification of general families of arbitrary high order numerical methods, characterized by an iterative procedure gaining one order of accuracy at each iteration, e.g., DeC and ADER methods. In particular, the modification consists in introducing intermediate embeddings between the iterations in order to increase the accuracy of the discretization together with the order of accuracy along the iterative procedure. The modified methods have several advantages, among which: they are cheaper than the original ones and they have a natural adaptive character, which allows to easily prescribe p-adaptivity. In the talk, the application of the proposed modification to several different schemes will be discussed. More in detail: to ADER-DG for hyperbolic PDEs [2], to ADER methods for ODEs with stability analysis and applications to hyperbolic PDEs via the method of lines [3], and to DeC methods for ODEs with stability analysis and applications to mass matrix-free continuous Galerkin formulations for hyperbolic PDEs [1].

References

[1] L. Micalizzi and D. Torlo, *A new efficient explicit deferred correction framework: analysis and applications to hyperbolic PDEs and adaptivity*, Commun. Appl. Math. Comput. (2023), (1–36).
[2] L. Micalizzi, D. Torlo, and W. Boscheri, *Efficient iterative arbitrary high-order methods: an adaptive bridge between low and high order*, Commun. Appl. Math. Comput. (2023), 1–38.
[3] M. H. Veiga, L. Micalizzi, and D. Torlo, *On improving the efficiency of ader methods*, Appl. Math. Comput. **466** (2024), 128426.

High-Order Moment Scaling of Near-Wall Turbulence for Arbitrary Velocities: An Extended Symmetry Approach

Martin Oberlack
(joint work with Simon Görtz, Jonathan Laux, Sergio Hoyas)

Introduction. Presently, we derive and validate scaling laws for arbitrary turbulent one-point velocity moments in wall-bounded flows, focusing on moments from spanwise and wall-normal velocity components. The scaling laws are derived using a symmetry analysis of the underlying set of Navier-Stokes equations from which the infinite moment hierarchy is derived and are therefore first principle-based. They are subsequently validated using new direct numerical simulation (DNS) data, revealing a hidden Reynolds number dependency and the fact that scaling is determined by the lowest order moment. Consistency with DNS data confirms the validity of the scaling laws even for sensitive fluctuating moments.

Derivation of Scaling Laws. The subsequent analysis is based on the Navier-Stokes equations,

$$\frac{\partial U_i}{\partial t} + U_k \frac{\partial U_i}{\partial x_k} + \frac{\partial P}{\partial x_i} - \nu \frac{\partial^2 U_i}{\partial x_k \partial x_k} = 0\,, \quad \frac{\partial U_k}{\partial x_k} = 0, \tag{1}$$

where $t \in \mathbb{R}^+$, $\boldsymbol{x} \in \mathbb{R}^3$, $\boldsymbol{U} = \boldsymbol{U}(\boldsymbol{x}, t)$, $P = P(\boldsymbol{x}, t)$, and ν represent time, position vector, instantaneous velocity vector, pressure, and kinematic viscosity, respectively. In contrast to Reynolds' decomposition, i.e. $U_k = \bar{U}_k + u_k$, where $\overline{(\cdot)}$ and u_k are respectively mean and fluctuation quantities, we consider statistical moments based on the instantaneous flow quantities. Consequently, the generic multipoint velocity moments in multi index notation are defined by

$$H_{i_{\{n\}}} = H_{i_{(1)} \ldots i_{(n)}} = \overline{U_{i_{(1)}}(\boldsymbol{x}_{(1)}, t) \cdot \ldots \cdot U_{i_{(n)}}(\boldsymbol{x}_{(n)}, t)}\,. \tag{2}$$

With that definition and analogous to [8], the multipoint moment equation (MPME) for the velocity yields

$$\frac{\partial H_{i_{\{n\}}}}{\partial t} + \sum_{l=1}^{n} \left[\frac{\partial H_{i_{\{n+1\}}[i_{(n)} \mapsto k_{(l)}]}[\boldsymbol{x}_{(n)} \mapsto \boldsymbol{x}_{(l)}]}{\partial x_{k_{(l)}}} + \frac{\partial I_{i_{\{n-1\}}[l]}}{\partial x_{i_{(l)}}} - \nu \frac{\partial^2 H_{i_{\{n\}}}}{\partial x_{k_{(l)}} \partial x_{k_{(l)}}} \right] = 0. \tag{3}$$

The moment $I_{i_{\{n-1\}}[l]}$ refers to the pressure-velocity correlation and correlates the pressure at l-th. point with $n-1$ velocities [10, 11].

In the following, we carry out a symmetry analysis, based on the Navier-Stokes equation (1) and the infinite dimensional system (3). Details on the symmetry theory for generic multipoint moments are presented in depth in the planned publication by [1]. In the current work we aim to compare the theory with new DNS data, why we restrict the consideration to on one-point statistics, i.e. $\boldsymbol{x} = \boldsymbol{x}_{(1)} = \boldsymbol{x}_{(2)} = \ldots = \boldsymbol{x}_{(n)}$. The corresponding one-point moments are accordingly denoted by $H^{(0)}_{i_{\{n\}}}$. As the theory was successfully presented in [8] and

validated in [3] for mean velocity moments composed of U_1, we focus in the current work on the n^{th} moments of U_2 and U_3, i.e. $\overline{U_{[i]}}$, where the square bracket indicates that no summation is applied.

Very briefly, let us introduce the idea of a form-invariant Lie symmetry transformation $\boldsymbol{x}^* = \boldsymbol{\phi}(\boldsymbol{x}, \boldsymbol{y}; a)$, $\boldsymbol{y}^* = \boldsymbol{\psi}(\boldsymbol{x}, \boldsymbol{y}; a)$, leaving a differential equation $\boldsymbol{F} = 0$ unchanged. Globally, this means that

(4)
$$\boldsymbol{F}\left(\boldsymbol{x}, \boldsymbol{y}, \boldsymbol{y}^{(1)}, \boldsymbol{y}^{(2)}, \ldots, \boldsymbol{y}^{(p)}\right) = 0 \quad \Leftrightarrow \quad \boldsymbol{F}\left(\boldsymbol{x}^*, \boldsymbol{y}^*, \boldsymbol{y}^{*(1)}, \boldsymbol{y}^{*(2)}, \ldots, \boldsymbol{y}^{*(p)}\right) = 0,$$

with the p^{th} derivatives of $\boldsymbol{y}$ is defined as $\boldsymbol{y}^{(p)}$.

The symmetry transformations of the system (3) known so far are divided into (i) those inherited from the Navier-Stokes equations (1) to (3) and (ii) those based on the statistical treatment which are found only in (3) and are therefore called statistical symmetries.

Of the nine symmetries of the inviscid Navier-Stokes equations (1), i.e. the Euler equations, the combined space-time scaling symmetry, including scaling of pressure and velocity, transforms for in the moment frame to

(5)
$$\bar{T}_{Sx/St}: \; t^* = \mathrm{e}^{a_{St}} t, \; \boldsymbol{x}^*_{(i)} = \mathrm{e}^{a_{Sx}} \boldsymbol{x}_{(i)}, \; \bar{\boldsymbol{U}}^* = \mathrm{e}^{a_{Sx} - a_{St}} \bar{\boldsymbol{U}}^*, \mathbf{H}^*_{\{n\}} = \mathrm{e}^{n(a_{Sx} - a_{St})} \mathbf{H}_{\{n\}}.$$

The translation symmetry of space is simply preserved in the moment frame,

$$\bar{T}_{x_i}: \; t^* = t, \; \boldsymbol{x}^*_{(i)} = \boldsymbol{x}_{(i)} + \boldsymbol{a}_{\boldsymbol{x}}, \; \bar{\boldsymbol{U}}^* = \bar{\boldsymbol{U}}^*, \; \mathbf{H}^*_{\{n\}} = \mathbf{H}_{\{n\}}. \tag{6}$$

The proof of form invariance is easily obtained by substituting (5) and (6) into (3).

As mentioned before, different scalings in space and time require vanishing of the viscous term. Therefore, caution is required at this point, because in principle, the Navier-Stokes equation (1) admits only one scaling symmetry. Only the Euler equations admit the two scaling symmetries (5). A detailed explanation why preservation of both scaling symmetries and consideration of the asymptotic limit $\nu \to 0^+$ is reasonable for the construction of scaling laws is presented in [1]. There, we carry out a boundary layer-like singular asymptotics in distance space $\boldsymbol{r}_{(i)} = \boldsymbol{x}_{(i)} - \boldsymbol{x}_{(0)}$. The small expansion parameter is the Kolmogorov length scale η determining the small scales where viscosity and dissipation act. This expansion was first derived in [9] for isotropic turbulence and the two-point moment equation. Subsequently, the MPME decompose into two equations. The large scales, much larger than η, are simply determined by equation (3) with $\nu = 0$. Therefore, scaling laws for moments even of high order are based on this equation why it is, together with its special scaling symmetry (5), the basis for the subsequent analyses. The second equation stemming from the asymptotic analysis is similar to the classical boundary layer equation. It acts on small scales on the order of η where viscosity and dissipation are dominant.

As mentioned above, the statistical symmetries play a central role in the derivation of scaling laws. They were first derived in [10] and in [13] their physical

meaning were pointed out. The translation symmetry in the moments

$$\bar{T}'_{\{n\}}: \; t^* = t\,, \;\; \boldsymbol{x}^*_{(i)} = \boldsymbol{x}_{(i)}\,, \;\; \bar{\boldsymbol{U}}^* = \bar{\boldsymbol{U}} + \boldsymbol{a}\,, \;\; \mathbf{H}^*_{\{n\}} = \mathbf{H}_{\{n\}} + \mathbf{a}^H_{\{n\}} \tag{7}$$

conforms to non-gaussianity. The statistical scaling symmetry in the moments only

$$\bar{T}'_s: \; t^* = t\,, \;\; \boldsymbol{x}^*_{(i)} = \boldsymbol{x}_{(i)}\,, \;\; \bar{\boldsymbol{U}}^* = \mathrm{e}^{a_{Ss}}\bar{\boldsymbol{U}}\,, \;\; \mathbf{H}^*_{\{n\}} = \mathrm{e}^{a_{Ss}}\mathbf{H}_{\{n\}}\,, \tag{8}$$

can be traced back to intermittency. It stems from the linearity of the infinite system (3).

Finally for the consideration of plane shear flows as it is done in this work, the MPME (3) admits additional symmetries. With x_2 the wall-normal coordinate it allows translation of moments with a linear term in x_2,

$$\bar{T}'_L: \; t^* = t\,, \;\; \boldsymbol{x}^*_{(i)} = \boldsymbol{x}_{(i)}\,, \;\; \bar{\boldsymbol{U}}^* = \bar{\boldsymbol{U}}\,, \;\; \mathbf{H}^*_{\{n\}} = \mathbf{H}_{\{n\}} + x_2\mathbf{a}^L_{\{n\}}\,, \tag{9}$$

This symmetry has already been discovered in [12] and is further specified in [1]. As we will see later, it leads to a linear correction of the scaling laws in the log region of the channel flow. For the core region, this symmetry is broken as it is inconsistent with the requirement of scaling symmetric to the center of the channel. We see later that the prefactor of the linear term is very small for both the U_2 and U_3 moments in the logarithmic region, but by no means negligible.

With this, invariant solutions for $\overline{U^n_{[i]}}$ for $i = 2, 3$ and $n \geq 2$ are derived from the discussed symmetries, rather similar to $\overline{U^n_1}$ in [8]. Also in this work, we restrict ourselves to one-point statistics in comparison with the DNS data. One point moments arise as special case of the complete set of invariant solution for arbitrary multi-point moments $\mathbf{H}_{\{n\}}$ derived in [1]. There, also the symmetry reduction of the MPME (3) is proven. We combine the groups (5), (7), (8) and (9), which gives us the global form of the transformation,

$$\begin{aligned}
\bar{T}: \; & x_2^* = \mathrm{e}^{a_{Sx}} x_2, \;\; \overline{U_1}^* = \mathrm{e}^{a_{Sx}-a_{St}+a_{Ss}}\overline{U_1}\,, \\
& \overline{U^2_{[i]}}^* = \mathrm{e}^{2(a_{Sx}-a_{St})+a_{Ss}}\overline{U^2_{[i]}} + x_2 a^L_{[i]_{\{2\}}} + a^H_{[i]_{\{2\}}}, \ldots\,, \\
& \overline{U^n_{[i]}}^* = \mathrm{e}^{n(a_{Sx}-a_{St})+a_{Ss}}\overline{U^n_{[i]}} + x_2 a^L_{[i]_{\{n\}}} + a^H_{[i]_{\{n\}}}
\end{aligned} \tag{10}$$

Here, a_{Sx}, a_{St}, and a_{Ss} are the parameters of the combined three-parameter scaling group. The first moment of $i = 2, 3$ does not appear, since there is no mean flow in these directions. The characteristic system, describing invariant solutions of the

spanwise and wall-normal velocity moments, reads

$$\begin{aligned}(11)\quad \frac{\mathrm{d}x_2}{a_{Sx}x_2+a_{x_2}} &= \frac{\mathrm{d}\overline{U_1}}{[a_{Sx}-a_{St}+a_{Ss}]\,\overline{U_1}+a^H_{[1]_{\{1\}}}} = \dots \\ &\frac{\mathrm{d}\overline{U^2_{[i]}}}{[2(a_{Sx}-a_{St})+a_{Ss}]\,\overline{U^2_{[i]}}+a^H_{[i]_{\{2\}}}+x_2a^L_{[i]_{\{2\}}}} = \dots \\ &= \frac{\mathrm{d}\overline{U^n_{[i]}}}{[n(a_{Sx}-a_{St})+a_{Ss}]\,\overline{U^n_{[i]}}+a^H_{[i]_{\{n\}}}+x_2a^L_{[i]_{\{n\}}}}.\end{aligned}$$

For details on deriving the characteristic system from the global form of transformations, we refer to [1].

In the context of integrating (11), we need to distinguish two cases, i.e. the solutions corresponding to the logarithmic and the center region of the channel flow [8]. Depending on where scaling laws are considered, different parameters turn out to be symmetry breaking, i.e. restricting the group parameters. The pivotal parameter governing the logarithmic wall-near region is the wall shear stress velocity $u_\tau = \sqrt{\tau_w/\rho}$, where τ_w is the wall shear stress, and ρ represents density. u_τ subsequently forms the exclusive near-wall velocity scale. Consequently, for a prescribed specific value, adherence to the scaling of the mean velocity as dictated by Eq.(10), the wall shear stress velocity leads to the symmetry-breaking and, hence, $a_{Sx}-a_{St}+a_{Ss}=0$. Consequently, the integration of Eq.(11) under this restriction leads to a reduced parameter dependence for the scaling laws in the logarithmic region due to integration of the first two terms in (11), and the higher moments follow from the first and further terms.

$$\begin{aligned}(12)\quad \overline{U^n_{[i]}} &= \tilde{C}_{[i]_{\{n\}}}\left(x_2+\frac{a_{x_2}}{a_{Sx}}\right)^{\omega(n-1)} + \frac{a^L_{[i]_{\{n\}}}}{a_{Sx}(1+\omega(1-n))}x_2 \\ &+ \frac{a^H_{[i]_{\{n\}}}(1+\omega(1-n)) - a^L_{[i]_{\{n\}}}\frac{a_{x_2}}{a_{Sx}}}{a_{Sx}\omega(1-n)(1+\omega(1-n))}.\end{aligned}$$

Here, $\omega = 1-a_{St}/a_{Sx}$ is a universal constant, and $\tilde{C}_{n,[i]}$ emerges as constant of integration. Similar to the results in [8] for the U_1 moments, we find three key results: (i) moments $n \geq 2$ have a power law behavior, where (ii) all n^{th}-order moments are linked with each other by the exponent ω, (iii) the power law behavior is the same for all three U_i components, which will later clearly be proven by the DNS data.

For the scaling laws in the channel core region, as mentioned above, the symmetry of the flow with respect to the channel center is symmetry breaking, i.e. $\mathbf{a}^L_{\{n\}} = 0$. Subsequently, in eq. (11), the factors $(a_{Sx}-a_{St}+a_{Ss}),\dots,n(a_{Sx}-a_{St})+a_{Ss}$ are all non-zero. This again gives us power-laws for all moments n, including the mean flow component of U_1, i.e. the first moment. We further find that we can summarize a_{Sx}, a_{St}, and a_{Ss} as two free parameters, since they only occur as ratios. From the exponents for the first two moments, σ_1 and σ_2, the scaling laws

for the channel core region follow as

$$\overline{U^n_{[i]}} = \tilde{C}'_{[i]_{\{n\}}} \left(x_2 + \frac{a_{x_2}}{a_{Sx}} \right)^{n(\sigma_2-\sigma_1)+2\sigma_1-\sigma_2} - \frac{a^H_{[i]_{\{n\}}}}{n(a_{Sx}-a_{St})+a_{Ss}}\,, \tag{13}$$

Again, all $\tilde{C}'$ are constants of integration, and the group parameters are summarized as $\sigma_1 = 1 - a_{St}/a_{Sx} + a_{Ss}/a_{Sx}$ and $\sigma_2 = 2(1 - a_{St}/a_{Sx}) + a_{Ss}/a_{Sx}$. As can be seen from the scaling laws, the latter exponents of the first two moments determine the exponent of all power laws for the higher order moments.

Comparison With DNS Data. The scaling laws (12) and (13) are in the following validated using new DNS data of a plane turbulent channel flow, with a Reynolds number of $Re_\tau = 10^4$ using the code LISO with a grid of about 80 billion points. For further details on this simulation, the reader is referred to [3], where, however, for the current comparison, the length of the DNS was doubled again compared to the aforementioned work. In addition to the validation presented in [8], we will in the following validate the scaling laws for moments from velocity components $i = 2, 3$. These are of special interest since no mean flow in this direction exists. Therefore, in this case instantaneous moments are identical with the fluctuating moments. In other words, the scaling laws derived in the previous section hold for fluctuating as well as for instantaneous moments.

Validation in the logarithmic region. In the following, the wall normal coordinate in the logarithmic region is denoted by y^+, i.e. $y^+ = 0$ defines the wall. Accordingly, the scaling laws to be validated in the logarithmic region are given by

$$\overline{U^n_{[i]}}^+ = C_{[i]_{\{n\}}} \left(y^+ + A \right)^{\omega(n-1)} + B_{[i]_{\{n\}}} + L_{[i]_{\{n\}}} y^+, \quad \text{for } n \geq 2, \tag{14}$$

where we have summarized the various constant group parameters appearing in eq. (12). For a similar validation of the logarithmic law for the averaged mean velocity, see [3] where the von Kármán constant a value was obtained to $\kappa = 0.394$. It is subject of ongoing research whether the data below shows that C_n and B_n result in a simple exponential function in n as already shown for the U_1-moments in [8].

Fig. 1a and Fig. 1b show the higher U_2 and U_3-moments for $n = 2, 4, 6$ in the logarithmic layer. Therein, we find a comparison between the DNS data and the fitted theoretical result (12). The power law scaling behavior is clearly visible by the double logarithmic plotting. The universal scaling factor is chosen to $\omega = 0.1$, matching the DNS data and obtaining the best fit for both figures. This again reveals that both moments obey the same scaling behavior.

The two key results of these fits are (i) an extremely good match of the power law with the DNS data for all moments. Their power law scaling is solely determined by the single parameter ω and (ii) the validity of the scaling laws in the log law's range of validity of $y^+ \simeq 400 \ldots 2500$. This range of validity is obtained by considering a power law indicator function analogous to the consideration in [8].

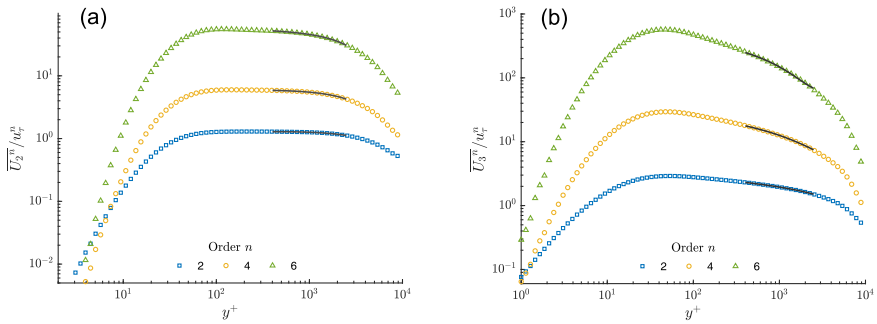

FIGURE 1. Comparison of moments between theory (solid) and DNS data at $Re_\tau = 10000$ in the range $y^+ \in [400, 2500]$ for U_2 (a) and U_3-moments (b) of order 2, 4, 6 in the logarithmic region. The mentioned y^+ range corresponds to the range of validity of the log-law for the given Reynolds number as shown in [8].

Validation in the centre region. In the centre region of the channel, we use the common way to formulate moments in deficit form. This is done by using a shifted coordinate x_2, with origin $x_2 = 0$ on the channel center. First ideas on a symmetry based power law similar to (13) in the centre of a channel flow were formulated in [7]. Therein, the mean velocity was derived in deficit form, which is in the current work used for arbitrary moments of U_i with $i = 2, 3$. Therefore, the power law scaling (13) is transformed to the universal deficit form

$$\frac{\overline{U_i^n}^{(0)} - \overline{U_i^n}}{u_\tau^n} = C'_{i,n} \left(\frac{x_2}{h}\right)^{n(\sigma_2-\sigma_1)+2\sigma_1-\sigma_2} \tag{15}$$

The exponent (0) in $\overline{U_i^n}^{(0)}$ refers to the value of the moment in the centre of the channel at $x_2 = 0$ and, similar to Eq. (14), α' and β' subsume various constants and are presumed to be universal in the core region.

In Fig. 2, we show the moments from the DNS at $Re_\tau = 10^4$ according to the deficit form up to order $n = 6$. It is obvious that for a large range, the moments show identical gradients, independent from the order n. This behavior is, according to the scaling law (15), reachable if $\sigma_1 = \sigma_2$. Consistent with this, the parameters in eq. (15) were fitted, namely to $\sigma_1 = 1.95$ and $\sigma_2 = 1.94$. Indeed, the fit of the core moments here shows a larger relative deviation from the DNS data than for the U_1-moments in [8], which might be due to the extremely sensitive fluctuating moments here. However, we argue that against this background eq. (15) represents the scaling very well, which is further supported by it being an invariant solution of the moment equations, as we show in [1].

Summing up, like the U_1 moments, all U_2 and U_3 moments in the core region scale with a single exponent which is independent of n, i.e. these moments clearly

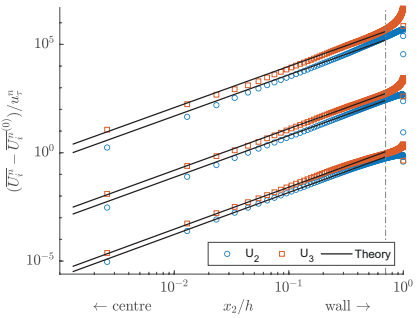

FIGURE 2. Comparison between theory (solid) and DNS data at $Re_\tau = 10000$ for U_2 and U_3-moments of order 2, 4, 6 (from bottom to top) in the core region.

admit strong anomalous scaling. This is accompanied by strongly intermittent *instantaneous* velocities in the channel center, to which we will assign the initially indeterminate velocity scale u^*. Regarding the symmetries in (5) shows that the constant exponent for all velocity moments is accompanied by symmetry breaking

$$a_{Sx} = a_{St}.$$

Thus, the scaling of the instantaneous velocities in (5) is broken by the velocity scale u^* and the scaling of moments by the intermittency symmetry (8) alone is preserved, leading to the observed anomalous scaling. Summing up, scaling of moments in the channel center is fundamentally determined by the statistical symmetries.

Reynolds number dependency. In [1] we show how viscosity and Reynolds number affect the scaling laws via deriving an integral constraint for the constants and group parameters in the scaling laws, which subsequently depend on the Reynolds number. This integral constraint includes an integration over the interface between logarithmic region and viscous sublayer. At this surface, values of moments and pressure-velocity correlations are determined by viscous dissipation in the sublayer. This effect is carried through the logarithmic region up into the core region, even though, according to the asymptotic expansion in [1], the large structures are mainly determined by inviscid equations. Consequently, in comparison to the logarithmic region, the Reynolds number dependency of the parameters in the deficit law core region is significantly weaker than in the log region, which is right next to the viscous sublayer. For reasons of shortness, the analysis in the current work is restricted to the Reynolds number dependency of the parameters in the logarithmic region. However, as we aim to compare the coefficients for a broad number of Reynolds numbers, we are restricted to second order U_1 moments, since for these moments a large number of data sets exists.

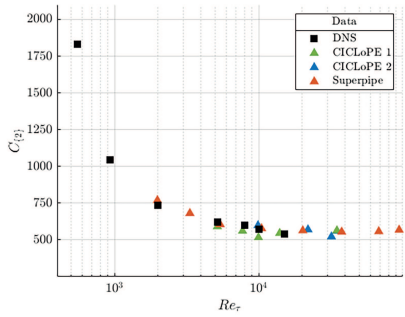

FIGURE 3. Values for scaling prefactor $C_{[1]_{\{2\}}}$ from eq. (16) fitted for $Re_\tau = 180 \ldots 9.4 \cdot 10^4$

Recall that the scaling law for these moments in the log region is given by

$$\overline{U_1^2}^+ = C_{[1]_{\{2\}}} \left(y^+ + A\right)^\omega + B_{[1]_{\{2\}}} + L_{[1]_{\{2\}}} y^+, \tag{16}$$

admitting the same power law form as for higher U_2 and U_3 moments as given in (14). It is to point out that the exponent $\omega = 0.1$, determining the power law behavior, is universal and the same for all velocities.

From the statement made above, we assume the Reynolds number dependency to be hidden in C, A, B, L, which are in the following compared for different Reynolds numbers. For the fits of (16), we used DNS data as well as experimental data. The set of experimental data contains data from [4] measured at the Princeton Superpipe for $Re_\tau = 2000 \ldots 9.4 \cdot 10^4$ and [15] and [16] measured at the CICLoPE facility of the University of Bologna for $Re_\tau = 5200 \ldots 3.5 \cdot 10^4$. Fitted parameters referring to experimental data are marked with a triangle ▲. Regarding DNS data, we used data from [2] in a Reynolds number range between $Re_\tau = 180 \ldots 2000$, [6] at $Re_\tau = 5200$, [14] at $Re_\tau = 8000$ and DNS from [3] at $Re_\tau = 10^4, 1.5 \cdot 10^4$. Fitted parameters referring to DNS data are marked with a square ■. Note that the fitting range, i.e. the range of y^+ where the constants in the scaling law are fitted, depends on the Reynolds number. This is quite intuitive as the logarithmic region increases with increasing Reynolds number. For the sake of shortness, the fitting range is not displayed here. Figs. 3-6 show the values for the parameters in (16) displayed in semi-logarithmic form over different Reynolds numbers. The first central result, universal for all parameters, is that all data points, regardless of the source of the data, lie consistently on a line, tending to a constant value for high Reynolds numbers. This indicates that from a certainly high Reynolds number, the scaling and therefore the values of the coefficients is truly independent from the Reynolds number. From fig. 4, we further find that the linear term in (16) tends to zero for sufficiently high Reynolds number and is only of notably relevance in the case of lower Reynolds numbers. For the DNS data, the linear term is fitted to zero from a lower Reynolds number than it is for the experimental data. The reason for that might lie in the quality of the measured data but is to be further

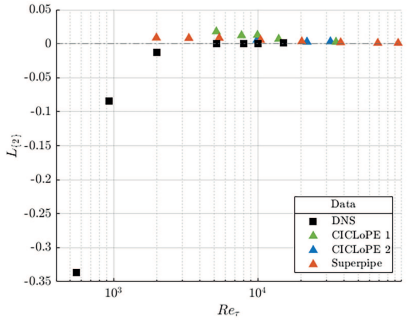

FIGURE 4. Values for constant $L_{[1]_{\{2\}}}$ from eq. (16), fitted for $Re_\tau = 180 \ldots 9.4 \cdot 10^4$

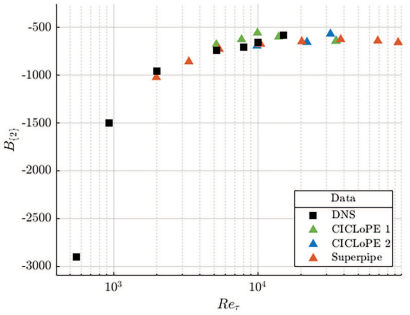

FIGURE 5. Values for constant $B_{[1]_{\{2\}}}$ from eq. (16), fitted for $Re_\tau = 180 \ldots 9.4 \cdot 10^4$

investigated in future work. It is to note that the offset A, displayed in fig. 6, is universal for all higher moments, independent from their direction and order. This is since A is defined as the ratio between the group parameters a_{x_2}/a_{Sx} and therefore universal for the logarithmic region. In the present work, we have set it to zero throughout due to the sufficiently high Reynolds number.

Conclusion. From the above considerations and scaling laws, two main aspects can be concluded. First, for the U_2 and U_3 moments, the exponent of the second order moment is sufficient to obtain the scaling of all higher moments. The scaling is determined in the logarithmic region by ω and for the deficit law by σ_1 respective σ_2. Second, we have shown how the scaling laws are affected by the Reynolds number and how this influence is reduced when moving towards the core region. This has practical importance for turbulence models, especially if statistical symmetries are included as for example in [5].

Summarizing, in this work we have extended the ideas from the works of [8] and [3] to higher moments from U_2 and U_3. Compared to the considerations in these

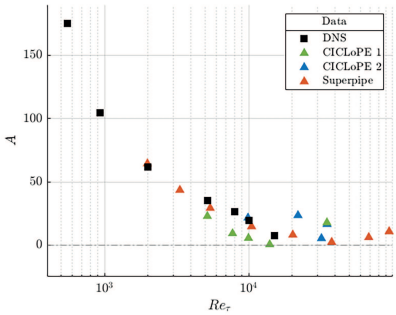

FIGURE 6. Values for constant $A = a_{x_2}/a_{Sx}$ from eq. (16) fitted for $Re_\tau = 180 \ldots 9.4 \cdot 10^4$

two works, the instantaneous moments in the current work are not affected by the mean flow in x_1-direction and are therefore identical with the fluctuating moments in the respective direction. For these moments, we have shown that scaling laws derived from first principle symmetry theory and based on the underlying set of Navier-Stokes and statistical equations are valid and therefore hold even for fluctuating moments with much smaller absolute values and much more sensitive behavior than the moments in mean flow direction.

SG and MO acknowledge funding by the Deutsche Forschungsgemeinschaft (DFG, German Research Foundation) - SPP 2410 Hyperbolic Balance Laws in Fluid Mechanics: Complexity, Scales, Randomness (CoScaRa), within the Project "Approximation Methods for Statistical Conservation Laws of Hyperbolically Dominated Flow" under project number 526024901. SH is partially funded by project PID2021-128676OB-I00 by Ministerio de Ciencia, innovación y Universidades / FEDER.

REFERENCES

[1] S. Görtz and M. Oberlack, *High-moment scaling laws of wall-bounded turbulent shear flows: Invariant solutions to the multi-point moment equations*, under review with Phys. Rev. Fluids, (2024).

[2] S. Hoyas and J. Jiménez, *Scaling of the velocity fluctuations in turbulent channels up to* $Re_\tau = 2003$, Phys. Fluids, **18**, (2006), 011702.

[3] Hoyas, S. and Oberlack, M. and Alcántara-Ávila, F. and Kraheberger, S. V. and Laux, J., *Wall turbulence at high friction reynolds numbers*, Phys. Rev. Fluids, **7**, (2022), 014602.

[4] Hultmark, M. and Vallikivi, M. and Bailey, S. C. C. and Smits, A. J., *Turbulent pipe flow at extreme reynolds numbers*, Phys. Rev. Lett., **108**, (2012), 094501.

[5] Klingenberg, D. and Plümacher, D. and Oberlack, M., *Symmetries and turbulence modeling*, Phys. Fluids, **32**, (2020), 025108.

[6] Lee, M. and Moser, R. D., *Direct numerical simulation of turbulent channel flow up to* $Re_\tau \approx 5200$. J. Fluid Mech., **774**, (2015) 395–415.

[7] Oberlack, M., *A unified approach for symmetries in plane parallel turbulent shear flows*, J. Fluid Mech., **427**, (2001), 299–328.

[8] Oberlack, M. and Hoyas, S. and Kraheberger, S. V. and Alcántara-Ávila, F. and Laux, J., *Turbulence statistics of arbitrary moments of wall-bounded shear flows: A symmetry approach*, Phys. Rev. Lett., **128**, (2022), 024502.
[9] Oberlack, M. and Peters, N., *Closure of the Two-Point Correlation Equation in Physical Space as a Basis for Reynolds Stress Models*, (1993), 85–94. Elsevier Science.
[10] Oberlack, M. and Rosteck, A., *New statistical symmetries of the multi-point equations and its importance for turbulent scaling laws*, Discrete Continuous Dyn. Syst, **3**, (2010), 451–471.
[11] Oberlack, M. and Wacławczyk, M. and Rosteck, A. and Avsarkisov, V., *Symmetries and their importance for statistical turbulence theory*, Mechanical Engineering Reviews, **2**, (2015), 15–00157.
[12] Rosteck, A. M., *Scaling laws in turbulence - a theoretical approach using lie-point symmetries*, PhD thesis, Technische Universität, Darmstadt, (2014).
[13] Wacławczyk, M. and Staffolani, N. and Oberlack, M. and Rosteck, A. and Wilczek, M. and Friedrich, R., *Statistical symmetries of the lundgren-monin-novikov hierarchy*, Physical Review E, **90**, (2014), 013022.
[14] Yamamoto, Y. and Tsuji, Y., *Numerical evidence of logarithmic regions in channel flow at* $\mathrm{Re}_\tau = 8000$, Phys. Rev. Fluids, **3**, (2018), 012602.
[15] Zimmerman, S. and Philip, J. and Monty, J. and Talamelli, A. and Marusic, I. and Ganapathisubramani, B. and Hearst, R. J. and Bellani, G. and Baidya, R. and Samie, M. and et al. *A comparative study of the velocity and vorticity structure in pipes and boundary layers at friction reynolds numbers up to* 10^4, J. Fluid Mech., **869**, (2019), 182–213.
[16] Örlü, R. and Fiorini, T. and Segalini, A. and Bellani, G. and Talamelli, A. and Alfredsson, P. H., *Reynolds stress scaling in pipe flow turbulence–first results from ciclope*, Philosophical Transactions of the Royal Society A: Mathematical, Physical and Engineering Sciences, **375**, (2017), 20160187.

Convergence of structure-preserving FE schemes for the Euler equations - Extension to the stochastic Euler system

Philipp Öffner

(joint work with Rémi Abgrall, Dominic Breit, Dmitri Kuzmin, Thamsanqa Castern Moyo, Mária Lukáčová-Medvid'ová)

Many problems in computational fluid dynamics are described via the compressible Euler or Navier-Stokes (NS) equations. Recently, dissipative weak (DW) solutions have been introduced as a generalization to classical solution concepts. In the first part of the talk, we focus on the Euler equation of gas dynamics given by

$$\begin{aligned} &\partial_t \varrho + \mathrm{div}_x(\varrho \mathbf{u}) = 0 \\ &\partial_t(\varrho \mathbf{u}) + \mathrm{div}_x\left(\varrho \mathbf{u} \otimes \mathbf{u}\right) + \nabla_x p = 0 \quad \Longleftrightarrow \partial_t \mathbf{U} + \mathrm{div}_x\, \mathbf{f}(\mathbf{U}) = 0. \\ &\partial_t E + \mathrm{div}_x\left[(E+p)\mathbf{u}\right] = 0 \end{aligned} \tag{1}$$

Here, ϱ denotes the density, E the total energy, $\mathbf{u}$ the velocity, $\mathbf{m} = \rho\mathbf{u}$ the momentum, and p the pressure. We further denote by $\mathbf{U} = (\varrho, \mathbf{m}, E)^T$ the conserved vector and by $\mathbf{f}i(\mathbf{U}) = (\varrho u_i, u_i\mathbf{m} + p, u_i(E+p))^T$ the flux function. We focus on perfect gas and consider the Euler system (1) with no-flux or periodic boundary condition and certain initial data. The second law of thermodynamics dictates that the convex entropy function η must satisfy the inequality

$$\partial_t \eta + \mathrm{div}_x\, F \leq 0.$$

Following the work of [4] and guided by numerical insights, we introduce DW solutions and revisit their key properties. DW solutions need not satisfy the equations weakly but rather up to certain measures of defect and oscillations. They serve as a natural extension of classical solutions, as they coincide with them under conditions such as the existence of classical solutions (referred to as the weak-strong uniqueness principle) or certain degrees of smoothness. Moreover, DW solutions can be identified as limits of consistent and stable approximations. Convergence towards DW solutions has been demonstrated for various structure-preserving numerical methods [1, 4, 5, 6]. Here, we particularly focus on high-order flux-corrected finite-element (FC-FE) schemes and establish their convergence to DW solutions for the multi-dimensional Euler equations. Crucially, this convergence relies on three essential properties:

- A priori estimates on the approximate solutions,
- structure-preserving properties of the schemes, and
- consistency relation with the continuous system.

We delve into each of these properties in depth and provide a detailed sketch of the proof for the consistency of the FC-FE schemes. It's noteworthy that consistency, in this context, differs from the typical approach in numerical methods where a smooth solution is assumed within the scheme, and the local truncation error is analyzed. In our context, consistency entails utilizing the numerical solution within the weak formulation of the Euler equations (1), with the remaining error diminishing as the grid is refined. We draw parallels to similar research based on this concept and provide a few examples. Subsequently, we prove the following convergence theorem [5]:

Theorem 7. *Let $\mathbf{U}^h = \{\varrho^h, \mathbf{m}^h, \eta^h\}_{h\to 0}$ be a family of numerical solutions obtained by the consistent and structure-preserving FE schemes on a shape regular mesh. Then, there exists a subsequence (also denoted by $\mathbf{U}^h$) such that*

$$\begin{aligned}\varrho^h &\to \varrho \text{ weakly-}(*) \text{ in } L^\infty((0,T)\times\mathcal{O})\\ \eta^h &\to \eta \text{ weakly-}(*) \text{ in } L^\infty((0,T)\times\mathcal{O})\\ \mathbf{m}^h &\to \mathbf{m} \text{ weakly-}(*) \text{ in } L^\infty((0,T)\times\mathcal{O};\mathbb{R}^d)\end{aligned}$$

as $h \to 0$ where $\mathbf{U} = (\varrho, \mathbf{m}, \eta)^T$ is a DW solution of the Euler system.

Additionally, we find that strong convergence is achieved when $\mathbf{U}$ represents a weak entropy, strong, or classical solution. In numerical simulations, we confirm strong convergence towards classical solutions. Employing Cesàro averaging, we convert weak-$(*)$ convergence into strong convergence, concentrating on the Kelvin-Helmholtz test case. Ultimately, we demonstrate strong convergence for this particular test case.

In the second part of the discussion, we broaden our exploration to include the stochastic Euler equations [7]:

$$
\begin{aligned}
&\mathrm{d}\,\varrho + \mathrm{div}_x \mathbf{m}\,\mathrm{d}\,t = 0,\\
&\mathrm{d}\,\mathbf{m} + \mathrm{div}_x\Big(\frac{\mathbf{m}\otimes\mathbf{m}}{\varrho}\Big)\,\mathrm{d}\,t + \nabla_x p\,\mathrm{d}\,t = \varrho\phi\,\mathrm{d}\,W,\\
&\mathrm{d}\,E + \mathrm{div}_x\left((E+p)\,\frac{\mathbf{m}}{\varrho}\right)\mathrm{d}\,t = \frac{1}{2}\varrho\|\phi\|_{\ell_2}^2\,\mathrm{d}\,t + \phi\cdot\mathbf{m}\,\mathrm{d}\,W,
\end{aligned}
\tag{2}
$$

where W is a (cylindrical) Wiener process on a filtered probability space $(\Omega, \mathfrak{F}, (\mathfrak{F}_t)_{t\geq 0}, \mathbb{P})$ and ϕ is the diffusion coefficient (a Hilbert-Schmidt operator). We commence our exploration by establishing a comparison with the deterministic scenario. Initially, the incorporation of stochastic perturbations aimed to introduce a regularization effect. However, in the Euler case, this alone proves insufficient to salvage well-posedness. Even in multi-dimensions, the problem remains ill-posed [3]. Consequently, we introduce the concept of dissipative measure-valued martingale solution [7] and reiterate some recent findings within this framework. Specifically, we concentrate on

- existence of dissipative martingale solutions,
- pathweise weak-strong uniqueness, and
- convergence of FE schemes.

To prove convergence, we need

- a priori estimates on the approximate solutions, and
- structure-preserving and consistent schemes from the deterministic setting.

In the subsequent discussion, we highlight that a straightforward assumption mirroring the deterministic case, such as uniformly bounding the density from below and the energy from above, is unrealistic for stochastic PDEs. Thus, we refine this assumption by introducing a stopping time. Consequently, we conduct our investigation under the following premise:

Assumption 1. *There is a stopping time* $\mathfrak{t}$ *with* $\mathbb{P}(\mathfrak{t} > 0) = 1$ *and deterministic constants* $K > 0$ *such that* $\mathbb{P}$*-a.s.*

$$
\inf_{t\in[0,\mathfrak{t}],x\in\mathcal{O}} \varrho^h(t,x) \geq \frac{1}{K}, \qquad \sup_{t\in[0,\mathfrak{t}],x\in\mathcal{O}} \mathcal{E}^h(t,x) \leq K,
$$

uniformly in h.

We finally summarize and explain further our main results from [2], namely we are able to prove:

- Ensuring consistency between a DG/FV discretization and dissipative martingale solutions.
- Achieving convergence in law up to a subsequence using stochastic compactness arguments.
- Demonstrating convergence to a pathwise strong solution throughout their lifespan.

- Establishing convergence rates of at least order 1/2 in the L^1-norm of the relative energy.

Towards the conclusion of the presentation, we provide an outlook on forthcoming projects. Currently, our focus lies on numerically validating our convergence results and error estimates for dissipative martingale solutions, particularly in the context of high-order methods. Moreover, we aim to extend the concept of DW solutions and the construction of high-order, structure-preserving numerical methods to encompass the Navier-Stokes-Korteweg equations and multicomponent/phase flows. Additionally, we are actively working on adapting our investigation to address incompressible equations.

References

[1] R. Abgrall, M. Lukáčová-Medvid'ová, and P. Öffner, *On the convergence of residual distribution schemes for the compressible Euler equations via dissipative weak solutions*, Math. Models Methods Appl. Sci. **33** (01), (2023), 139–173.

[2] D. Breit, T. Moyo, and P. Öffner, *Discontinuous Galerkin methods for the complete stochastic Euler equations*, in preparation, (2024).

[3] D. Breit, E. Feireisl, and M. Hofmanova, *On solvability and ill-posedness of the compressible Euler system subject to stochastic forces*, Anal. PDE **13**(2), (2020), 271–402.

[4] E. Feireisl, M. Lukáčová-Medvid'ová, H. Mizerová, and B. She *Numerical analysis of compressible fluid flows*, MS&A, Model. Simul. Appl., Springer, (2021).

[5] D. Kuzmin, M. Lukáčová-Medvid'ová, and P. Öffner, *Consistency and convergence of flux-corrected finite element methods for nonlinear hyperbolic problems*, arXiv: 2308.14872, (2023).

[6] M. Lukáčová-Medvid'ová and P. Öffner, *Convergence of discontinuous Galerkin schemes for the Euler equations via dissipative weak solutions*, Appl. Math. Comput. **436**, (2023).

[7] T. Moyo, *Dissipative solutions and Markov selection to the complete stochastic Euler system*, J. Diff. Equ. **365**, (2023), 408–464.

On the linear growth of the mixing zone in a semi-discrete model of Incompressible Porous Medium (IPM) equation

Yulia Petrova

(joint work with Sergey Tikhomirov, Yalchin Efendiev)

We present a semi-discrete model (5)–(8) of the two-dimensional viscous incompressible porous medium (IPM) equation describing gravitational fingering instability. The IPM equation describes evolution of concentration carried by the flow of incompressible fluid determined via Darcy's law in the field of gravity:

$$\partial_t c + \operatorname{div}(uc) = \nu \Delta c, \tag{1}$$

$$\operatorname{div}(u) = 0, \tag{2}$$

$$u = -\nabla p - (0, c). \tag{3}$$

Here $c = c(t, x, y)$ is the transported concentration, $u = u(t, x, y)$ is the vector field describing the fluid motion, $p = p(t, x, y)$ is the pressure, and $\nu \geq 0$ is a dimensionless parameter equal to an inverse of the Peclet number. Usually the

spatial domain (x, y) is either the whole space $\mathbb{R}^2$ or cylinder $[0, 1]\times\mathbb{R}$ with periodic or no-flux boundary conditions, but here we consider a discretization in x.

We are interested in studying the *exact rate of the linear growth of mixing zone* (see Fig. 1) formed when the initial condition is close to the unstable stratification:

$$c(0, x, y) = \begin{cases} +1, & y \geq 0, \quad \text{(heavy fluid)} \\ -1, & y < 0. \quad \text{(light fluid)} \end{cases} \tag{4}$$

The theoretical bounds on the speed of the linear growth for (1)–(3) are obtained in [2], see also numerical results both for gravitational and viscous fingering [3, 4, 6]. *Our goal* is to answer the question: can the bounds in [2] be improved?

The semi-discrete model consists of a system of advection-reaction-diffusion equations on concentrations $c_k = c_k(t, y)$, velocities $u_k = u_k(t, y)$, pressures $p_k = p_k(t, y)$, describing motion of miscible liquids in several vertical tubes (n real lines, $y \in \mathbb{R}$, $k = 1..n$) and interflow between them (governed by velocities $w_{k+1/2}$).

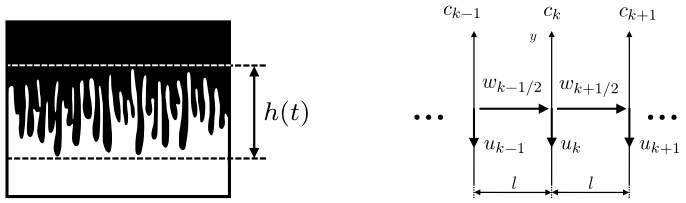

FIGURE 1. Left: gravitational fingering instability, $h(t) \sim \alpha t$ — scaling of the size of the mixing zone. Right: the n-tubes model

The advantage of the semi-discrete model is that it explicitly shows the possible (interconnected) mechanisms of slowing down the fingers' growth: (1) the convection in the transverse direction of the flow; (2) intermediate concentration, that is the typical concentration inside the finger is $c^* \in (-1, 1)$, see also discussion in [5].

Let $n \in \mathbb{N}, n \geq 2$, be the number of tubes. The *n-tubes IPM model* is obtained as a formal limit of the upwind finite-volume scheme and reads as follows, $k = 1..n$:

$$\text{(transport eq. in } k\text{-th tube)} \quad \partial_t c_k + \partial_y(u_k c_k) - \nu\partial_{yy} c_k = f_{k-1/2} - f_{k+1/2}, \tag{5}$$

$$\text{(incompressibility condition)} \quad l \cdot \partial_y u_k - w_{k-1/2} + w_{k+1/2} = 0. \tag{6}$$

Function $f_{k+1/2}$ is responsible for the interflow between k-th and $(k + 1)$ tubes:

$$f_{k+1/2} = \begin{cases} c_k \cdot \frac{w_{k+1/2}}{l}, & w_{k+1/2} \geq 0, \text{ (fluid flows from tube } k \text{ to } (k+1)) \\ c_{k+1} \cdot \frac{w_{k+1/2}}{l}, & w_{k+1/2} \leq 0. \text{ (fluid flows from tube } (k+1) \text{ to } k) \end{cases} \tag{7}$$

The velocities u_k and $w_{k+1/2}$ are given by the Darcy's law:

$$u_k = -\partial_y p_k - c_k, \qquad w_{k+1/2} = \frac{p_{k+1} - p_k}{l}. \tag{8}$$

Here $l > 0$ is a parameter equal to the distance between the tubes. We assume that the last, n-th tube, is connected with the 1-st tube, thus all the indexes in the equations should be understood modulo n.

Numerical modelling shows that the typical asymptotic solution as $t \to \infty$ for initial data close to (4) for a small number of tubes looks like a stacked combination of traveling waves which we call a propagating terrace (see Fig. 2).

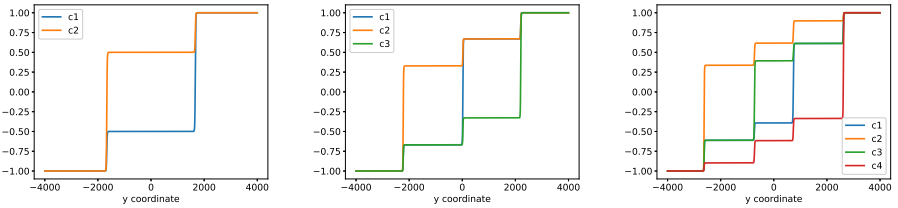

FIGURE 2. Typical asymptotic solution c_k, $k = 1..n$ for $n = 2, 3, 4$ tubes

In the talk we present a rigorous justification of the existence of a propagating terrace in the simplest setting of two tubes (see preprint [1]). The *main result* of [1] claims that for fixed $\nu > 0$ and sufficiently small values of $l > 0$ there exist two intermediate concentrations $c_1^*(l) \in (-1, 1)$, $c_2^*(l) \in (-1, 1)$ and two traveling wave (TW) solutions that connect the states:

$$(-1, -1) \xrightarrow{TW} (c_1^*(l), c_2^*(l)) \xrightarrow{TW} (1, 1). \tag{9}$$

Moreover, the speeds of the traveling waves approach $-1/4$ and $1/4$ as $l \to 0$.

The main tool in the proof in [1] is geometric singular perturbation theory. We represent the travelling wave dynamical system for the n-tubes IPM model as a singular perturbation of the pressure-free transverse flow equilibrium (TFE) model.[1] The only difference between the n-tubes IPM and n-tubes TFE models is the Darcy's law — instead of (8), TFE model states

$$u_k = \left(\frac{1}{n} \cdot \sum_{i=1}^{n} c_i\right) - c_k =: \bar{c} - c_k, \qquad \sum_{i=1}^{n} w_{k-1/2} = 0. \tag{10}$$

The TFE model turns out to be easier to analyze, in particular, for the two-tubes TFE model (5)–(7) and (10) we find explicit solutions in terms of traveling waves.[2]

There are several interesting *open questions* on the n-tubes IPM/TFE models:

(1) describe all possible asymptotic solutions of (5)–(8) as $t \to \infty$ for $n \geq 3$. For $n \geq 4$, we observe that the asymptotic solution is non-unique. In many situations a propagating terrace as in Fig. 2 appear.
   - how to determine the constant states between the traveling waves?

[1] In the literature describing viscous fingering TFE model has an analogue called vertical (flow) equilibrium, see e.g. [7].

[2] In this case the Hugoniot loci form straight lines and coincide with the rarefaction curves, making the 2-tubes TFE system to be of Temple type [8].

- the speeds of the fastest and the slowest traveling waves play an important role as they determine the rate of growth of the mixing zone — how to find them explicitly?

(2) study the limit as the number of tubes $n \to \infty$. Do the solutions of the system (5)–(8) approximate the solutions of the original IPM model (1)–(3) as $n \to \infty$? In which sense?
(3) study the well-posedness of the "hyperbolic" problem (5)–(8) with $\nu = 0$. What can we say about the vanishing viscosity limit as $\nu \to 0$?
(4) study the existence of the propagating terrace (9) for the two-tubes model for all values of $l > 0$ (now the result of [1] is valid only for l small enough). Study the stability properties of the propagating terrace.
(5) study the above questions for the n-tubes model for viscous fingering:

$u = -Km(c)\nabla p$, $\quad K$ — permeability tensor, $m(c)$ — mobility function.

References

[1] Y. Petrova, S. Tikhomirov, and Y. Efendiev, *Propagating terrace in a two-tubes model of gravitational fingering*, (2024) arXiv:2401.05981.
[2] G. Menon and F. Otto, *Dynamic scaling in miscible viscous fingering*, Commun. Math. Phys., **257** (2005), 303–317.
[3] F. Bakharev, A. Enin, A. Groman, A. Kalyuzhnyuk, S. Matveenko, Y. Petrova, I. Starkov, and S. Tikhomirov, *Velocity of viscous fingers in miscible displacement: Comparison with analytical models*,J. Comput. Appl. Math., **402** (2022), 113808.
[4] J.S. Nijjer, D.R. Hewitt, and J. A. Neufeld, *The dynamics of miscible viscous fingering from onset to shutdown*, J. Fluid Mech., **837** (2018), 520–545.
[5] F. Bakharev, A. Enin, S. Matveenko, N. Rastegaev, D. Pavlov, and S. Tikhomirov, *Relation between size of mixing zone and intermediate concentration in miscible displacement*, (2023), arXiv:2310.14260.
[6] G. Boffetta and S. Musacchio, *Dimensional effects in Rayleigh–Taylor mixing*, Philosophical Transactions of the Royal Society A **380** (2022), 20210084.
[7] A. Armiti-Juber and C. Rohde, *On Darcy-and Brinkman-type models for two-phase flow in asymptotically flat domains*, Computat. Geosci., **23** (2019), 285–303.
[8] B. Temple, *Systems of conservation laws with invariant submanifolds*, Trans. Amer. Math. Soc., **280**(2) (1983), 781–795.

Implicit Quinpi schemes for systems of conservation laws

Gabriella Puppo

(joint work with Matteo Semplice, Giuseppe Visconti)

Systems of hyperbolic conservation laws often present different scales linked to the magnitude of the eigenvalues of the Jacobian of the flux function. Numerical schemes used to integrate hyperbolic problems usually are explicit, because in many applications one is interested in resolving all scales. Borrowing our terminology from the most typical example of this class of problems, given by gas dynamics, explicit schemes resolve both convective and acoustic waves.

However, when the flow is considerably slower than the sound speed, the stability condition required by an explicit scheme may become too restrictive. In this

case, an implicit integration may become attractive. Implicit schemes typically require more computational work in each time step, but permit to use much larger steps. Thus, in many cases, they become competitive with respect to explicit schemes. The issue is how to reduce the computational load required by implicit schemes per time step, without giving up accuracy and the lack of spurious oscillations.

The literature on implicit schemes for hyperbolic problems is not yet well developed. Our work on implicit schemes [5] stems from previous work appeared in [1] and [3].

In the scheme we propose, the system is first integrated implicitly with a backward Euler scheme based on a piecewise constant reconstruction. This provides a first estimate of the solution at the new time step t^{n+1}, that we call the *predictor*, u_P^{n+1}. It is well known that backward Euler with piecewise constant reconstruction yields an unconditionally stable, total variation non increasing solution. The predictor therefore possesses these characteristics. However, this solution is very diffusive.

To increase the order of the scheme, it is necessary to use higher order schemes, based on piecewise polynomials in space, and a correspondingly high order time integrator. The problem is that to prevent spurious oscillations, one must rely on algorithms which are heavily non linear. In this work, we use the CWENO reconstruction of [2], which produces a local polynomial in each cell of the form

$$R_j(x) = \sum_{\ell=-p}^{p} \omega_{j+l}(\mathbf{u}_j^{n+1}) u_{j+\ell}^{n+1},$$

where j denotes a general space cell, $2p+1$ yields the amplitude of the stencil on which the reconstruction is based (linked to the degree of the interpolating polynomial), $\mathbf{u}_j$ denotes all the data in the stencil of the j-th cell, u_j^{n+1} is the solution sought at the new time step, and $\omega_{j+\ell}$ are the non linear weights, computed extracting information on the local smoothness of the solution from the data $\mathbf{u}_j$ contained in the stencil of the j-th cell.

In our approach, we use the solution obtained with the predictor to estimate the non linear weights. Thus the reconstruction becomes

$$R_j(x) = \sum_{\ell=-p}^{p} \omega_{j+l}(\mathbf{u_P}_j^{n+1}) u_{j+\ell}^{n+1}.$$

In this fashion, the weights depend on information provided by the scheme u_P at the correct time, i.e. t^{n+1}, and the reconstruction is linear in the solution one wants to compute. Next, we apply a high order implicit time integrator, such as a DIRK scheme. The final high order solution $\mathbf{u}^{n+1}$ is high order accurate, non oscillatory in space, and it is linear on linear problems. Its non linearity depends only on the non linearity of the flux.

The scheme we obtain still contains spurious oscillations on shocks and discontinuities. This is due to the fact that underlying each DIRK scheme, sits a polynomial interpolation in time, which can develop oscillations in the presence

of shocks. In other words, time limiting is also necessary. We achieve this with an a posteriori blending of the low order non oscillatory solutions provided by the predictor u_P^{n+1} and the high order solution u^{n+1}. The blending is driven by a smoothness indicator based on the local cell entropy production defined in [4] produced by the two schemes.

Numerical results on the non linear Euler equations of gas dynamics can be found in the forthcoming [6].

References

[1] T. Arbogast, C. S. Huang, X. Zhao, and D. N. King, *A third order, implicit, finite volume, adaptive Runge-Kutta WENO scheme for advection-diffusion equations*, Comput. Methods Appl. Mech. Engrg. **368** (2020).

[2] I. Cravero, G. Puppo, M. Semplice, and G. Visconti, *CWENO: uniformly accurate reconstructions for balance laws*, Math. Comput., **87** (2018), 1689–1719.

[3] S. Gottlieb, J. S. Mullen, and S. J. Ruuth, *A Fifth Order Flux Implicit WENO Method*, J. Sci. Comp. **27** (2006), 271–287.

[4] G. Puppo and M. Semplice, *Numerical entropy and adaptivity for finite volume schemes*, Commun. Comput. Phys., **10** (2011), 1132–1160.

[5] G. Puppo, M. Semplice, and G. Visconti, *Quinpi: Integrating conservation laws with CWENO implicit methods*, Comm. Appl. Math. & Comput., **5** (2023), 343–369.

[6] G. Puppo, M. Semplice, and G. Visconti, *Quinpi: Integrating stiff hyperbolic systems with implicit high order finite volume schemes*, arXiv:2307.14685, submitted to Commun. Comput. Phys., (2024).

A (global flux) quadrature based framework to construct arbitrary order steady state preserving schemes in 1D and multi-D

Mario Ricchiuto

(joint work with Wasilij Barsukow, Mirco Ciallella, Maria Kazolea, Yogiraj Mantri, Lorenzo Micalizzi, Philipp Öffner, Carlos Parés, Davide Torlo)

We consider the approximation of solutions to hyperbolic balance laws

$$u_t + \mathsf{div} F(u) = S(u, \vec{x})$$

in one as well as multiple dimensions. The above equation many admit complex steady states of practical interest in themselves, or as a background state of which perturbations are pf practical interest. The construction of steady state preserving, also called well balanced, numerical discretization tackles the issue of approximating non-trivial steady states with high precision. This talk gives an overview of recent and ongoing work [1, 2, 3, 4, 5] which proposes numerical discretizations based on a modified quadrature of the source term $S(u, x)$ which allow great enhancements in the resolution of steady equilibria. The main focus of the presentation is on the issue of characterizing explicitly the discrete steady equilibria. The main issue is summarized in the sketch below.

We can associate to the continuous PDE its steady state limit, and to this the steady equilibrium u^{eq}. For the discrete problem we can say the same. The discrete equations have a steady limit, and we can denote by u_h^{eq} the solution satisfying

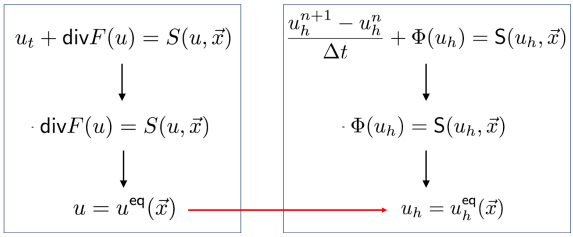

this limit. We are interested in characterizing explicitly the map from u^{eq} to u_h^{eq}. The reason for this is to

- characterize quantitatively the quality of the steady equilibrium and the expected enhancements for a well balanced method;
- understand if the above properties can be modified and/or further improved and by which modification to the scheme;
- possibly construct a projection operator $P : u^{\mathsf{eq}} \mapsto u_h^{\mathsf{eq}}$ allowing, without running the actual steady simulations, to construct initial discrete states which are preserved by the scheme to machine accuracy.

The approach used in the ongoing work is to systematically replace local values of the source terms (nodal values, cell average) with the derivative of a source primitive computed with appropriate quadrature formulas. In one space dimention, this allows to write the original problem in the modified form

$$u_t + \Big[F(u) - \mathcal{I}\big(S(u,x)\big)\Big]_x$$

Where the operator $\mathcal{I}$ is essentially a linear operator associated to a well chosen quadrature formula. The remaining spatial derivative can be approximated with any classical approach (DG, continuous FEM. WENO FV or FD). The main result is now that of course the pointwise values of the steady states of the above method are described by

$$F(u) - \mathcal{I}\big(S(u,x)\big) = F_0$$

which is nothing else that an ODE integrator applied to

$$F' = S(u(F),x)$$

If the operator $\mathcal{I}$ is now appropriately chosen, we can embed in this formulation exact consistency with higher order ODE integrators, such as collocation of high order multi-step methods. The talk reviews some application of this principle in finite elements and WENO finite differences.

In two space dimensions, we use a tensor/dimension by dimension generalization on Cartesian grids in the finite element setting. The notion of In this case, we show the existence of

(1) a high order approximation of the div operator, which for elements of degree p has consistency h^{p+1} instead of the usual h^p;
(2) a projection of given continuous vectorial fields on the a discrete space which is discretely div free if the initial field is solenoidal;

(3) estimates proving for the above projection nodal consistency of ordre h^{p+1} for general vectorial fields, and h^{p+2} for solenoidal fields;
(4) a generalization allowing to include sources in order to preserve a non-homogenous constraint of the type $\mathsf{div}\vec{v} = S$ with the same consitency properties.

Some details on each aspect, discussed in [5], are included in the talk. Numerical experiments in one and two dimensions confirm all the theoretical predictions.

References

[1] M. Ciallella, D. Torlo, and M. Ricchiuto, *Arbitrary High Order WENO Finite Volume Scheme with Flux Globalization for Moving Equilibria Preservation*, J. Sci. Comp., **96** (2023).
[2] Y. Mantri, P. Öffner, and M. Ricchiuto, *Fully well balanced entropy controlled DGSEM for shallow water flows: global flux quadrature and cell entropy correction*, J. Comput. Phys., **498** (2024).
[3] L. Micalizzi, M. Ricchiuto, and R. Abgrall, *Novel well-balanced continuous interior penalty stabilizations*, J. Sci. Comp., to appear.
[4] M. Kazolea, C. Parés, and M. Ricchiuto, *Discrete well-balanced WENO finite difference schemes via a global flux quadrature method using multi-step ODE integrator weights*, in preparation.
[5] W. Barsukow, M. Ricchiuto, and D. Torlo, *Structure preserving methods via Global Flux quadrature: divergence preservation and curl involution with continuous Finite Elements*, in preparation.

A multiscale model for weakly nonlinear quasilinear hyperbolic systems

Giovanni Russo
(joint work with David Ketcheson)

Waves propagating in media with periodic structures have attracted a lot of attention in recent years. These media show interesting macroscopic properties, which may be quite different from those of the individual materials constituting the stratified system. More recently, waves on fluids and gases with an underlying periodic structure have been studied. On a macroscopic scale, such a system can be considered a sort of fluid meta material.

These waves present a peculiar, somehow unexpected, behavior. For example, there is evidence that in spite of the fact that the waves are governed by genuinely quasi-linear hyperbolic system, they do not break into a shock.

As specific case, we study the propagation of small amplitude waves in shallow water over a periodic bathymetry [1]. We assume the wavelength is much larger than the period δ of the bathymetry.

The evolution equations for the water elevation $\eta(x,t)$ and the discharge $q(x,t)$ over a δ-periodic bathymetry $b(x)$ are written below, and the setup is illustrated in the figure to the right of the equations.

$$\eta_t + q_x = 0$$
$$q_t + \left(\frac{q^2}{\eta - b}\right)_x + g(\eta - b)\eta_x = 0.$$

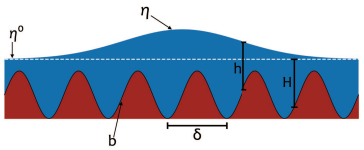

It is shown that an initial pulse of small amplitude will not produce a shock. Indeed, after a long time, an initial Gaussian pulse splits into several waves of various amplitude. The phenomenon is not related to the dispersive waves generated from deep water effect, and is explained in terms of dispersive waves satisfying a model system obtained from the original one by suitable asymptotic expansion, truncated at various orders in the small parameter δ denoting the periodicity of the bathymetry.

The evolution of an initial Gaussian pulse $\eta(x, 0)$ centered at the origin is illustrated below at various times (see Figure 1). The accurate computations are

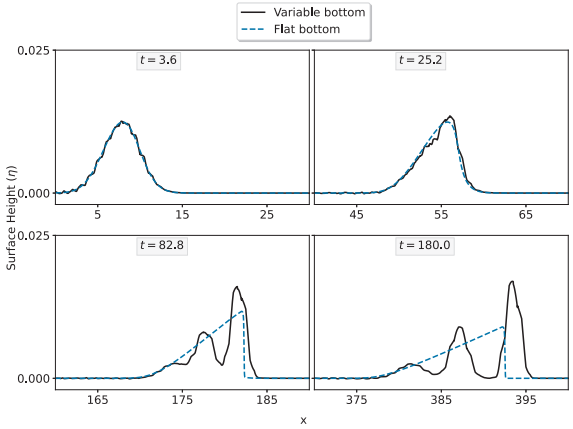

FIGURE 1. Evolution of an initial Gaussian pulse over periodic bathymetry. The surface elevation is shown, measured in meters. For comparison, the dashed blue line shows the solution for flow over a flat bottom.

obtained using package *SharpClaw* [2], which is based on WENO 5 reconstruction in space and Runge-Kutta 4 in time. The grid is refined until the relative error between the numerical solution obtained with Δx and with $\Delta x/2$ is less that 10^{-5}.

The numerical computation shows that the behaviour of the waves in presence of a periodic bathymetry is quite different than in the case of a flat bottom. In particular, no shock develops, rather several waves form, and evolve with a pattern characteristic of dispersive systems.

In order to understand the phenomenon, we adopted a technique developed by Yong and Kevorkian [3], and already adopted in a different context by LeVeque and Young [4].

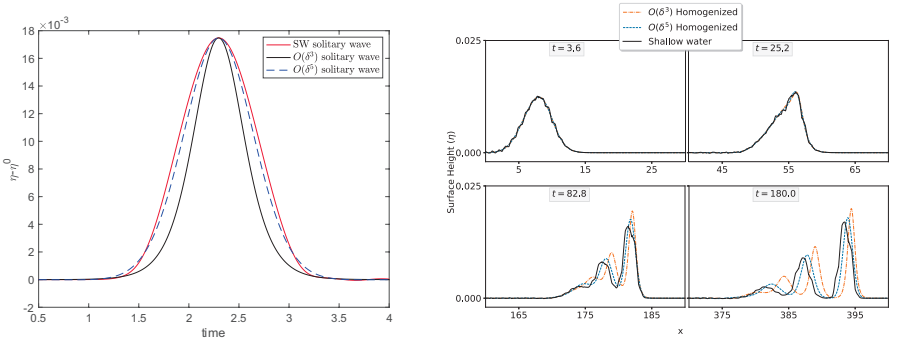

FIGURE 2. Comparison between the direct solution of the shallow water equations and the solutions of the homogenized equations. Left panel: comparison of the traveling waves, plotted as a function of time. The red line represents the value of $\eta(\bar{x}, t-\tau)$. The parameter τ is adjusted to align the computed solution with the traveling wave solutions. The black line is the $O(\delta^3)$-accurate solitary wave, while the blue dashed line is accurate up to $O(\delta^5)$. Right panel: time dependent solutions at various times. The bathymetry is piecewise constant. The surface elevation $\eta - \eta^0$ is shown, with the x-axis shifted to show the wave structure at each time.

The technique is based on the so called multiple scale expansion. The solution is assumed to depend on a slow variable x, on time t, and on a fast variable x/δ. The dependence on the latter, induced by the bathymetry, is assumed to be 1-periodic.

An asymptotic expansion of the solution in the small parameter δ is performed, and a set of equations with space independent coefficients is derived to various order in the small parameter δ. In particular the set of equations, neglecting terms of $O(\delta^3)$, takes the form

$$\eta_t + q_x = 0$$
$$q_t + c^2\eta_x + \delta\beta_1((q^2)_x - \eta q_x) + \delta^2(F_1(\eta, q, q_x, q_t) - \mu_1 q_{ttt}) = 0$$

with suitable function F_1. Linear stability analysis show that the initial value problem for this system is ill posed. To the same accuracy, one obtains a different form of the system, namely

$$\eta_t + q_x = 0$$
$$q_t + c^2\eta_x + \delta\alpha_0\left(c^2\eta\ \eta_x + (q^2)_x\right) + \delta^2(F_2(\eta, \eta_x, q, q_x) - \mu q_{xxt}) = 0$$

Linear stability analysis shows well posedness of such system for all wave numbers. A similar system, which contains fifth order derivatives, can be derived by continuing the expansion and neglecting terms of $O(\delta^5)$.

The two systems admit traveling waves that depend only on $\xi = x - Vt$. A comparison between the traveling waves of the homogenised systems and one that emerges from the original shallow water system is illustrated in Figure 2 together with a comparison between time dependent solutions.

In both cases, it is evident that by increasing the order of the expansion in δ the solution of the homogenised system become closer and closer to the numerical solution of the original shallow water system.

A similar behaviour is observed in several other hyperbolic systems, including the classical Euler equations of compressibe gas dynamics.

References

[1] David I. Ketcheson, L. Lóczi, and G. Russo, *An effective medium equation for weakly nonlinear shallow water waves over periodic bathymetry*, SIAM MMS, submitted.

[2] D. I. Ketcheson, M. Parsani, and R. J. LeVeque, *High-order Wave Propagation Algorithms for Hyperbolic Systems*, SIAM J. Sci. Comput., **35** (2013), A351–A377.

[3] D. H. Yong and J. Kevorkian, *Solving boundary-value problems for systems of hyperbolic conservation laws with rapidly varying coefficients*, Studies in Applied Mathematics, **108** (2002), 259–303.

[4] R. J. LeVeque and D. H. Yong, *Solitary waves in layered nonlinear media*, SIAM J. Appl. Math., **63** (2003), 1539–1560.

Compressible Navier-Stokes equations with potential temperature transport: strong solutions and conditional regularity

Andreas Schömer

(joint work with Mária Lukáčová-Medvid'ová)

A model for the fluid flow in meteorological applications is given by the compressible Navier-Stokes equations with potential temperature transport; see [2], [3]. Neglecting external forces such as gravity, this system reads

$$\begin{aligned} \partial_t \varrho + \operatorname{div}_{\mathbf{x}}(\varrho \mathbf{u}) &= 0, \\ \partial_t(\varrho \mathbf{u}) + \operatorname{div}_{\mathbf{x}}(\varrho \mathbf{u} \otimes \mathbf{u}) + \nabla_{\mathbf{x}} p(\varrho\theta) &= \operatorname{div}_{\mathbf{x}}(\mathbb{S}(\nabla_{\mathbf{x}}\mathbf{u})), \\ \partial_t(\varrho\theta) + \operatorname{div}_{\mathbf{x}}(\varrho\theta \mathbf{u}) &= 0, \end{aligned} \tag{1}$$

where ϱ denotes the density, $\mathbf{u}$ the velocity, and θ the potential temperature of the fluid. The viscous stress tensor $\mathbb{S}$ is given by

$$\mathbb{S}(\nabla_{\mathbf{x}}\mathbf{u}) = \mu\left(\nabla_{\mathbf{x}}\mathbf{u} + (\nabla_{\mathbf{x}}\mathbf{u})^T - \frac{2}{3}\operatorname{div}_{\mathbf{x}}(\mathbf{u})\,\mathbb{I}\right) + \lambda \operatorname{div}_{\mathbf{x}}(\mathbf{u})\,\mathbb{I}$$

with the viscosity constants $\mu > 0$, $\lambda \geq -\mu/3$. The system is closed by the pressure state equation

$$p(\varrho\theta) = a(\varrho\theta)^\gamma$$

with constants $a > 0$ and $\gamma > 1$. Weak solutions to (1) are known to exist under the assumption $\gamma \geq 9/5$; see [10, Theorem 1]. However, the physically relevant values of the adiabatic index γ lie in the interval $(1, 5/3]$. To circumvent this

problem, we can move on to the framework of dissipative measure-valued (DMV) solutions, where we can ensure existence of solutions to (1) for all $\gamma > 1$; see [5]. It should be noted that there is a DMV-strong uniqueness principle for (1) stating that if there are a DMV solution and a strong solution to (1) emanating from the same initial data, then they coincide as long as the latter exists; see [4].

The aim of this talk (based on [6]) is to uncover the full importance of the DMV-strong uniqueness principle. To this end, we prove the local-in-time existence of strong solutions to (1) using the approach of Valli [8] and Valli, Zajączkowski [9] based on Schauder's fixed-point theorem. In a second step, we prove a conditional regularity result for the strong solution following Sun, Wang, Zhang [7] and Huang, Xin [1]. More precisely, we show the following result: If the maximal existence time $T_{\max}$ of the strong solution is finite, then

$$\limsup_{t \uparrow T_{\max}} (||\varrho(t)||_{L^\infty} + ||\mathbf{u}(t)||_{L^\infty}) = \infty.$$

Consequently, if the density and the velocity remain uniformly bounded, then the strong solution is global in time and, in particular, every DMV solution starting from the same initial data coincides with it.

References

[1] X. Huang and Z. Xin, *A blow-up criterion for classical solutions to the compressible Navier-Stokes equations*. Sci. China Math., **53** (2010), 671–686.

[2] R. Klein, *An applied mathematical view of meteorological modelling*, In: Applied Mathematics Entering the 21st Century, pp. 227–269. SIAM, Philadelphia, PA, 2004.

[3] M. Lukáčová-Medvid'ová, J. Rosemeier, P. Spichtinger, and B. Wiebe, *IMEX Finite Volume Methods for Cloud Simulation*. In: Finite Volumes for Complex Applications VIII - Hyperbolic, Elliptic and Parabolic Problems, pp. 179–187. Springer International Publishing, Cham, 2017.

[4] M. Lukáčová-Medvid'ová and A. Schömer, *Compressible Navier–Stokes equations with potential temperature transport: stability of the strong solution and numerical error estimates*, **25**(1), 2023.

[5] M. Lukáčová-Medvid'ová and A. Schömer, *Existence of dissipative solutions to the compressible Navier-Stokes system with potential temperature transport*. J. Math. Fluid Mech., **24**(82), 2022.

[6] M. Lukáčová-Medvid'ová and A. Schömer, *Compressible Navier-Stokes equations with potential temperature transport: strong solutions and conditional regularity*. (in preparation)

[7] Y. Sun, C. Wang, and Z. Zhang, *A Beale–Kato–Majda blow-up criterion for the 3-D compressible Navier–Stokes equations*. J. Math. Pures Appl., **95**(2011), 36–47.

[8] A. Valli, *Periodic and stationary solutions for compressible Navier-Stokes equations via a stability method*, Ann. Sc. Norm. Super. Pisa Cl. Sci., **10** (1983), 607–647.

[9] A. Valli and W. M. Zajączkowski, *Navier-Stokes equations for compressible fluids: global existence and qualitative properties of the solutions in the general case*. Comm. Math. Phys., **103** (1986), 259–296.

[10] D. Maltese, M. Michálek, P. B. Mucha, A. Novotný, M. Pokorný, and E. Zatorska, *Existence of weak solutions for compressible Navier-Stokes equations with entropy transport*. J. Differential Equations, **261** (2016), 4448–4485.

Monte Carlo for random Navier–Stokes–Fourier system

Bangwei She
(joint work with Mária Lukáčová-Medvid'ová, Yuhuan Yuan)

Randomness is an inherent property of models in science and engineering. Model parameters as well as initial and boundary data are typically known only from observations or measurements that can be affected by several errors. In order to investigate data uncertainty in the solution of an underlying model, different methods have been developed in the recent years. Monte Carlo method that is based on statistical sampling is probably the most popular among them.

The aim of the present paper is to rigorously analyze Monte Carlo method for heat conductive, viscous compressible fluid flows subjected to random data. We recall the Navier–Stokes–Fourier system governing the motion of such fluid flows

$$\begin{aligned}
\partial_t \varrho + \nabla \cdot (\varrho \mathbf{u}) &= 0,\\
\partial_t(\varrho \mathbf{u}) + \nabla \cdot (\varrho \mathbf{u} \otimes \mathbf{u}) + \nabla p &= \nabla \cdot \mathbb{S}(\mu, \lambda, \nabla \mathbf{u}) + \varrho \mathbf{g},\\
c_v(\partial_t(\varrho \vartheta) + \nabla \cdot (\varrho \mathbf{u} \vartheta)) - \kappa \Delta \vartheta &= \mathbb{S}(\mu, \lambda, \nabla \mathbf{u}) : \nabla \mathbf{u} - p \nabla \cdot \mathbf{u},\\
c_v = 1/(\gamma - 1),\ \gamma > 1,\ \mathbb{S}(\mu, \lambda, \nabla \mathbf{u}) &= \mu\Big(\nabla \mathbf{u} + \nabla^t \mathbf{u} - \frac{2}{d} \nabla \cdot \mathbf{u} \mathbb{I}\Big) + \lambda \nabla \cdot \mathbf{u} \mathbb{I}
\end{aligned}$$

on $\mathbb{T} \equiv \big([-1,1]|_{\{-1,1\}}\big)^d$, $d = 2, 3$, with the initial data

$$\varrho(0, \cdot) = \varrho_0,\ \mathbf{u}(0, \cdot) = \mathbf{u}_0,\ \vartheta(0, \cdot) = \vartheta_0.$$

Here $\varrho, \mathbf{u}$ and ϑ are the fluid density, velocity, and absolute temperature, respectively. For pressure p, we assume the perfect gas law, i.e. $p = \varrho\, \vartheta$. Further, γ is the adiabatic coefficient, c_v is the specific heat per constant volume.

We consider the initial data, external force, viscosity coefficients, and heat conductivity coefficient as *random model data*

driving force ..... $\mathbf{g} = \mathbf{g}(\mathbf{x})$;
viscosity coefficients ..... $\mu > 0$, $\lambda \geq 0$;
heat conductivity coefficient ..... $\kappa > 0$;
initial data ..... ϱ_0, $\mathbf{u}_0$, ϑ_0.

In order to study such a problem numerically, we combine Monte Carlo method with a convergent finite volume (FV) method [3]. Our goal is to derive rigorous convergence and error analysis both with respect to statistical sampling as well as space-time discretizations. Although Monte Carlo approximations, such as Monte Carlo FV methods, are routinely used for uncertainty quantification in computational fluid dynamics or in meteorology, their rigorous convergence and error analysis for compressible viscous and heat conducting fluid flows is still missing in the literature. This paper presents the first results in this direction.

We refer to our recent work [4], where convergence and error estimates of a Monte Carlo FV method for the random compressible barotropic Navier–Stokes system were analyzed. In contrary to the viscous barotropic case, the analysis of heat conductive viscous compressible fluid flow is more involved. First, the existence of global weak solution for the Navier–Stokes–Fourier equations with

perfect gas law $p = \varrho\vartheta$ is an open problem. There are only some results on the global-in-time existence of weak solutions available, however certain structural restrictions on p, e, s and the coefficients μ, κ are required, see [5, Theorem 3.1].

One of the main tool in the convergence analysis of deterministic discretization methods, e.g. FV methods, is the so-called *weak-strong uniqueness principle* [2]. This means that a generalized solution (dissipative weak solution), that is identified as a limit of a sequence of discrete solutions, coincides with the strong solution as long as the latter exists. Second problem lies in the fact that the (dissipative) weak-strong uniqueness results are only conditional for the Navier–Stokes–Fourier system, see [1]. For example, boundedness of density and temperature has to be assumed for the weak-strong uniqueness principle.

The structure of the paper is organized as follows. Firstly, we present statistical analysis of Monte Carlo estimators for the expectation and deviation of the statistical strong solution to the Navier-Stokes-Fourier system. Secondly, we show the convergence of a finite volume method with random data by applying genuine stochastic compactness arguments under the assumption that the numerical density and temperature are bounded in probability. Consequently, we derive the main results of this paper: convergence and error estimates of Monte Carlo FV method for the random Navier–Stokes–Fourier system. Finally, several numerical results are presented to illustrate the theoretical results.

References

[1] J. Březina, E. Feireisl, and A. Novotný, *Stability of strong solutions to the Navier-Stokes-Fourier system*, SIAM J. Math. Anal., **52** (2020), 1761–1785.

[2] E. Feireisl, M. Lukáčová-Medvid'ová, H. Mizerová, and B. She, *Numerical Analysis of Compressible Fluid Flows*, Springer-Verlag, Cham, 2021.

[3] E. Feireisl, M. Lukáčová-Medvid'ová, H. Mizerová, and B. She, *On the convergence of a finite volume method for the Navier–Stokes–Fourier system*, IMA J. Numer. Anal., **41** (2021), 2388-2422.

[4] E. Feireisl, M. Lukáčová-Medvid'ová, B. She, and Y. Yuan, *Convergence and error analysis of compressible fluid flows with random data: Monte Carlo method*, Math. Models Methods Appl. Sci., **32** (2022), 2887–2925.

[5] E. Feireisl and A. Novotný, *Singular Limits in Thermodynamics of Viscous Fluids*, Birkhäuser–Basel, 2017.

High-order alternative finite difference WENO (A-WENO) schemes and their applications

Chi-Wang Shu

The essentially non-oscillatory (ENO) and weighted ENO (WENO) finite difference schemes are popular high order numerical methods for solving hyperbolic conservation laws, balance laws and related equations. Comparing with finite volume ENO/WENO schemes, finite difference schemes have a dimension by dimension feature and are much cheaper in computational cost for multi-dimensional problems. Most finite difference ENO/WENO solvers are based on the Shu-Osher lemma [4], converting the design of numerical flux in a conservative finite difference

scheme to that of the one-dimensional finite volume reconstruction. This approach has the advantage of simplicity and easiness in coding, as the same finite volume reconstruction routine can be used in the finite difference code. For this reason, the original approach in the Shu-Osher 1988 JCP paper [3], which is based on ENO interpolation rather than on ENO reconstruction, had largely been forgotten until 2013, when Jiang, Shu and Zhang revived this "alternative formulation" and used it to obtain more effective WENO schemes with Lax-Wendroff time discretization and for free-stream preserving [1, 2]. Later referred to as alternative WENO, or A-WENO, this approach has recently been explored to yield several interesting results, including effective finite difference A-WENO schemes for compressible two-medium flows [7], local characteristic decomposition free high order finite difference A-WENO schemes for hyperbolic systems endowed with a coordinate system of Riemann invariants [5], and a high-order well-balanced A-WENO method with the exact conservation property for certain systems of hyperbolic balance laws [6]. In this talk we survey the A-WENO schemes and their recent applications.

References

[1] Y. Jiang, C.-W. Shu, and M. Zhang, *An alternative formulation of finite difference weighted ENO schemes with Lax-Wendroff time discretization for conservation laws*, SIAM Journal on Scientific Computing, **35** (2013), A1137–A1160.

[2] Y. Jiang, C.-W. Shu, and M. Zhang, *Free-stream preserving finite difference schemes on curvilinear meshes*, Methods and Applications of Analysis, **21** (2014), 1–30.

[3] C.-W. Shu and S. Osher, *Efficient implementation of essentially non-oscillatory shock-capturing schemes*, Journal of Computational Physics, **77** (1988), 439–471.

[4] C.-W. Shu and S. Osher, *Efficient implementation of essentially non-oscillatory shock-capturing schemes, II*, Journal of Computational Physics, **83** (1989), 32–78.

[5] Z. Xu and C.-W. Shu, *Local characteristic decomposition free high order finite difference WENO schemes for hyperbolic systems endowed with a coordinate system of Riemann invariants*, SIAM Journal on Scientific Computing, to appear.

[6] Z. Xu and C.-W. Shu, *A high-order well-balanced alternative finite difference WENO (A-WENO) method with the exact conservation property for systems of hyperbolic balance laws*, Preprint.

[7] F. Zheng, C.-W. Shu, and J. Qiu, *A high order conservative finite difference scheme for compressible two-medium flows*, Journal of Computational Physics, **445** (2021), 110597.

Computing statistical Navier–Stokes solutions

Stephan Simonis

(joint work with Siddhartha Mishra)

We develop stochastic lattice Boltzmann methods (LBMs) for efficiently approximating statistical solutions to the incompressible Navier–Stokes equations (NSE) in three spatial dimensions. Entropic space-time adaptive kinetic relaxation frequencies allow for stable and consistent numerical solutions with decreasing viscosity. Single level Monte Carlo (MC) and stochastic Galerkin (SG) methods (Zhong *et al.*, 2024) are used to approximate responses, e.g. from random perturbations

of the initial flow field. The novel schemes are implemented in the parallel C++ data structure *OpenLB* (Krause *et al.*, 2021) and executed on heterogeneous high-performance computing machinery[1]. In exploratory computations, we observe scaling of the energy spectra and structure functions in terms of Kolmogorov's K41 theory. For the first time, we compute along the inviscid limit (Fjordholm *et al.*, 2021) of statistical solutions of the incompressible NSE toward weak-strong unique statistical solutions of the incompressible EE in three dimensions.

Let $\Omega \subseteq \mathbb{R}^d$ and $I \subseteq \mathbb{R}_+$. The force-free, incompressible NSE for modeling viscous ($\varepsilon > 0$) Newtonian fluid flows read

$$\begin{cases} \operatorname{div}(\boldsymbol{u}) = 0 & \text{in } \Omega \times I, \\ \partial_t \boldsymbol{u} + \operatorname{div}_{\boldsymbol{x}}(\boldsymbol{u} \otimes \boldsymbol{u}) - \varepsilon \boldsymbol{\Delta}_{\boldsymbol{x}} \boldsymbol{u} + \boldsymbol{\nabla}_{\boldsymbol{x}} p = \boldsymbol{0} & \text{in } \Omega \times I, \\ \boldsymbol{u}|_{t=0} = \overline{\boldsymbol{u}} & \text{in } \Omega, \end{cases} \tag{1}$$

where $\boldsymbol{u}\colon \Omega \times I \to U \coloneqq \mathbb{R}^d$, $d \in \{2, 3\}$ is the flow velocity, $p\colon \Omega \times I \to \mathbb{R}$ denotes the rescaled pressure (Lagrange multiplier), $\varepsilon > 0$ is the kinematic viscosity, and $\overline{\boldsymbol{u}}\colon \Omega \to \mathbb{R}^d$ is the initial data $\overline{\boldsymbol{u}} \in L^2_{\operatorname{div}}(\Omega; U)$. An inviscid flow assumption ($\varepsilon \to 0$) reduces the NSE (1) to the incompressible EE. Let $\boldsymbol{u}_0 = \overline{\boldsymbol{u}} + \boldsymbol{s}$, where $\boldsymbol{s}$ is a random vector, such that $\boldsymbol{u}_0 \sim \mu_0^\varepsilon$. Statistical solutions of the NSE (Foiaş and Prodi, 1976) are time-parametrized Young measures $\boldsymbol{\mu}^\varepsilon = (\mu_t^\varepsilon)_{0 \le t \le T}$ on $L^2_{\operatorname{div}}(\Omega; U)$ (see Definition 3.6 in Fjordholm *et al.*, 2021, and references therein). It is proven by Fjordholm *et al.* (2021) that statistical solutions of the NSE limit to inviscid statistical solutions of the EE for $\varepsilon \to 0$ under a weak scaling assumption on the structure functions $|S^2(\tau, r)| < Cr^\alpha$, where $\alpha > 0$ and $\tau \in (0, T]$, $r > 0$ (see e.g. Lye (2020), Theorem 3.1.1.(iii) for a definition of S^p). For small ε,

$$E_T(\mu_t^\varepsilon, \kappa) = \int_0^T \int_{L^2_{\operatorname{div}}} E(\kappa, t) \, \mathrm{d}\mu_t^\varepsilon(\boldsymbol{u}) \, \mathrm{d}t \lesssim \kappa^{-2\beta} \quad \Rightarrow \quad S^2(T, r) \lesssim r^{\beta - 1/2}, \tag{2}$$

where $1 < 2\beta < 3$ (here $\beta = \frac{5}{6}$) and $E(\kappa, t)$ is the band-averaged energy spectrum (Lanthaler *et al.*, 2021a). If the energy spectrum scales according to (2), then a limit statistical solution of the EE exists. Further, weak-strong uniqueness of statistical solutions is based on the p-Wasserstein distance

$$W_p(\mu_t^\Delta, \mu_t^{\mathrm{ref}}) = \left(\inf_{\pi \in \Pi\left(\mu_t^\Delta, \mu_t^{\mathrm{ref}}\right)} \int_{X^2} |x - y|^p \, \mathrm{d}\pi(x, y) \right)^{\frac{1}{p}}, \tag{3}$$

where $\pi \in \Pi(\mu, \rho) \subset \mathcal{P}(X^2)$ are transport plans between $\mu, \rho \in \mathcal{P}(X)$ with finite p-moments and $\forall F, G \in C_b(X)\colon \int_{X^2} F(x) + G(y) \, \mathrm{d}\pi(x, y) = \int_X F(x) \, \mathrm{d}\mu(x) + \int_X G(y) \, \mathrm{d}\rho(y)$ on the separable Banach space X. Let $1 \le p < \infty$. According to Lanthaler *et al.* (2021a, 2021b), weak convergence of $\{\boldsymbol{\mu}^\Delta\}_{\Delta > 0}$ to a reference solution $\boldsymbol{\mu}^{\mathrm{ref}}$ is obtained by $\boldsymbol{\mu}^\Delta \rightharpoonup \boldsymbol{\mu}^{\mathrm{ref}} \Leftrightarrow W_p\left(\boldsymbol{\mu}^\Delta, \boldsymbol{\mu}^{\mathrm{ref}}\right) \to 0$. We provide exploratory computations using MC LBMs with entropic multi-relaxation (Karlin

[1]S. Simonis acknowledges support by the state of Baden-Württemberg through bwHPC.

et al., 2014) in *OpenLB*. Given the spatial grid resolution N and initial data $\mu_0^\varepsilon \in \mathcal{P}(L^2_{\mathrm{div}})$, we generate M independent and identically distributed samples

$$\left\{ \boldsymbol{u}_0^{(1)}, \boldsymbol{u}_0^{(2)}, \ldots, \boldsymbol{u}_0^{(M)} \right\} \sim \mu_0^\varepsilon,$$

which are evolved in time $t > 0$ with LBMs to obtain $\{\boldsymbol{u}^{(m)} | m = 1, 2, \ldots, M\}$. Thus, for $\varepsilon \to 0$, a weak-strog unique statistical solution is approximated by

$$\mu_t^\varepsilon \approx \mu_t^{\varepsilon,N,M} := \frac{1}{M} \sum_{m=1}^{M} \delta_{\boldsymbol{u}^{(m)}(t)},$$

where $\delta_{\boldsymbol{u}^{(m)}(t)}$ is the Dirac measure at $\boldsymbol{u}^{(m)}(t)$. We compute the flow field from a uniformly randomized Taylor–Green vortex (RTGV) initial condition (samples and mean fields shown in Fig. 1) and observe that the scaling assumption holds (see Simonis *et al.* (2024)). The convergence of the Wasserstein distance toward the fine resolution reference (see Fig. 2) approves the analytical results of Fjordholm *et al.* (2021). Conclusively, we provide first computational evidence of weak convergence of statistical solutions of the NSE toward weak-strong unique statistical solutions of the EE in three dimensions. In future research, we will apply SG LBMs (Zhong *et al.*, 2024) to initial boundary value problems of turbulent fluid flows.

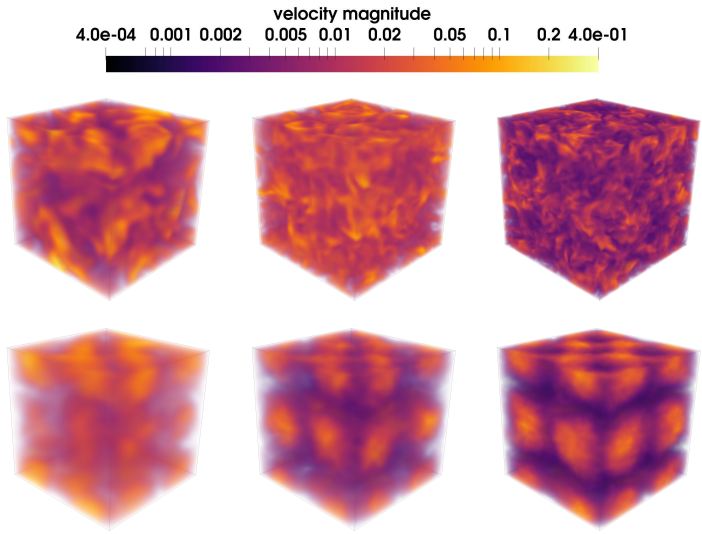

FIGURE 1. Velocity field iso-volumes of RTGV flow $t \approx 30$s. Single sample computations (top row) and expected mean (bottom row) for $Re = 1280, 2560, 5120$ (row-wise from left to right).

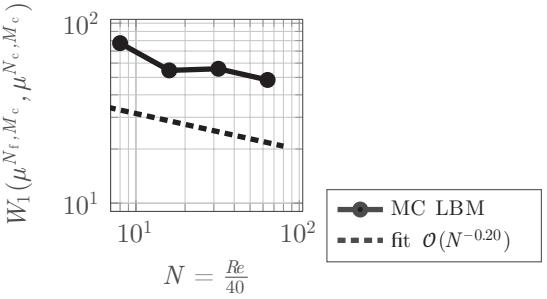

FIGURE 2. Approximated 1-Wasserstein distances (3) at $t \approx 30$s (Algorithm A.2.2 in Lye, 2020), with fine $(\cdot_f)$ and coarse $(\cdot_c)$ samples and resolutions $(M_f, M_c) = (N_f, N_c)$.

REFERENCES

[1] U. S. Fjordholm, S. Mishra, and F. Weber, *On the vanishing viscosity limit of statistical solutions of the incompressible Navier–Stokes equations*, ArXiv preprint (2021). doi: 10.48550/ARXIV.2110.04674

[2] C. Foias and G. Prodi, *Sur les solutions statistiques des équations de Navier-Stokes*, Annali di Matematica Pura ed Applicata **111**(1) (1976), 307–330. doi: 10.1007/BF02411822

[3] I. V. Karlin, F. Bösch, and S. S. Chikatamarla, *Gibbs' principle for the lattice-kinetic theory of fluid dynamics*, Physical Review E **90**(3) (2014), 031302. doi: 10.1103/PhysRevE.90.031302

[4] M. J. Krause, A. Kummerländer, S.J. Avis, H. Kusumaatmaja, D. Dapelo, F. Klemens, M. Gaedtke, N. Hafen, A. Mink, R. Trunk, J. E. Marquardt, M.-L. Maier, M. Haussmann, and S. Simonis, *OpenLB—Open source lattice Boltzmann code*, Computers & Mathematics with Applications **81** (2021), 258–288. doi: 10.1016/j.camwa.2020.04.033

[5] S. Lanthaler, S. Mishra, and C. Parés-Pulido, *Statistical solutions of the incompressible Euler equations*, Mathematical Models and Methods in Applied Sciences **31**(02) (2021a), 223–292. doi: 10.1142/S0218202521500068

[6] S. Lanthaler, S. Mishra, and C. Parés-Pulido, *On the conservation of energy in two-dimensional incompressible flows*, Nonlinearity **34**(2) (2021b), 1084. doi: 10.1088/1361-6544/abb452

[7] K.O. Lye, *Computation of statistical solutions of hyperbolic systems of conservation laws*, ETH Zürich (2020), Doctoral thesis. doi: 10.3929/ethz-b-000432014

[8] S. Simonis, T. Rohner, and S. Mishra, *Computing statistical Navier–Stokes solutions with stochastic lattice Boltzmann methods*, *In preparation* (2024).

[9] M. Zhong, T. Xiao, M.J. Krause, M. Frank, and S. Simonis, *A stochastic Galerkin lattice Boltzmann method for incompressible fluid flows with uncertainties*, SSRN preprint (2024). doi: 10.2139/ssrn.4739337

Vanishing viscosity solutions of characteristic initial-boundary value problems for systems of conservation laws

Laura V. Spinolo
(joint work with Fabio Ancona, Andrea Marson)

In the recent work [2] we consider a nonlinear systems of conservation laws in one space variable

$$\mathbf{g}(\mathbf{v})_t + \mathbf{f}(\mathbf{v})_x = \mathbf{0}_N \tag{1}$$

where the unknown $\mathbf{v}$ attains values in $\mathbb{R}^N$ and $\mathbf{g}, \mathbf{f} : \mathbb{R}^N \to \mathbb{R}^N$ are smooth functions satisfying suitable assumptions that we touch upon in the following. The archetype of (1) are the celebrated compressible Euler equations modeling the dynamics of an ideal, compressible fluid. Other famous examples include the inviscid Magneto-Hydro-Dynamic (MHD) equations describing the propagation of plane waves in an electrically charged, compressible and ideal fluid.

Formally, the inviscid system (1) can be recovered as the $\varepsilon \to 0^+$ limit of the viscous approximation

$$\mathbf{g}(\mathbf{v}^\varepsilon)_t + \mathbf{f}(\mathbf{v}^\varepsilon)_x = \varepsilon\Big(\mathbf{D}(\mathbf{v}^\varepsilon)\mathbf{v}^\varepsilon_x\Big)_x, \quad \mathbf{v} \in \mathbb{R}^N, \tag{2}$$

where $\mathbf{D}$ is a positive semi-definite $N \times N$ matrix depending on the physical model under consideration. For instance, the compressible Navier-Stokes (or Navier-Stokes-Fourier) equations and the viscous MHD equations are the most obvious choices for approximating the Euler and inviscid MHD equations, respectively. Coupling (1) with the underlying viscous mechanism (2) is of particular importance in the case of initial-boundary value problems since, even in the most elementary linear case, the limit in general depends on $\mathbf{D}$ and changes as $\mathbf{D}$ changes, see [7]. Note however that establishing convergence of the physical viscosity approximation (2) is presently a challenging open question, for both Cauchy and initial-boundary value problems.

In the physical cases of the fluid-dynamics and MHD equations, the matrix $\mathbf{D}$ in (2) is singular (non-invertible), which poses severe additional technical challenges for the analysis of the inviscid limit. As an instance of this fact, the initial-boundary value problem for (2) is in general overdetermined if one imposes a *full* boundary condition like $\mathbf{v}^\varepsilon(t,0) = \mathbf{v}_b(t)$. To restore well-posedness, we couple (2) with the initial and boundary conditions

$$\mathbf{v}^\varepsilon(0,\cdot) = \mathbf{v}_0, \qquad \widetilde{\boldsymbol{\beta}}(\mathbf{v}^\varepsilon(\cdot,0), \mathbf{v}_b) = \mathbf{0}_N, \tag{3}$$

where $\widetilde{\boldsymbol{\beta}}$ is a suitable function defined in [2, §2.2]. At the heuristic level, the basic idea underpinning the construction of $\widetilde{\boldsymbol{\beta}}$ is imposing a full boundary condition on the *parabolic* component of $\mathbf{v}^\varepsilon$, and a boundary condition along the characteristic fields of the *hyperbolic* component entering the domain.

In [2] we regard the initial-boundary value problem for (1) as the vanishing viscosity limit of system (1) coupled with the initial and boundary conditions (3).

This is expressed through the boundary condition, that we assign on (1) as in the below equation:

$$\mathbf{v}(0,\cdot) = \mathbf{v}_0, \qquad \mathbf{v}(\cdot,0) \sim_{\mathbf{D}} \mathbf{v}_b. \tag{4}$$

If we assume that every vector field for (1) is either genuinely nonlinear or linearly degenerate, the relation $\sim_{\mathbf{D}}$ is defined as follows.

Definition 3. *Given system* (2) *and* $\bar{\mathbf{v}}$, $\mathbf{v}_b \in \mathbb{R}^N$, *we say that "*$\bar{\mathbf{v}} \sim_{\mathbf{D}} \mathbf{v}_b$*" if there is* $\underline{\mathbf{v}} \in \mathbb{R}^N$ *such that the following conditions are both satisfied:*

i) $\mathbf{f}(\bar{\mathbf{v}}) = \mathbf{f}(\underline{\mathbf{v}})$ *and the* 0*-speed discontinuity between* $\bar{\mathbf{v}}$ *(on the right) and* $\underline{\mathbf{v}}$ *(on the left) satisfies the Lax admissibility condition;*

ii) *there is a so-called "boundary layer"* $\mathbf{w} : \mathbb{R}_+ \to \mathbb{R}^N$ *such that*

$$\begin{cases} \mathbf{D}(\mathbf{w})\mathbf{w}' = \mathbf{f}(\mathbf{w}) - \mathbf{f}(\underline{\mathbf{v}}) \\ \widetilde{\boldsymbol{\beta}}(\mathbf{w}(0), \mathbf{v}_b) = \mathbf{0}, \quad \lim_{y\to+\infty} \mathbf{w}(y) = \underline{\mathbf{v}}. \end{cases} \tag{5}$$

Note that, in the above definition, the need for considering the state $\underline{\mathbf{v}}$ stems from the fact that we deal with the boundary characteristic case, namely we take into account the possibility that an eigenvalue of the jacobian matrix $\mathbf{Df}$ vanishes. This happens in the case of the Euler and inviscid MHD equations if for instance the fluid velocity vanishes. Note furthermore that if the boundary characteristic field is linearly degenerate condition i) in Definition 3 boils down to the requirement that $\mathbf{f}(\bar{\mathbf{v}}) = \mathbf{f}(\underline{\mathbf{v}})$. The main result of [2] reads as follows.

Theorem 8. *Assume Hypotheses* $1, \cdots, 5$ *in* [2, §2] *and fix* $\mathbf{v}^* \in \mathbb{R}^N$*; then there is a constant* $\delta^* > 0$ *only depending on the functions* $\mathbf{g}$, $\mathbf{f}$, $\mathbf{D}$ *in system* (2) *such that the following holds. If* $\mathbf{v}_0, \mathbf{v}_b \in BV(\mathbb{R}_+)$ *satisfy*

$$\text{TotVar } \mathbf{v}_0 + \text{TotVar } \mathbf{v}_b + |\mathbf{v}_0(0^+) - \mathbf{v}_b(0^+)| \le \delta^*, \quad |\mathbf{v}_0(0^+) - \mathbf{v}^*| \le \delta^* \tag{6}$$

there is a global-in-time, Lax admissible distributional solution $\mathbf{v} \in BV_{\text{loc}}(\mathbb{R}_+ \times \mathbb{R}_+)$ *of* (1) *satisfying the initial and boundary conditions* (4) *in the sense of traces. Also, if system* (1) *admits a convex entropy then the solution we construct is entropy admissible.*

In the statement of the above result, TotVar $\mathbf{v}$ and BV denote the total variation of the function $\mathbf{v}$ and the space of bounded total variation functions. To the best of our knowledge, Theorem 8 yields the first global existence result for the initial-boundary value problem (1),(4) in the boundary characteristic case. Note indeed that the boundary condition considered in the related work [1] is different from (4) and in general is not consistent with the underlying viscous approximation (2). Note furthermore that Hypotheses $1, \cdots, 5$ in [2, §2] are satisfied by the Navier-Stokes-Fourier and viscous MHD equations (with both null and positive electrical resistivity) written in both Eulerian and Lagrangian coordinates. The small total variation assumption (6) is obviously highly restrictive, but also necessary to establish global-in-time existence of admissible solutions: in this regard we refer to the counterexamples in [8] and also the the more recent analysis in [6], which provides a strong indication of total variation blow up (starting from data of finite, but large, total variation) for the p-system of isentropic gas dynamics.

The proof of Theorem 8 relies on the introduction of a wave front-tracking algorithm inspired by [5]. This is a boon to the analysis, since it is known that limits of wave front-tracking approximations enjoy better regularity properties than general BV functions, see for instance [5, Chapter 10]. Also, the introduction of a wave front-tracking algorithm is pivotal to the proof of uniqueness results via the Standard Riemann Semigroup approach. We are confident one could use these techniques to establish uniqueness of the admissible solution of (1) satisfying (4), but this was left open in [2] due to the considerable length and technicality of the proof of Theorem 8.

Compared to the wave front-tracking analysis in [5], the main difficulty posed by the presence of the boundary is dealing with interactions between the wave fronts and the boundary. This is particularly challenging in the boundary characteristic case, where there is no clear discrimination between wave fronts entering and leaving the domain and in principle very complicated interaction patterns can arise, with wave fronts bouncing back and forth from the boundary. In [2], we tackle this challenge by carefully controlling the strength of the wave fronts entering the domain after an interaction at the boundary. These estimates and the consequent introduction of a new Glimm-type functional are in our opinion one of the most innovative points of the whole paper from the technical standpoint, and their proof relies on the very detailed analysis of the structure of the so-called boundary Riemann problem performed in [3, 4]. Another innovative point in [2] is the proof of the fact that the limit of the wave front-tracking approximation satisfies the boundary condition (4), proof which requires a very precise analysis of the behavior of the wave fronts at the boundary and in turn we feel is of independent interest.

References

[1] D. Amadori, *Initial-boundary value problems for nonlinear systems of conservation laws*, NoDEA Nonlinear Differential Equations Appl. **4** (1997), 1–42.

[2] F. Ancona, A. Marson, and L. V Spinolo, *Existence of vanishing physical viscosity solutions of characteristic initial-boundary value problems for systems of conservation laws*, submitted. Also arXiv:2401.14865.

[3] S. Bianchini and L. V. Spinolo, *The boundary Riemann solver coming from the real vanishing viscosity approximation*, Arch. Ration. Mech. Anal., **191** (2009), 1–96.

[4] S. Bianchini and L. V. Spinolo, *Characteristic boundary layers for mixed hyperbolic-parabolic systems in one space dimension and applications to the Navier-Stokes and MHD equations*, Comm. Pure Appl. Math., **73** (2020), 2180–2247.

[5] A. Bressan, *Hyperbolic systems of conservation laws, volume 20 of Oxford Lecture Series in Mathematics and its Applications*, Oxford University Press, 2000.

[6] A. Bressan, G. Chen, and Q. Zhang, *On finite time BV blow-up for the p-system.* Comm. Partial Differential Equations **43** (2018), 1242–1280.

[7] M. Gisclon, *Étude des conditions aux limites pour un système strictement hyperbolique, via l'approximation parabolique*, J. Math. Pures Appl. **75** (1996), 485–508.

[8] H. K. Jenssen, *Blowup for systems of conservation laws*, SIAM J. Math. Anal. **31** (2000), 894–908.

[9] D. Serre, *Systems of conservation laws. 1 & 2* Cambridge University Press, 1999.

Runge-Kutta methods are stable

Eitan Tadmor

We consider the class of Runge-Kutta (RK) methods for the approximate integration of *arbitrarily large* systems of ODEs, $\dot{\mathbf{y}} = \mathbf{F}(t, \mathbf{y})$. The *linearized stability* of such methods is concerned with the behavior of the RK iterations

$$\mathbf{u}_{n+1} = \mathcal{P}_s(\Delta t \mathbb{L}_N)\mathbf{u}_n, \quad n = 0, 1, \dots. \tag{1}$$

Here $\mathbb{L}_N$ is the $N \times N$ Jacobian matrix of $\mathbf{F}$ 'freezed' at arbitrary state, $\frac{\partial \mathbf{F}(t_*, \mathbf{y}(t_*))}{\partial \mathbf{y}}$, and $\mathcal{P}_s(z) = 1 + z + \sum_{k=2}^{s} a_k z^k$ is an s-stage RK method of interest; it is rth-order accurate, $r \le s$, if $|\mathcal{P}_s(z) - e^z| \le \mathcal{O}(|z|^{r+1})$. The stability of (1) is dictated by its region of absolute stability,

$$\mathcal{A}_s := \{z \ : \ |\mathcal{P}_s(z)| \le 1\}.$$

Specifically — let $\Lambda(\mathbb{L}_N)$ denote the spectrum of $\mathbb{L}_N$; then the RK iterations,

$$|\mathbf{u}_n| \le K|\mathbf{u}_0|, \qquad n = 1, 2, \dots, \tag{stability}$$

are *stable* in the sense of uniformly bounded growth, provided (1) is implemented with a small enough time step, Δt, so that,

$$\Delta t \Lambda(\mathbb{L}_N) \subset \mathcal{A}_s. \tag{2}$$

This notion of uniform bounded stability involves a constant K which is independent of n. However, this classical stability paradigm for RK methods, "(2) $\rightsquigarrow$ (stability)" *does not* hold uniformly in the increasingly large dimension N. Indeed, (2) fails to secure different notion of stability — power-boundedness, resolvent stability, strong stability, uniformly in N. Instead, in [5] we proved that uniform-in-N stability holds if we replace the spectrum $\Lambda(\mathbb{L}_N)$ with the larger set of *numerical range*, $W(\mathbb{L}_N) := \{\langle \mathbb{L}_N \mathbf{w}, \mathbf{w}\rangle \ : \ |\mathbf{w}| = 1\}$. Specifically assume that RK method is implemented with a small enough time step, Δt, so that,

$$\Delta t \cdot W(\mathbb{L}_N) \subset \mathcal{A}_s, \tag{3}$$

then we have the alternative paradigm, "(3) $\rightsquigarrow$ (stability)", with K uniformly bound both in n and in N; indeed, $K = 1 + \sqrt{2}$. The result is based on the remarkable work of M. Crouzeix on the numerical range $W(A)$ serving as K-spectral set of arbitrary matrix A, [1, 2].

To verify (3) requires the geometry of the numerical range, which is less accessible than the spectrum of a matrix. To this end assume that an *imaginary interval condition* holds, so that $\mathcal{A}_s$ includes a non-trivial interval along the imaginary axis, $[-i\mathcal{R}_s, i\mathcal{R}_s] \subset \mathcal{A}_s$. Clearly, such a condition is necessary for stability of all semi-bounded $\mathbb{L}$'s, which are encountered in hyperbolic systems. The imaginary interval condition was introduced in H. O. Kreiss et. al., [3, 4]; they proved that it implies $\mathcal{A}_s$ contains a non-trivial semi-disc, $B_{\mathcal{C}_s}(z) = \{\Re z \le 0; \ |z| \le \mathcal{C}_s\}$ with $0 < \mathcal{C}_s \le \mathcal{R}_s$, which in turn implies resolvent stability (but again, the passage to (stability) lacks uniformity in N).

For example, for classical 3rd-rd order RK method, RK3 one has $\mathcal{C}_3\mathcal{R}_3 = \sqrt{3}$; however for erg classical RK4, $\mathcal{C}_4 = 2.61$ which is more restrictive than the usual $\mathcal{R}_4 = 2\sqrt{2}$ encountered when using the standard (2). In[5] we prove uniform in N stability follows for small enough time step Δt such that

$$\Delta t \cdot r(\mathbb{L}_N) \le \mathcal{C}_s, \qquad r(A) := \max_{|\mathbf{w}|=1} |\langle A\mathbf{w}, \mathbf{w}\rangle|. \tag{4}$$

The implication "(4) $\rightsquigarrow$ (stability)" involves the *numerical radius* $r(\mathbb{L}_N)$ which can be estimated in many cases; in particular, since $\|A\| \le 2r(A)$ one can simply use the norm, $\Delta t\|\mathbb{L}_N\| \le \mathcal{C}_s/2$, which secures the (stability) uniform in N.

References

[1] M. Crouzeix, *Numerical range and functional calculus in Hilbert space*, J. Funct. Anal., **244** (2007), pp. 668–690.

[2] M. Crouzeix and C. Palencia, *The numerical range is a* $(1+\sqrt{2})$*-spectral set*, SIAM J. Matrix Anal. Appl., **38** (2017), pp. 649–655.

[3] H.-O. Kreiss and G. Scherer, *Method of lines for hyperbolic differential equations*, SINUM **29**(3), 1992, 640–646.

[4] H.-O. Kreiss and L. Wu, *On the stability definition of difference approximations for the initial boundary value problem*, Appl. Numerical Math., **12** (1-3) 1993, 213–227.

[5] E. Tadmor, *Runge-Kutta methods are stable*, ArXiv:2312.15546 (2023).

Stabilization of a Multi–Dimensional System of hyperbolic Balance Laws

Ferdinand Thein

(joint work with Michael Herty)

We are interested in the boundary feedback stabilization of multi–dimensional hyperbolic PDEs. Two cases are discussed in this talk. For each case a proper Lyapunov function is defined. With this we show stabilization in L^2 for the arising system using a suitable feedback control.

Consider the following initial boundary value problem (IBVP) for a given hyperbolic system

$$\begin{cases} \dfrac{\partial}{\partial t}\mathbf{w} + \displaystyle\sum_{k=1}^{d} \mathbf{A}^{(k)}(\mathbf{x})\frac{\partial}{\partial x_k}\mathbf{w}(t,\mathbf{x}) + \mathbf{B}(\mathbf{x})\mathbf{w}(t,\mathbf{x}) & = 0,\ (t,\mathbf{x}) \in [0,T)\times\Omega \\ \mathbf{w}(0,\mathbf{x}) & = \mathbf{w}_0(\mathbf{x}),\ \mathbf{x}\in\Omega, \\ \mathbf{w}(t,\mathbf{x}) & = \mathbf{w}_{BC}(t,\mathbf{x}), (t,\mathbf{x}) \in [0,T)\times\partial\Omega \end{cases} \tag{1}$$

Here $\mathbf{w} \equiv (w_1(t,\mathbf{x}),\dots,w_n(t,\mathbf{x}))^T$ is the vector of unknowns and $\Omega \subset \mathbb{R}^d$ a bounded domain with sufficiently smooth boundary $\partial\Omega$. Moreover, $\mathbf{A}^{(k)}$ and $\mathbf{B}$ are sufficiently smooth and bounded $n \times n$ real matrices. We define the matrix

$$\mathbf{A}^*(\mathbf{x},\nu) := \sum_{k=1}^{d} \nu_k \mathbf{A}^{(k)}(\mathbf{x})$$

with $\nu = (\nu_1, \dots, \nu_d)^T \in \mathbb{S}^{d-1}$ being a unit vector in $\mathbb{R}^d$. System (1) is said to be hyperbolic if the matrix $\mathbf{A}^*(\mathbf{x}, \nu)$ has n real eigenvalues $\lambda_i = \lambda_i(\mathbf{x}, \nu)$, $i = 1, \dots, n$, and n corresponding linearly independent right eigenvectors $\mathbf{r}_i = \mathbf{r}_i(\mathbf{x}, \nu), i = 1, \dots, n$ for all $\nu \in \mathbb{S}^{d-1}$. Note that by choosing

$$\nu = \mathbf{e}_k = (0, \dots, 0, \underbrace{1}_{k}, 0, \dots, 0)^T$$

we have $\mathbf{A}^*(\mathbf{x}, \mathbf{e}_k) = \mathbf{A}^{(k)}(\mathbf{x})$ and thus the individual Jacobians $\mathbf{A}^{(k)}(\mathbf{x})$ are also diagonalizable with real eigenvalues. The boundary $\partial\Omega$ will be separated in the controllable and uncontrollable part, i.e. for $i = 1, \dots, n$

$$\Gamma_i^+ := \{\, \mathbf{x} \in \partial\Omega \mid \lambda_i(\mathbf{x}, \mathbf{n}(\mathbf{x})) \geq 0 \},$$
$$\Gamma_i^- := \{\, \mathbf{x} \in \partial\Omega \mid \lambda_i(\mathbf{x}, \mathbf{n}(\mathbf{x})) < 0 \}.$$

Case 1: Diagonal Jacobians. Here we consider system (1) where the matrices $\mathbf{A}^{(k)}(\mathbf{x}) = (a_{ii}^{(k)}(\mathbf{x}))_{i=1,\dots,n}$ are assumed to be diagonal matrices and hence have a full set of eigenvectors. It is shown in [4] that such systems for example arise in the study of Hamilton–Jacobi equations. For the eigenvalues we have that $\lambda_i(\mathbf{x}, \mathbf{n}(\mathbf{x})) = \mathbf{a}_i(\mathbf{x}) \cdot \mathbf{n}(\mathbf{x})$ with $\mathbf{a}_i := (a_{ii}^{(1)}, \dots, a_{ii}^{(d)})$. We introduce the following abbreviations

$$\mathcal{E}(\mu(\mathbf{x})) := \operatorname{diag}(\exp(\mu_1(\mathbf{x})), \dots, \exp(\mu_n(\mathbf{x}))),$$
$$\mathcal{M}^{(k)}(\mathbf{x}) := \operatorname{diag}\left(\frac{\partial}{\partial x_k}\mu_1(\mathbf{x}), \dots, \frac{\partial}{\partial x_k}\mu_n(\mathbf{x})\right),\ k = 1, \dots, d.$$

The Lyapunov function is then defined as follows

$$L(t) = \int_\Omega \mathbf{w}(t, \mathbf{x})^T \mathcal{E}(\mu(\mathbf{x})) \mathbf{w}(t, \mathbf{x}) \, \mathrm{d}\mathbf{x} \tag{2}$$

where the functions $\mu_1(\mathbf{x}), \dots, \mu_n(\mathbf{x})$ are defined by

$$\sum_{k=1}^{d} \left(\mathcal{M}^{(k)} \mathbf{A}^{(k)} + \frac{\partial}{\partial x_k} \mathbf{A}^{(k)} \right) + \mathcal{D} = -\operatorname{diag}\left(C_L^{(i)}\right) \tag{3}$$

$$\text{or written row-wise} \quad \mathbf{a}_i \cdot \nabla \mu_i(\mathbf{x}) + \nabla \cdot \mathbf{a}_i + \mathcal{D}_{ii} = -C_L^{(i)},\ C_L^{(i)} \geq C_L > 0$$

for some value $C_L \in \mathbb{R}_{>0}$. Further, we assume that there exists a diagonal matrix $\mathcal{D}$ such that we have

$$-\mathbf{v}^T \left(\mathbf{B}^T \mathcal{E} + \mathcal{E} \mathbf{B} \right) \mathbf{v} \leq \mathbf{v}^T \mathcal{D} \mathcal{E} \mathbf{v},\ \forall \mathbf{v} \in \mathbb{R}^n. \tag{4}$$

This kind of dissipativity condition for the linear source term ensures that we find suited weights μ_i using (3). There are different possible choices for $\mathcal{D}$ depending on the problem under consideration. The imposed boundary controls $u_i, i \in \{1, \dots, n\}$ satisfy

$$-\sum_{i=1}^{n} \int_{\Gamma_i^-} u_i(t, \mathbf{x})^2 \, (\mathbf{a}_i \cdot \mathbf{n}) \exp(\mu_i(\mathbf{x})) \, \mathrm{d}\mathbf{x} \leq \sum_{i=1}^{n} \int_{\Gamma_i^+} w_i^2 \, (\mathbf{a}_i \cdot \mathbf{n}) \exp(\mu_i(\mathbf{x})) \, \mathrm{d}\mathbf{x}. \tag{5}$$

The main results states the exponential decay of the Lyapunov function under suited conditions, see [4, Main Thm.].

Case 2: Symmetric Hyperbolic Systems. Second, we study (1) being symmetric hyperbolic, i.e. the $\mathbf{A}^{(k)}(\mathbf{x})$ are in particular assumed to be symmetric. The assumption of symmetry is no major restriction since it includes all systems equipped with an additional conservation law, cf. [2]. This includes most systems relevant for applications, see [1].

For these systems there exists a well-conditioned orthogonal matrix $\mathbf{T}(\mathbf{x}, \nu)$ such that

$$\mathbf{\Lambda}^*(\mathbf{x}, \nu) = \mathbf{T}^T(\mathbf{x}, \nu)\mathbf{A}^*(\mathbf{x}, \nu)\mathbf{T}(\mathbf{x}, \nu) \tag{6}$$

It is further assumed that there exists a *feasible Lyapunov potential* $\overline{\mu}(\mathbf{x})$ such that

$$\overline{\mathbf{m}} := \nabla\overline{\mu}(\mathbf{x}) \quad \text{and} \quad \overline{\mathbf{A}}(\overline{\mathbf{m}}) := -\mathbf{Id} + \sum_{k=1}^{d} \overline{m}_k \mathbf{A}^{(k)} \geq 0. \tag{7}$$

Then the linear matrix inequality (LMI)

$$\mathbf{A}(\mathbf{m}) := C\mathbf{Id} + \sum_{k=1}^{d} m_k \mathbf{A}^{(k)} \leq 0,\ C \in \mathbb{R}_{>0} \tag{8}$$

holds for system (1) with $\mu(\mathbf{x}) = -C\overline{\mu}(\mathbf{x})$ and $\mathbf{m} = \nabla\mu(\mathbf{x})$. It is remarked in [5] that the LMI (8) can be modified if certain reminder terms, such as the coupling matrix $\mathbf{B}$, should be taken into account. Therefore we introduce with $\mathbf{B}^{sym} = \frac{1}{2}\left(\mathbf{B} + \mathbf{B}^T\right)$

$$\mathcal{R}(\mathbf{x}) := \sum_{k=1}^{d} \frac{\partial}{\partial x_k} \mathbf{A}^{(k)}(\mathbf{x}) - 2\mathbf{B}^{sym}(\mathbf{x})$$

and demand

$$\mathbf{A}(\mathbf{m}) := C\mathbf{Id} + \mathcal{R}(\mathbf{x}) + \sum_{k=1}^{d} m_k(\mathbf{x})\mathbf{A}^{(k)}(\mathbf{x}) \leq 0,\ C \in \mathbb{R}_{>0}. \tag{9}$$

The LMI (9) then replaces (8). For example in the case of $\mathcal{R}(\mathbf{x}) < 0$ we could benefit from this additional term in order to find suited coefficients $\mathbf{m}$. The Lyapunov function is then defined as follows

$$L(t) = \int_\Omega \mathbf{w}(t, \mathbf{x})^T \mathbf{w}(t, \mathbf{x}) \exp(\mu(\mathbf{x}))\, \mathrm{d}\mathbf{x}.$$

The imposed feedback controls $\mathbf{u} = (u_1, \ldots, u_n)^T$ satisfy $\mathbf{u} = \mathbf{T}\tilde{\mathbf{u}}$

$$\begin{aligned} &-\sum_{i=1}^{n} \int_{\Gamma_i^-} \lambda_i(\mathbf{x}, \mathbf{n}(\mathbf{x}))\tilde{u}_i(t, \mathbf{x})^2 \exp(\mu(\mathbf{x}))\, \mathrm{d}\mathbf{x} \\ &\leq \sum_{i=1}^{n} \int_{\Gamma_i^+} \lambda_i(\mathbf{x}, \mathbf{n}(\mathbf{x}))v_i(t, \mathbf{x})^2 \exp(\mu(\mathbf{x}))\, \mathrm{d}\mathbf{x}, \end{aligned}$$

with $\mathbf{v} = \mathbf{T}^T\mathbf{w}$ and (6). It is then shown that the Lyapunov function decays exponentially, see [5, Thm. 2.4].

It will be an interesting question for future research to identify structural properties of symmetric hyperbolic systems such that (8) holds, see also [3].

References

[1] G. Boillat, *Nonlinear hyperbolic fields and waves*, In Recent mathematical methods in nonlinear wave propagation (Montecatini Terme, 1994), volume 1640 of Lecture Notes in Math., pages 1–47. Springer, Berlin, 1996.

[2] K. O. Friedrichs and P. D. Lax, *Systems of conservation equations with a convex extension*, Proc. Nat. Acad. Sci. U.S.A., **68** (1971), 1686–1688.

[3] J. W. Helton and V. Vinnikov, *Linear matrix inequality representation of sets*, Comm. Pure Appl. Math., **60** (2007), 654–674.

[4] M. Herty and F. Thein, *Stabilization of a multi-dimensional system of hyperbolic balance laws*, Mathematical Control and Related Fields, https://doi.org/10.3934/mcrf.2023033, 2023.

[5] M. Herty and F. Thein, *Boundary feedback control for hyperbolic systems*, ESAIM: Control, Optimisation and Calculus of Variations (submitted), http://arxiv.org/abs/2303.05598, 2023.

All-speed IMEX schemes for two-fluid flows

Andrea Thomann

(joint work with Aaron Brunck, Mária Lukáčová-Medvid'ová, Ilya Peshkov)

We are interested in the numerical simulation of mixtures composed of a gas and/or a liquid phase, where the sound speeds of the gas and liquid phase respectively are much faster than the material wave which is of the order of the transport velocity. Thus, three different scales can arise in the model. In regimes which are characterized by small, potentially different phase Mach numbers, using an explicit scheme requires a time step that scales with the smallest appearing Mach number. This is especially problematic when phenomena in a low Mach number regime are monitored over a long time period. Moreover, the main interest often lies on a sharp resolution of the interface which is transported with the local fluid speed and thus would allow for a much larger time step. Therefore, we use implicit-explicit (IMEX) time integrators where fast waves are treated implicitly leading to a CFL condition which is restricted by the material velocity only.

For the mixture description, we use a symmetric hyperbolic thermodynamically compatible (SHTC) diffusive interface model given in [1, 2] which is composed of the dynamics for volume fractions α_1, α_2 obeying a saturation constraint $\alpha_1+\alpha_2 = 1$, partial densities $\alpha_1\rho_1$ and $\alpha_2\rho_2$ yielding the mixture density $\rho = \alpha_1\rho_1 + \alpha_2\rho_2$, the mixture momentum $\rho\mathbf{v}$, relative velocity $\mathbf{w} = \mathbf{v}_1 - \mathbf{v}_2$ driven by the difference in chemical potentials μ_1, μ_2 of each phase, where $\mathbf{v}_j$ denote the phase velocities for $j = 1, 2$, and finally the total energy ρE. Note that in the SHTC theory, the model naturally comes with an equation for the entropy and the energy conservation as a consequence. However, since we apply a single temperature simplification $T_1 = T_2 = T$, for smooth flows, the energy and entropy equation are equivalent

and we chose to solve for the energy conservation law instead. This allows to apply classical semi-implicit approaches for the approximation of fluid dynamics systems [7, 8]. The model in compact notation can be written as follows

$$\partial_t \mathbf{q} + \nabla \cdot \mathbf{f}(\mathbf{q}) + \mathbf{B}(\mathbf{q})\nabla \mathbf{q} = \frac{1}{\tau}\mathbf{r}(\mathbf{q}), \tag{1}$$

where $\mathbf{q}$ denotes the state vector, $\mathbf{f}$ the flux tensor, $\mathbf{B}(\mathbf{q})\nabla\mathbf{q}$ a non-conservative product due to transport of α_1 and contributions of the relative velocity $\mathbf{w}$. In $\mathbf{r}$ the relaxation source terms are contained, i.e. an equilibrium processes for the pressures and velocities, acting on the volume fraction and relative velocity equation respectively. Therein, in short, $\tau = \tau^{(\alpha)}, \tau^{(w)}$ denotes the possibly different relaxation rates. The system is closed by considering an equation of state (EOS) per phase. Here, the ideal gas law or stiffened gas equation is applied. Thus for each phase $k = 1, 2$, a Mach number $M_k = \|\mathbf{v}\|/a_k$ is defined, where a^1, a^2 are the phase sound speeds given as usual by $a_k = \sqrt{\partial_{\rho_k} p_k}$. Rescaling system (1) based on a separation of each dimensional variable in $\mathbf{q}$ into a reference value q_j^r and a non-dimensional quantity $\tilde{q}_j$, yields the following non-dimensional system

$$\partial_t \tilde{\mathbf{q}} + \nabla \cdot \mathbf{f}^v(\tilde{\mathbf{q}}) + \nabla \cdot \mathbf{f}^M(\tilde{\mathbf{q}}, {M_k}^{-1}) + \mathbf{B}(\tilde{\mathbf{q}})\nabla\tilde{\mathbf{q}} = \frac{1}{\tau^{(w)}}\mathbf{r}^v(\tilde{\mathbf{q}}) + \frac{1}{\tau^{(\alpha)}}\mathbf{r}^M(\tilde{\mathbf{q}}, M_k^{-1}), \tag{2}$$

where the flux tensor $\mathbf{f}$ is split into a velocity based flux $\mathbf{f}^v$ and a pressure based flux $\mathbf{f}^M$ containing the dependence on the Mach numbers. Analogously the relaxation source term is split into $\mathbf{r}^v$ and $\mathbf{r}^M$. The non-conservative product does not depend on the Mach number.

For model (2) can be formally shown, following the seminal works of [5, 6], that in the low Mach number limit, the mixture is described by the incompressible Euler equations with variable volume fraction. Since we consider the case of a single temperature the phase Mach numbers are coupled, thus, if M^1 tends to zero, so does M^2. For details on the formal derivation of well-prepared initial data and the low Mach number limit, we refer to [4]. In the case of barotropic flows, the phase Mach numbers are independent of each other. We refer to [3] for formal limits with two distinct Mach numbers. Thus we require the numerical scheme to be consistent with the incompressible low Mach number limit and to be stable under a Courant-Friedrichs-Levy (CFL) condition independently of the Mach number flow regime dictated by the characteristics of the velocity based flux $\mathbf{f}^v$, thus asymptotic preserving (AP).

To achieve this, we apply an operator splitting on (2) and integrate explicitly the contributions $\mathbf{f}^v$ and $\mathbf{B}\nabla\mathbf{q}$, whereas $\mathbf{f}^M$ and $\mathbf{r}^v, \mathbf{r}^M$ are treated implicitly due possibly very fast relaxation processes, thus stiff relaxation source terms. To avoid the solution of non-linear implicit systems and at the same time obtain an AP scheme, we linearize pressure based terms in $\mathbf{f}^M$ with respect to a reference total energy $(\rho E)^{\mathrm{RS}} = \rho^{\mathrm{RS}} e^{\mathrm{RS}} + \rho^{\mathrm{RS}}(\|\mathbf{v}\|^2) + c_1 c_2 \|\mathbf{w}\|^2)/2$ composed of the leading order terms of the well-prepared initial density and internal energy. Since the pressure is already linear in ρE, we only need to linearize the chemical potential difference $\mu = \mu_1 - \mu_2$ in a non-linear part $\bar{\mu} \in \mathcal{O}(M_k^2)$ and a linear part $\hat{\mu} =$

$\mu^{\mathrm{RS}} + \left(\frac{\partial \mu}{\partial(\rho E)}\right)^{\mathrm{RS}} (\rho E - (\rho E)^{\mathrm{RS}})$. Since $\bar{\mu}$ vanishes as $M_k \to 0$, it can be treated explicitly without reducing the CFL condition, see [4].

The numerical scheme in a finite volume framework consists of first solving the velocity based contributions given by $\mathbf{f}^v$ and $\mathbf{B}\nabla\mathbf{q}$ explicitly with Rusanov numerical fluxes and integration of the non-conservative product. To avoid solving a large coupled linear implicit system, we substitute the implicitly treated momentum and relative velocity in the total energy update by their respective evolution equations combined with a linearization in time as done e.g. in [8]. Moreover, the linear relaxation source term acting on the relative velocity is included. This yields one scalar implicit equation containing Laplace operators which are discretized using second order central differences. It can be solved efficiently using direct or iterative solvers, e.g. GMRES. Once the total energy is obtained, $\mathbf{w}^{n+1}$ and $\rho\mathbf{v}^{n+1}$ are updated adding the implicit respective flux contributions from $\mathbf{f}^M(\mathbf{q}^{n+1})$. As a last step, the pressure relaxation in the evolution equation for α_1 is considered. Since it is an algebraic and non-linear source term, a Newton method is applied. Using semi-implicit stiffly accurate IMEX Runge Kutta methods [7], and second order interface reconstruction using a minmod limiter, the scheme is extended to second order accuracy [4]. The scheme is provably AP up to $\mathcal{O}(\Delta t)$, however for homogeneous mixtures and single phase flows it is AP up to $\mathcal{O}(M_k^2)$, see [4]. The proofs contain elements from the AP proof in [9] in the context of a numerical scheme for the Euler equations with gravity.

A suitable test case to visualize the AP property is a simulation of the Kelvin-Helmholtz instability. The initial data is well-prepared [4] and allows a direct comparison with the incompressible limit equations. The solution at time $t = 3$ is depicted in Fig. 1. On the left, the result for α_1 computed with the 2nd order AP solver for the two-phase flow model is depicted in a Mach number flow regime of $\mathcal{O}(M) = 10^{-2}$. On the right, the respective solution of the incompressible limit model using a finite element solver. We can observe, that both results are qualitatively in good agreement which underlines the AP property of the numerical scheme.

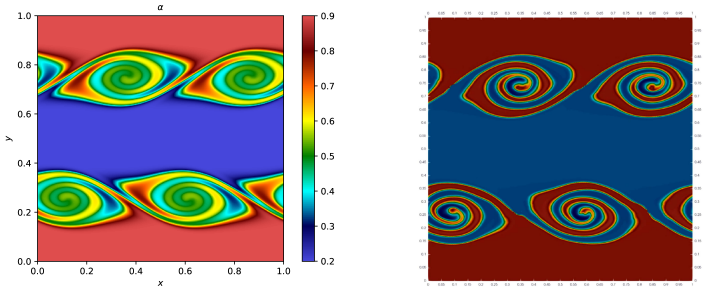

FIGURE 1. Kelvin-Helmholtz instability; numerical solution of α_1. Left: compressible two-fluid single temperature model. Right: incompressible Euler limit equations.

References

[1] E. Romenski and E. F. Toro, *Compressible Two-Phase Flows: Two-Pressure Models and Numerical Methods*, Comput. Fluid Dyn. J., **13** (2004), 403–416.
[2] E. Romenski, D. Drikakis, and E. F. Toro, *Conservative Models and Numerical Methods for Compressible Two-Phase Flow*, J. Sci. Comput., **42** (2010), 68–95.
[3] M. Lukáčová-Medvid'ová, G. Puppo, and A. Thomann, *An all Mach number finite volume method for isentropic two-phase flow*, J. Numer. Math., **31** (2023), 175–204.
[4] M. Lukáčová-Medvid'ová, I. Peshkov, and A. Thomann, *An implicit-explicit solver for a two-fluid single-temperature model*, J. Comput. Phys., **498** (2024), 112696.
[5] S. Klainerman and A. Majda, *Singular limits of quasilinear hyperbolic systems with large parameters and the incompressible limit of compressible fluids*, Commun. Pure Appl. Math., **34** (1981), 481–524.
[6] S. Dellacherie, *Analysis of Godunov type schemes applied to the compressible Euler system at low Mach number*, J. Comput. Phys., **229** (2010), 978–1016.
[7] S. Boscarino, F. Filbet, and G. Russo, *High Order Semi-implicit Schemes for Time Dependent Partial Differential Equations*, J. Sci. Comput., **68** (2016), 975–1001.
[8] S. Boscarino, G. Russo, and L. Scandurra, *All Mach number second order semi-implicit scheme for the Euler equations of gas dynamics*, J. Sci. Comput., **77** (2018), 850–884.
[9] G. Bispen, M. Lukáčová-Medvid'ová, and L. Yelash, *Asymptotic preserving IMEX finite volume schemes for low Mach number Euler equations with gravitation*, J. Comput. Phys., **335** (2017), 222–248.

Minimal Acceleration for the Multi-Dimensional Isentropic Euler Equation

Michael Westdickenberg

We consider the multi-dimensional isentropic Euler equations

$$\left.\begin{aligned} \partial_t \varrho + \nabla \cdot (\varrho \mathbf{u}) &= 0 \\ \partial_t(\varrho \mathbf{u}) + \nabla \cdot (\varrho \mathbf{u} \otimes \mathbf{u}) + \nabla P(\varrho) &= 0 \end{aligned}\right\} \quad \text{in } [0,\infty) \times \mathbf{R}^d, \tag{1}$$

$$(\varrho, \mathbf{u})(0,\cdot) =: (\bar{\varrho}, \bar{\mathbf{u}}) \quad \text{initial data.}$$

This system expresses local conservation of mass and momentum. We only consider polytropic gases, for which $U(\varrho) = \kappa \varrho^\gamma$ with constants $\kappa > 0$ and $\gamma > 1$ and

$$P(r) = U'(r) r - U(r) \quad \text{for } r \geq 0.$$

Smooth solutions $(\varrho, \mathbf{u})$ of (1) satisfy the additional conservation law

$$\partial_t \Big(\tfrac{1}{2} \varrho |\mathbf{u}|^2 + U(\varrho) \Big) + \nabla \cdot \left(\Big(\tfrac{1}{2} \varrho |\mathbf{u}|^2 + U'(\varrho) \varrho \Big) \mathbf{u} \right) = 0, \tag{2}$$

which expresses local conservation of total energy

$$E(\varrho, \mathbf{u}) := \tfrac{1}{2} \varrho |\mathbf{u}|^2 + U(\varrho),$$

which is the sum of kinetic and internal energy. Since solutions of (1) may become discontinuous in finite time, solutions must be considered in the weak sense and energy conservation (2) must be relaxed to an $\leq$ inequality.

Global existence of weak solutions to (1) is still an open problem in several space dimension. A useful relaxation with guaranteed global existence is the notion of

dissipative solutions, introduced in [1]. Dissipative solutions are defined as tuples of $(\varrho, \mathbf{m})$ and defect measures $\mathbf{R}, \phi$ that satisfy the continuity equation and

$$\partial_t \mathbf{m} + \nabla \cdot \left(\frac{\mathbf{m} \otimes \mathbf{m}}{\varrho} + P(\varrho)\mathbf{1} \right) + \boxed{\nabla \cdot (\mathbf{R} + \phi \mathbf{1})} = 0,$$

$$\frac{d}{dt} \int_{\mathbf{R}^d} \left(\tfrac{1}{2}\varrho |\mathbf{u}|^2 + U(\varrho) + \boxed{\frac{1}{2}\mathrm{tr}(\mathbf{R}) + \frac{1}{\gamma - 1}\phi} \right)(t, dx) \leq 0.$$

Here $\mathbf{R}$, ϕ are measures taking values in the symmetric, positive semidefinite matrices and the non-negative numbers, which form closed convex cones. Dissipative solutions become weak solutions of (1) iff the defect measures vanish a.e.

The construction of infinitely many weak solutions to (1), pioneered by De Lellis–Székelyhidi [3], starts from so-called subsolutions, which can be interpreted as dissipative solutions with defect measures nonvanishing in open sets. Superimposing over $(\varrho, \mathbf{m})$ highly oscillatory waves, one can then remove the discrepancy between dissipative and weak solutions. In contrast, our goal here is to construct dissipative solutions to the isentropic Euler equations (1) that minimizes the defect measures from the start. To this end, we reinterpret dissipative solutions in terms of Young measures, which has the advantage that Young measures come with a natural notion of weak* convergence and therefore compactness, by Banach-Alaoglu theorem. Dissipative solutions have the useful property that density and momentum are Lipschitz continuous in time, with densities measured with respect to the Wasserstein distance and momenta measured with respect to the bounded Lipschitz norm, which is defined in terms of testing against bounded and Lipschitz continuous test functions. These are the natural topologies we suggest should be used. In fact, since for given initial data all dissipative solutions to this data must have the same total momentum, because of the momentum equation, it is sufficient to consider a distance that uses test functions with bounded Lipschitz seminorm only, without the need to restrict to bounded functions. More precisely, let

$$d(\boldsymbol{m}_s, \boldsymbol{m}_t) := \sup \left\{ \int_{\mathbb{R}^d} \zeta(x) \cdot \big(\boldsymbol{m}_s(dx) - \boldsymbol{m}_t(dx)\big) : \|\zeta\|_{\mathrm{Lip}(\mathbb{R}^d)} \leq 1 \right\} \tag{3}$$

for $0 \leq s \leq t$. With momentum flux

$$\mathbb{U} := \left(\frac{\mathbf{m} \otimes \mathbf{m}}{\varrho} + P(\varrho)\mathbf{1} \right) + \boxed{\mathbf{R} + \phi \mathbf{1}}. \tag{4}$$

the metric derivative of $t \mapsto \boldsymbol{m}_t$ induced by the distance (3) is given by

$$|\boldsymbol{m}'|(t) = \int_{\dot{\mathbf{R}}^d} \mathrm{tr}\big(\mathbb{U}(t, dx)\big) \quad \text{for a.e. } t \in [0, \infty). \tag{5}$$

We refer the reader to [5] for more information. The metric derivative is a measure for the rate of change in time of the momentum. As such it can also be understood as a measure of the acceleration of the fluid. We will be interested in dissipative solutions that minimize the metric derivative $|\boldsymbol{m}'|$, i.e., the acceleration.

Since the metric derivative is a function of time, its minimization yields a multi-objective optimization problem. Several strategies have been devised to deal with such problems. We consider two: scalarization and seeking minimal elements.

Shortest Solutions. Scalarization means to build one objective function out of the many. In our case, one natural approach is to consider the integral

$$\int_0^T |\boldsymbol{m}'|(t)\,dt =: \mathcal{L}(\boldsymbol{m}). \tag{6}$$

Since the metric derivative measures the rate of change of the momentum, we can think of $\mathcal{L}(\boldsymbol{m})$ as the length of the momentum curve. Given initial data, we then consider the set X of all dissipative solutions to this initial data. The set X is not empty as dissipative solutions are known to exist globally; see [5] for example. It may contain only one element when the data is such that a unique strong solution to (1) exists. Indeed, since dissipative solutions have the weak-strong uniqueness property, they coincide with strong solutions of (1) as long as the latter do exist. One can check that the set of dissipative solutions to given initial data is compact with respect to the topology of weak* convergence of Young measures. Moreover, combining (6) with (5)/(4), one can check that the length (6) is continuous with respect to this topology, so existence of dissipative solutions minimizing (6) follows easily. We call such dissipative solutions shortest solutions.

Minimal Elements. Inspired by Dafermos' [2] entropy rate admissibility condition, one might also be interested in dissipative solutions that minimize (5) for every t. It is not clear to us whether this amounts to a well-posed problem. We can look instead for Pareto-optimal solutions, i.e., for minimal elements with respect to a suitable quasi-order defined on the set of dissipative solutions in terms of comparing the metric derivative (5) of different dissipative solutions at all times. A quasi-order is a binary relation that is reflexive and transitive, but not necessarily antisymmetric. If this quasi-order is compatible with a topology, then one can use the following existence result due to Wallace [4].

Theorem 9 (Wallace)**.** *Suppose that X is a nonempty compact set with a quasi-order R such that the set of predecessors $P(x)$ of x is closed for every $x \in X$. Then X has a minimal element, i.e., an element $m \in X$ with the property that,*

$$\textit{if } y \in X \textit{ and } m \textit{ can be compared at all, then } (m, y) \in R.$$

This result can be applied with X the set of dissipative solutions of (1) to given initial data, and with the quasi-order defined in terms of the metric derivative (5). A suitable topology is again the weak* convergence of Young measures. Wallace's result constructs minimal elements starting from totally ordered subsets of X, which exist because of the Hausdorff maximal principle (i.e., the axiom of choice). The construction does, however, not minimize over the whole set X.

The motivation for our approach is that it may well be the case that for certain "wild" initial data, weak solutions of (1) cannot be expected to exist for all times. For configurations such as Kelvin-Helmholtz instabilities, defect measures may not vanish because oscillatory features persist at arbitrarily small length scales in the

absence of viscosity. One can try to construct solutions that are as close to being a weak solution as possible. In regions with nonvanishing defect measures, a more robust version of the De Lellis–Székelyhidi method may then be tried to repair the dissipative solution to become a (or infinitely many) weak solution(s).

References

[1] D. Breit, E. Feireisl, and M. Hofmanová, *Solution semiflow to the isentropic Euler system*, Arch. Ration. Mech. Anal. **235** (2020), 167–194.

[2] C. M. Dafermos, *The entropy rate admissibility criterion for solutions of hyperbolic conservation laws*, J. Differential Equations **14** (1973), 202–212.

[3] C. De Lellis and L. Székelyhidi, Jr., *On admissibility criteria for weak solutions of the Euler equations*, Arch. Ration. Mech. Anal. **195** (2010), 225–260.

[4] A. D. Wallace, *A fixed-point theorem*, Bull. Amer. Math. Soc. **51** (1945), 413–416.

[5] M. Westdickenberg, *Minimal acceleration for the multi-dimensional isentropic Euler equations*, Arch. Ration. Mech. Anal. **247** (2023), Paper No. 35, 37.

Reporter: Yongle Liu

Participants

Prof. Dr. Remi Abgrall
Institut für Mathematik
Universität Zürich
Winterthurerstrasse 190
8057 Zürich
SWITZERLAND

Dr. Wasilij Barsukow
Centre de Recherche en Mathématique de Bordeaux, CNRS
Université de Bordeaux 1
351 Cours de la Liberation
33405 Talence Cedex
FRANCE

Prof. Dr. Sebastiano Boscarino
Dipartimento di Matematica e Informatica
Citta Universitaria
Viale A. Doria, 6 - 1
95125 Catania
ITALY

Prof. Dr. Alina Chertock
Department of Mathematics
North Carolina State University
SAS Hall 4152
Raleigh, NC 27695-8205
UNITED STATES

Prof. Dr. Rinaldo M. Colombo
INdAM Unit - c/o DII
Università degli Studi di Brescia
Via Branze, 38
25123 Brescia
ITALY

Prof. Dr. Michael Dumbser
DICAM
Universita degli Studi di Trento
Via Mesiano, 77
38123 Trento
ITALY

Prof. Dr. Eduard Feireisl
Institute of Mathematics of the AS CR
Charles University
Žitná 25
115 67 Praha 1
CZECH REPUBLIC

Prof. Dr. Heinrich Freistühler
Fachbereich Mathematik und Statistik
Universität Konstanz
Universitätsstraße 10
78457 Konstanz
GERMANY

Prof. Dr. Mauro Garavello
Dipartimento di Matematica e Applicazioni
Università di Milano-Bicocca
Via Roberto Cozzi 55
20125 Milano
ITALY

Prof. Dr. Jan Giesselmann
Fachbereich Mathematik
Technische Universität Darmstadt
Dolivostraße 15
64293 Darmstadt
GERMANY

Prof. Dr. Christiane Helzel
Mathematisches Institut
Heinrich-Heine-Universität Düsseldorf
Universitätsstraße 1
40225 Düsseldorf
GERMANY

Prof. Dr. Michael Herty
Lehrstuhl für Numerische Mathematik
Institute für Geometrie und Praktische Mathematik
RWTH Aachen University
Templergraben 55
52062 Aachen
GERMANY

Prof. Dr. Helge Holden
Department of Mathematical Sciences
Norwegian University of Science and Technology
A. Getz vei 1
7491 Trondheim
NORWAY

Prof. Dr. Christian Klingenberg
Institut für Mathematik
Universität Würzburg
Emil-Fischer-Straße 40
97074 Würzburg
GERMANY

Prof. Dr. Dietmar Kröner
Abteilung für Angewandte Mathematik
Universität Freiburg
Hermann-Herder-Straße 10
79104 Freiburg i. Br.
GERMANY

Prof. Dr. Igor Kukavica
Department of Mathematics
University of Southern California, Dornsife
KAP 104
3620 S. Vermont Avenue
Los Angeles, CA 90089-2532
UNITED STATES

Prof. Dr. Alexander Kurganov
Department of Mathematics
Southern University of Science and Technology (SUSTech)
1088 Xueyuan Ave. Nanshan
Shenzhen, Guangdong Province 518 055
CHINA

Dr. Yongle Liu
Institute of Mathematics
University of Zurich
Winterthurerstrasse 190
Zürich CH 8057
SWITZERLAND

Prof. Dr. Mária Lukáčová-Medvidová
Institut für Mathematik
Fachbereich Mathematik/Physik/Informatik
Johannes-Gutenberg-Universität Mainz
Staudingerweg 9
55128 Mainz
GERMANY

Dr. Pierre-Henri Maire
CEA-CESTA
15 avenue des sablier CS 60001
33116 Le Barp cedex
FRANCE

Assc. Prof. Dr. Sandra May
Department of Information Technology
Uppsala Universitet
Box 337
751 05 Uppsala
SWEDEN

Lorenzo Micalizzi
Department of Mathematics
North Carolina State University
SAS Hall 2108
2311 Stinson Dr
Raleigh, NC 27607
UNITED STATES

Dr. Claudia Nocita
Dipartimento di Matematica
Universita di Pavia
Via Ferrata, 1
27100 Pavia
ITALY

Prof. Dr. Martin Oberlack
TU Darmstadt, Department of Mechanical Engineering, Chair of Fluid Dynamics
Otto-Bernd-Str. 2, 3 Stock
64287 Darmstadt 64287
GERMANY

Dr. Philipp Öffner
Institut für Mathematik
Johannes-Gutenberg-Universität Mainz
Staudingerweg 9
55128 Mainz
GERMANY

Prof. Dr. Iuliia Petrova
Pontifical Catholic University of Rio de Janeiro - PUC-Rio
Rua Marquês de São Vicente, 225, Gávea
22451-900 Rio de Janeiro, RJ
BRAZIL

Prof. Dr. Gabriella A. Puppo
Dipartimento di Matematica
Universita di Roma "La Sapienza"
Istituto "Guido Castelnuovo"
Piazzale Aldo Moro, 5
00185 Roma
ITALY

Dr. Mario Ricchiuto
INRIA at University of Bordeaux
200, Ave. de la Vieille Tour
33405 Talence Cedex
FRANCE

Prof. Dr. Christian Rohde
Institut für Angewandte Analysis und Numerische Simulation
Universität Stuttgart
Pfaffenwaldring 57
70569 Stuttgart
GERMANY

Prof. Dr. Giovanni Russo
Dipartimento di Matematica e Informatica
Citta Universitaria
Viale A. Doria, 6
95125 Catania
ITALY

Andreas Schömer
Institut für Mathematik
Johannes-Gutenberg-Universität Mainz
Staudingerweg 9
55128 Mainz
GERMANY

Bangwei She
Academy for Multidisciplinary Studies
Capital Normal University
West 3rd Ring North Road 105, Haidian
Beijing 100048
CHINA

Prof. Dr. Chi-Wang Shu
Division of Applied Mathematics
Brown University
Box F
182 George Street
Providence, RI 02912
UNITED STATES

Dr. Stephan Simonis
Institut für Angewandte und Numerische Mathematik 2
Karlsruher Institut für Technologie (KIT)
76049 Karlsruhe
GERMANY

Dr. Laura Spinolo
IMATI-CNR, Pavia
Via Ferrata, 5
27100 Pavia
ITALY

Prof. Dr. Eitan Tadmor
Department of Mathematics
University of Maryland
4176 Campus Drive
College Park, MD 20742-4015
UNITED STATES

Dr. Ferdinand Thein
Institut für Geometrie und Praktische Mathematik
RWTH Aachen
Templergraben 55
52056 Aachen
GERMANY

Dr. Andrea Thomann
Inria Nancy Grand-Est
Université de Strasbourg
615, rue du Jardin Botanique
54600 Villers-lès-Nancy
FRANCE

Prof. Dr. Konstantina Trivisa
Department of Mathematics
University of Maryland
College Park, MD 20742-4015
UNITED STATES

Dr. Francois Vilar
IMAG, Université de Montpellier
Place Eugene Bataillon
34095 Montpellier Cedex 5
FRANCE

Prof. Dr. Gerald Warnecke
Fakultät für Mathematik
Institut für Analysis und Numerik
Otto-von-Guericke-Universität Magdeburg
Universitätsplatz 2
39106 Magdeburg
GERMANY

Prof. Dr. Michael Westdickenberg
RWTH Aachen University
Templergraben 55
52062 Aachen
GERMANY

Dr. Yuhuan Yuan
School of Mathematics
Nanjing University of Aeronautics and Astronautics
Jiangjun Avenue No. 29
211106 Nanjing
CHINA